New synthetic and characterization strategies for polyolefins

by

Nyambeni Luruli

Dissertation

Presented for the degree of

Doctor

of

Philosophy (Polymer Science)

in the

Faculty of Science

at the

University of Stellenbosch

Supervisor: Prof H. G. Raubenheimer.
Co-supervisors: Prof. H. Pasch and Dr A. J. van Reenen

April 2006

DECLARATION

I, the undersigned, hereby declare that the work contained in this dissertation is my own original work and that I have not previously in its entirety or in part submitted it at any university for a degree.

Signature: .....…..... Date: .....

Summary

Metalloxycarbene complexes $[(CO)_5M^1{=}O(R)M^2(Cl)L_2]$ (M^1 = Cr , W; M^2 = Zr, Hf; L = Cp, Cp^*) were synthesized from the reaction between anionic Fischer-type carbene complex salts $[(CO)_5M^1{=}C(O)R][NEt_4]$ and metallocene chlorides. The molecular and crystal structures of $[(CO)_5W{=}C(Me)OZr(Cp)_2Cl]$, $[(CO)_5Cr{=}C(Me)OZr(Cp)_2Cl]$ and $[(CO)_5W{=}C(Ph)OHf(Cl)Cp_2]$ determined by X-ray methods, show a short $C_{carbene}$-O and relatively long O-Zr and O-Hf separations. Metalloxycarbene complexes in the presence of MAO are active catalysts for homo- and copolymerization of α-olefins and produce polymers with heterogeneous properties. 1-Pentene oligomers, homopolymers of ethylene and ethylene/1-pentene copolymers were successfully synthesized using metalloxycarbenes/MAO and the results obtained were critically compared with those synthesized with metallocene/MAO catalysts. The GC and GPC show that 1-pentene oligomers produced with both metalloxycarbenes and metallocenes catalysts range from simple dimers to more complicated high molecular weight (2 600 g/mol) products. The properties of polyethylene and ethylene/1-pentene copolymers were evaluated by, among others, GPC, SEC-FTIR, preparative molecular weight fractionation and HPer DSC. Generally the polymers obtained using metalloxycarbene/MAO catalysts have broad and bimodal molecular weight distributions. The copolymers have higher concentration of 1-pentene in the lower molecular weight fraction than those produced with

metallocene/MAO as shown by SEC-FTIR. Consequently, HPer DSC shows a decrease of melting and crystallization temperature towards the low molecular weight fractions.

Opsomming

Metaaloksikarbeenkomplekse [$(CO)_5M^1$=C(R)OM^2(Cl)L_2] (M^1 = Cr , W; M^2 = Zr, Hf; L = Cp, Cp^*] is gesintetiseer in die reaksie tussen anioniese Fischer-tipe karbeenkompleks-soute, [$(CO)_5M^1$=C(O)R][NEt_4], en metalloseen dichloriedes. Die molekulêre- en kristalstrukture van [$(CO)_5$W=C(Me)OZr$(Cp)_2$Cl], [$(CO)_5$Cr=C(Me)OZr$(Cp)_2$Cl] en [$(CO)_5$W=C(Ph)OHf(Cl)Cp_2] bepaal deur X-straalkristallografiese metodes, toon die aanwesigheid van kort $C_{karbeen}$-O- en relatief lang O-Zr- en O-Hf-bindings. Metaaloksikarbeenkomplekse, in die aanwesigheid van MAO, is aktiewe katalisatore vir die homo- en ko-polimerisering van α-olefiene en is verantwoordelik vir die vorming van polimere met heterogene eienskappe. 1-Penteen oligomere, homopolimere van etileen en etileen/1-penteen ko-polimere is suksesvol gesintetiseer met metaaloksikarbeenkomplekse/MAO en die resultate sodoende verkry, is krities vergelyk met produkte gesintetiseer vanuit metalloseen/MAO prekatalisatore.

Die GC en GPC resultate toon dat die 1-penteen oligomere, geproduseer met beide metaaloksikarbeenkomplekse en metallosene, kan wissel van eenvoudige dimere tot meer komplekse, hoë molekulêre massa (2 600g/mol) produkte. Die polietileen en etileen/1-penteen ko-polimere is gekarakteriseer deur onder andere gevorderde, GPC, SEC-FTIR, preparatiewe molekulêre massa fraksionering en HPer DSC. In die algemeen het die polimere verkry met metaaloksikarbeen/MAO katalisatore, breë en bimodale molekulêre massaverspreidings. Die ko-polimere bevat hoër konsentrasies van 1-penteen in die lae molekulêre massa fraksie in vergelyking met dié gevorm vanuit metalloseen/MAO–

gekataliseerde mengsels, soos aangedui deur SEC-FTIR-analise. HperDSC wys 'n verlaging in smelt- en kristallisasietemperature in die laer molekulêre massa fraksies.

ACKNOWLEDGEMENTS

My promoters **Prof. Helgard G. Raubenheimer** and **Prof. Harald Pasch** and **Dr. Albert J. van Reenen**, for their guidance and support

My mentors **Dr. Valerie Grumel**, **Dr. Robert Brull** and **Dr. Udo Wahner** for all the time and patience they have given me throughout this study

Thijs Pijpers, for assisting me with HPer DSC measurements. **Prof. Vincent Mathot**, for inviting me to work in his group at the Catholic University of Leuven, Belgium. The discussions we had were very helpful.

Christian Heinz and **Christoph Brinkmann** Deutsches Kunststoff-Institut (German Institute for Polymers) (DKI) for TREF and GPC experiments and the Lilien soccer matches we watched together. I really enjoyed the time we spent together.

Christel Hock and **Birgit Staben** for the FTIR and DSC measurements respectively

Jean Mckenzie, **Elsa Malherbe** and **Dr. Wolf Hiller** for NMR measurements

Aletta du Toit, Elzet Stander and Arno Neveling for helping me with the synthesis of carbene compexes.

My colleagues in the **Olefins** Lab at the University of Stellenbosch and **Analytics** at DKI

Department of Labour (South Africa) and NRF, BMBF, DAAD and Sasol for financial support

Mrs Elizabeth Zietsman at the US postgraduate bursary office for coordinating the funding.

This thesis is dedicated to

My wife, **Ndivhuwo**

16 December 2005

"…..Never turn your back on molecular side of things….."

J.R. Bull

TABLE OF CONTENTS

SYMBOLS AND ABBREVIATIONS USED

CCD	chemical composition distribution
Cp	cyclopentadienyl
Cp*	1,2,3,4,5-pentamethylcyclopentadienyl
CRYSTAF	crystallization analysis fractionation
Cy	cyclohexyl
DEA	dielectric analysis
DEGMBE	diethyleneglycolmonobutylether
DMA	dynamic mechanical analysis
DSC	differential scanning calorimetry
Flu	fluorenyl
FTIR	Fourier transform infrared
GC	gas chromatography
HDPE	high density polyethylene
HPer DSC	High Performance Differential Scanning Calorimetry
Ind	indenyl
i-Pr	iso-propyl
IR	infrared
LDPE	low density polyethylene
LLPE	linear low density polyethylene
MAO	Methylaluminoxane

Me	methyl
M_n	number-average molecular weight
M_w	weight-average molecular weight
MWD	molecular weight distribution
NMR	nuclear magnetic resonance
PDI	polydispersity index
Ph	phenyl
PMWF	Preparative Molecular Weight Fractionation
R	alkyl
SCBD	short chain branching distribution
SEC	size exclusion chromatography
SEC-FTIR	Combination of SEC and FTIR
SEC-HPer DSC	Combination of SEC and HPer DSC
T_g	glass transition
TGA	thermogravimetric analysis
TMA	thermomechanical analysis
TREF	Temperature rising elution fractionation

LIST OF FIGURES

Chapter 2

Chapter 3

Chapter 4

Chapter 5

Appendix

LIST OF SCHEMES

Chapter 2

Chapter 3

Chapter 4

Chapter 5

LIST OF TABLES

Chapter 3

Chapter 4

Chapter 5

Appendix

1 Aims and objectives of the project

1.1 Introduction

The discovery of Ziegler Natta catalyst systems generated a lot of interest in the fields of polyolefin synthesis and organometallic chemistry. These catalysts brought major improvements in the synthesis of polyolefins, especially polyethylene and polypropylenes. Since the discovery of these catalyst systems in the 1950's, a large number of catalyst systems which are based on organometallic complexes have been discovered[1-7], some of them being, metallocenes and post metallocenes. The main purpose for the modifications to existing catalyst systems has always been to finally improve the activity of a particular catalyst system as well as improving the end-properties of the polymer either by modifying the ligand, changing the metal or cocatalyst. Consequently, most of the post Ziegler-Natta catalyst systems have been shown to be superior in terms of their activity during polymerization[1-3,7]. In addition, they produce polymers with a wide variety of architecture and properties that were not previously accessible[3,5-7]. Examples are polymers with very narrow molecular weight distribution, block copolymers, and polyolefins with polar properties[178]. Despite all these advantages, it is generally known that no single class of catalyst system has the ability to control all macromolecular parameters that influence the final properties of the polymer. This simply means that the search for new or modified catalyst systems will remain an active area of research[4].

The complexity of polymer architecture arising from different synthetic methods or catalyst systems presents a challenge to analytical polymer chemists to develop

analytical methods that are suitable to characterize such materials in detail. Analytical methods allow one to study the microstructure of the polymers and to relate these to their macroscopic properties. In addition, sensitive analytical methods provide information about the polymerization behaviour of the catalyst system used thus providing valuable information needed to fine-tune the catalyst. Parameters that influence polymer properties include molecular weight (M_w) and molecular weight distribution (MWD), tacticity, endgroups, etc. In the case of random copolymers, comonomer content and comonomer distribution or short chain branching distribution (SCBD) remain important parameters.

Our group has studied metalloxycarbene complexes of the type $[(CO)_5M^1=C(R)O[M^2]$, i.e. the anionic Fischer-type carbene ligand bonded to a second organometallic unit M^2 through the negatively charged carbene oxygen atom. We have recently communicated that such metalloxycarbene with M^2 = Cp_2ZrCl, when activated with MAO, catalyses the oligomerization of 1-pentene and that the metalloxycarbene complex, $[(CO)_5W=C(Me)OZr(Cp_2)Cl]$, in the presence of MAO shows much higher catalytic activity for the oligomerzation of 1-pentene than the related compounds Cp_2ZrCl_2 and $Cp_2Zr(Cl)OMe$[9]. The high activities displayed by $[(CO)_5W=C(Me)OZr(Cp_2)Cl]$/MAO during the oligomerization of 1-pentene, encouraged us to explore other possibilities of using this and other related metalloxycarbene precursors, α-olefin oligomerization and copolymerization. In this dissertation, the metalloxycarbene catalysts were used to synthesize 1-pentene oligomers as well as homopolymers and copolymers of α-olefin are described.

The monomers chosen for the investigation were ethylene and 1-pentene. Ethylene is the simplest member of α-olefins monomers and it reacts readily due to the absence of bulky substituents around the olefinic bond. 1-Pentene was chosen due to its abundant availability in South Africa as a Fischer-Tropsch product from Sasol.

1.2 The aims of the study

The main aims of the study were to:

1.2.1. Perform oligomerization of 1-pentene and compare the results with those of the previous study[9].

1.2.2. Explore and compare the use of metalloxycarbenes as potential catalyst systems for α-olefin polymerization and copolymerizations. The metalloxycarbene complex catalyst precursors selected were $[(CO)_5W{=}C(Me)OZr(Cp_2)Cl]/MAO$, $[(CO)_5Cr{=}C(Me)OZr(Cp_2)Cl]/MAO$ and the corresponding Cp* analogue, $[(CO)_5Cr{=}C(Me)OZr(Cp^*_2)Cl]/MAO$. The Cp_2ZrCl_2 and $Cp^*_2ZrCl_2$ served as benchmark references.

1.2.3. Characterize the resulting oligomers, homopolymers and copolymers using standard analytical techniques such as gas chromatography (GC), nuclear magnetic resonance (NMR) spectroscopy, size exclusion chromatography (SEC), differential scanning calorimetry (DSC), Fourier transform infrared (FTIR) and crystallization analysis fractionation (CRYSTAF).

1.2.4. Use more advanced and recently developed fractionation analytical techniques to analyze short chain branching distribution along the molecular weight axis. The techniques are:

- Combination of SEC and FTIR (SEC-FTIR)
- Preparative molecular weight fractionation (PMWF)
- Combination of SEC and high performance DSC (SEC-HPer DSC)

1.3 The layout of the chapters

Chapter 2 covers the historic development of different catalyst systems and major developments in polyolefin chemistry in general with a bias towards ethylene and propylene polymerizations. Many excellent books and reviews are available covering different catalyst systems for polyolefins[1-7,10-13]. Therefore, the intention of this chapter is not to rewrite these reviews but to lay a general foundation for the following chapters. It also serves as a quick guide to different catalyst systems and terminology referred to in chapters to follow. Although this project did not focus particularly on propylene polymerization, the stereospecific polymerization associated with propylene, adds an interesting dimension to behaviour of different catalyst systems. Properties such as Mw and MWD, stereochemistry, SCBD of the polymers produced with various catalysts are discussed.

Chapter 3 focuses on the synthesis and characterization of several metalloxycarbene complexes. The resulting complexes are activated with MAO and used as catalyst systems to oligomerize/polymerize ethylene, propylene and 1-pentene. Results of oligomers and homopolymers produced with these catalysts are also discussed.

Chapter 4 focuses mainly on the copolymerization of ethylene with 1-pentene and the analyses of the copolymers using standard analytical methods (NMR, SEC, FTIR, and CRYSTAF).

Chapter 5 deals with advanced fractionation methods used to study SCBD. Special attention is paid to the distribution of 1-pentene (SCBD) along the molecular weight axis thus providing information on the polymerization behaviour of different catalyst systems.

Finally, overall conclusions are drawn in **Chapter 6** about the polymerization behaviour of metalloxycarbene catalysts and some of the analytical methods used. Recommendations are also discussed

1.4 Terminology

The term *molecular weight* is preferred throughout the dissertation instead of *molar mass*. These terms are used interchangeably in many scientific journals.

1.5 References

1. Mülhaupt, R.; *Macromol. Chem. Phys*. **2003**, 204, 289.

2. Alt, H. G.; Koppl, A. *Chem. Rev*. **2000,** 100, 1205.

3. Coates, G. W. *Chem. Rev*. **2000,** 100, 1223.

4. Bajgur, C. S.; Sivaram, S. *Curr. Sci.* **2000**, 78, 1325.

5. Coates, G. W.; Hustad, P. D.; Reinartz, S. *Angew. Chem. Int. Ed*. **2002**, 41, 2236.

6. Makio, H.; Kashiwa, N.; Fujita, T. *Adv. Synth. Catal*. **2002**, 344, 477.

7. Mitani, M.; Nakano, T.; Fujita, T. *Chem. Eur. J*. **2003**, 9, 2396.

8. Heinz, L.; Graef, S.; Macko, T.; Brüll, R.; Balk, S.; Keul, H.; Pasch, H. *e-Polymers*, **2005**, no. 054.

9. Brüll, R.; Kgosane, D.; Nevelling, A.; Pasch, H.; Raubenheimer, H. G.; Sanderson, R. D.; Wahner, U. M. *Macromol. Symp.* **2001**, 165, 11.

10. Prashar, S.; Antinolo, A.; Otero, A. *Coord. Chem. Rev.* **2005**, in press.

11. Gibson, V. C.; Spitzmesser, S. K. *Chem. Rev*. **2003**, 103, 283.

12. Britovsek, G. J. P.; Gibson, V. C.; Wass, D. F. *Angew. Chem. Int. Ed*. **1999**, 38, 428.

13. Ittel, S. D.; Johnson, L. K. *Chem. Rev*. **2000**. 100, 1169.

2 Literature review

2.1 Historical developments

Polyolefins, in general, are the most widely used polymers compared to other polymers such as polystyrene, polycarbonate and polyvinylchloride. Polyethylene and polypropylene (including their copolymers with other α-olefins) find many applications in packaging and in the automotive as engineering plastics. The annual world-wide total production of polymeric materials has been reported to be approximately 200 million metric tons[1]. The consumption volume of polyethylene and polypropylene (including their copolymers with other α-olefins) is believed to account for more than half of the total annual world-wide production.

In contrast, homopolymers made from α-olefin monomers with four carbons and higher have not found major industrial application. These monomers are widely used as comonomers in producing various grades of polyethylene and propylene copolymers. Other applications of homopolymers or oligomers synthesized from these monomers include their use in adhesives, paints, petrochemical and fragrance formulations[2]. For example, high molecular weight oligomers of 1-hexene, 1-octene and 1-decene are used to either decrease or increase oil viscosity. In addition to these applications, low molecular weight oligomers (dimers, trimers and oligomers) could be used to synthesize new monomers *via* olefinic group functionalization.

Three main grades of polyethylene exist (Figure 2.1), namely: linear low density polyethylene (LLDPE), low density polyethylene (LDPE), high density polyethylene (HDPE).

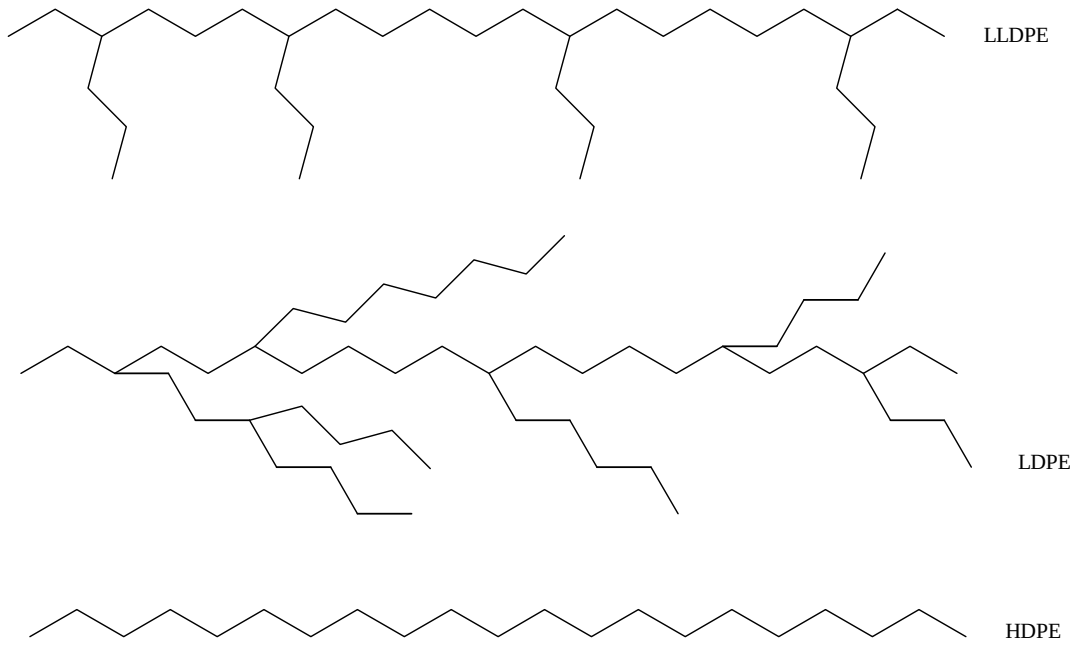

Figure 2.1:The molecular structures of polyethylenes

LLDPE is a slightly branched polymer with short branches that are introduced via copolymerization of ethylene with longer-chain olefins such as 1-butene, 1-pentene, 1-hexene, etc. LDPE is a highly branched polymer (with branches longer than those of LLDPE) which is commonly made by free radical polymerization processes. On the other hand, HDPE has virtually no branches. As a result of these variations in polymer structure, each type of polyethylene has different properties and applications. LLDPE has higher tensile and impact strength as well as puncture resistance. It is widely used in the packaging industry to manufacture flexible films. LDPE is

translucent or opaque, flexible and tough. It is mainly used for manufacturing various containers, dispensing bottles, wash bottles, tubing, etc. Lastly, HDPE is very tough and resistant to a variety of solvent. Its applications include piping and containers. Non-symmetrical polyolefins can be classified according to the pattern of the orientation (tacticity) of the substituent around the olefinic bond. For example, three main types of polypropylene namely, atactic, isotactic and syndiotactic polypropylene are illustrated in Figure 2.2.

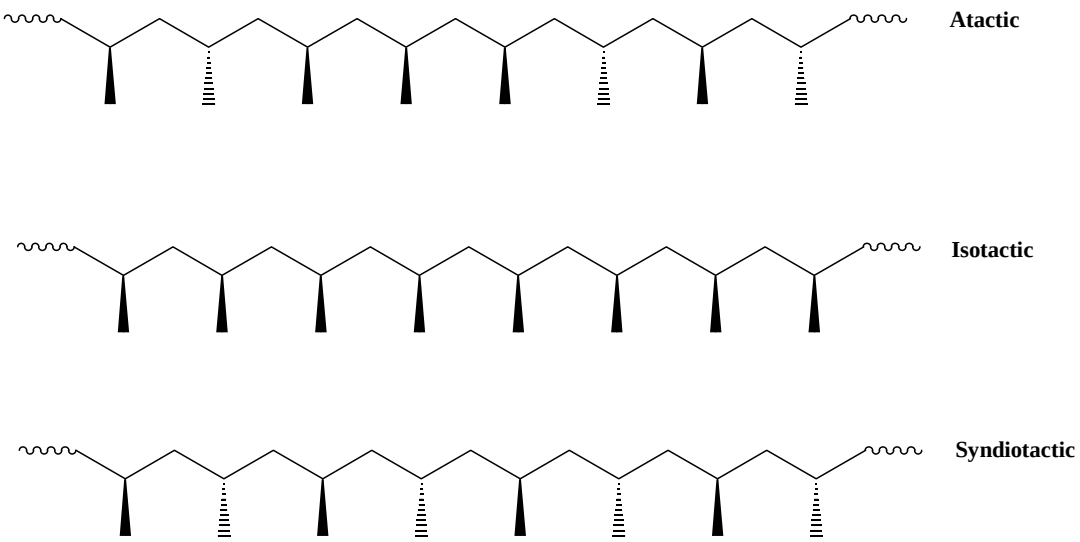

Figure 2.2: Structure of isotactic, syndiotactic and atactic polyolefins

The industrial success of polyolefins is directly linked to the development of various catalyst systems which led to either large scale industrial production or improvement of the polymer properties. The first breakthrough was due to Von Pechmann and co-

workers in 1898 when they synthesized polyethylene by accident. They termed it polymethylene since it contained long $–CH_2-$ chains[2].

Polyethylene was first synthesized industrially by Fawcett and Gibson at Imperial Chemical Industries (ICI) in 1933[3]. It polymerized accidentally when extremely high pressure was applied to a mixture of ethylene and benzaldehyde contaminated with oxygen. This process was reproduced in a high-pressure reactor by Perrin in 1935 leading to subsequent small scale industrial production of LDPE in 1939. Major industrial polyethylene syntheses which took place during the early 1950's were facilitated by discoveries of several highly active catalyst systems.

In 1951 Banks et al. synthesized polyethylene at Phillips Petroleum[3]. They used a SiO_2/CrO_3 catalyst to produce HDPE at mild temperatures and pressures compared to the ICI processes. Simultaneously, HDPE was produced at Standard Oil (Indiana) using molybdenum catalysts. Another landmark discovery for polyolefins occurred in 1952 when Karl Ziegler synthesized polyethylene under mild conditions (low pressure and temperature) using an early transition metal halide such as $TiCl_4$ or $TiCl_3$ and alkyaluminum referred to as a cocatalyst. It is believed that organometallics play an important role in such a heterogeneous catalyst[1-4].

Although Bunn predicted a helical form of crystalline polypropylene, it was Guilio Natta who first synthesized it in 1954 using a Ziegler-type system to polymerize ethylene[4]. Later in the same year Ziegler also prepared polypropylene using a

transition metal catalyst system. The achievements of these two scientists earned them a joint Nobel Prize in chemistry in 1963[1-4]. The catalyst systems discovered by both Ziegler and Natta are now referred to as Ziegler-Natta catalysts.

The industrial improvements brought about by Ziegler-Natta catalyst systems include, among others, industrial production of isotactic polypropylene and polymerization of various α-olefins. Most polyolefins are still industrially produced by Ziegler-Natta catalysts today. The discovery of these catalyst systems also saw the emergence of interface collaborative research between organometallic and polymer chemists. The knowledge of stereospecific polymerization can also be attributed to Ziegler-Natta catalyst systems.

The invention of Ziegler-Natta and Phillips catalyst systems allowed for the production of polyolefins materials with a wide variety of properties[13]. Examples of such materials include LLDPE, HDPE, isotactic polypropylenes, poly (1-butene), poly (4-methyl-1-pentene), ethylene/propylene copolymers and ethylene/propylene/diene rubbers[3].

After the discovery of Phillips, Ziegler-Natta catalysts and the subsequent industrial production of polyethylene and polypropylene, further milestones involving α-olefin synthesis, revolved around the development of catalyst systems that could improve polymer properties since the early catalyst systems, due to the heterogeneous nature

of the active sites, had difficulties in controlling the microstructures and the properties of the resulting polymer.

Increased control of polymer properties became possible with the discovery of group 4 metallocene catalysts[5]. Metallocenes as polymerization catalysts were discovered by Breslow and Newburg in the late 1950's[6]. Like Ziegler-Natta catalysts, they also consist of an organometallic component and a cocatalyst. The first metallocene catalyst systems (e.g. Cp_2TiCl_2/AlR_nCl_{3-n}) were considered as homogeneous Ziegler-Natta catalysts and they had low catalyst activities. They were merely used as models to study mechanistic details of the conventional Ziegler-Natta catalysts. However, the discovery of MAO by Kaminsky and Sinn in 1980 made the application of metallocenes as polymerization catalysts industrially possible[5-8].

MAO is now commercially available and is still widely used as a cocatalyst for metallocene catalyst systems. Its function is to activate metallocenes by alkylating the transition metal centre. The details of the mechanism for alkylaton will be explained later. Activating zirconocene with MAO results in the formation of very high active catalyst systems which produced high density polyethylene with molecular weights between 1 000 and 1 500 000 g/mol[5]. Sinn and Kaminsky were also the first to achieve the polymerization of propylene using a metallocene/MAO catalyzed system.

Although metallocenes are superior to Ziegler-Natta with respect to the control of polymer properties, they also have specific shortcomings. These include their

inability to tolerate polar monomers (as do Ziegler-Natta catalysts)[9] and to produce block copolymers[10]. A desire to overcome some of these shortcomings and to achieve greater control in polymer properties generated interest in finding other suitable catalysts. Concerted efforts were made to produce catalyst systems that are not based on cyclopentadienyl ligands. Such catalyst systems are referred to as non-metallocene or post metallocene catalyst systems[11].

Contrary to metallocene catalysts that are based on early transition metals, first post-metallocene precusors were based on late transition metals such as nickel, palladium and platinum. Nickel catalysts in particular were believed initially to effect the oligomerization of ethylene to form higher α-olefins. The first non-metallocene or post-metallocene catalyst system, based on nickel complexes with diimine ligands, which could polymerize ethylene, was discovered by Brookhart et al.[12] in 1995. They showed that when this complex was activated with MAO, it could polymerize ethylene, resulting in the formation of a highly branched and high molecular weight polyethylene. The activities of this catalyst and the molecular weight of the resulting polymers match those of metallocenes. This catalyst system generated a lot of interest into the search for new post metallocene catalysts. In 1996 McConville et al. reported titanium complexes with diamide ligands that showed high activities towards higher α-olefins[13].

Following these initial success, a number of other post-metallocene catalysts with extremely high activities have been reported[11,14]. Post-metallocenes offer a wide

range of choices with regard to both transition metal and cocatalyst. Various metals across the entire periodic table have been used with great success as will be shown in Section 2.2.3. Apart from MAO, various other types of co-catalysts such as $B(C_6F_5)_3$ and $Al(C_6F_5)_3$ are used for activation. Certain non-metallocene complexes are self-activating and require no cocatalyst for activation[15].

Post metallocenes produce polymers with very narrow molecular weight distributions and well defined properties[16]. Most of these systems control polymer properties to an even greater extent than metallocenes. Some of them are able to perform living polymerization and are, therefore, able to yield block copolymers. Successful studies of block copolymerization of ethylene and propylene with other α-olefins are known[16].

Living polymerization allows consecutive enchainment of monomer units without chain termination and thus greater control of molecular weight and polymers properties is achieved. Post metallocenes are the first catalyst systems to offer real opportunities towards block copolymers via coordination polymerization methods. Living or controlled polymerization methods have previously always been performed using anionic[17], cationic[18] or free radical methods[19-21]. Examples of materials with a wide array of architectures accessible through living polymerization methods include di- or triblock copolymers resulting from enchainment of two or three monomers, graft copolymers and star-branched polymers resulting from a central core that has the ability to initiate multiple polymer chains.

2.2 Organometallic and other coordination compounds in polyolefin catalyst systems

Coordination chemistry and organometallic chemistry in particular have played major roles in the development of various hetero- and homogeneous catalyst systems used in the synthesis of polyolefins, and new organic molecules in general. Most of the homogeneous polyolefin catalyst systems, as already mentioned, are composed of an organometallic complex and an activator. It has been demonstrated that improvements in the properties of polyolefins can be achieved by modifying the structures of these two components of a particular catalyst system[1-4,11,14,16]. The most important catalyst systems for polyolefin polymerization are now discussed as well as other organometallic complexes that are related to this study.

2.2.1 The Ziegler-Natta catalyst systems

Ziegler-Natta catalysts are heterogeneous particles which consist of two components. The first component is an early transition metal halide such as group 4-8 transition metal halide and the second main group organometallic compound normally referred to as a cocatalyst (Figure 2.3). Typical examples of cocatalysts are $Al(C_2H_5)_3$, $Al(i\text{-}C_4H_9)_3$, $Al(n\text{-}C_3H_7)_3$, $Al(C_2H_5)_2Cl$, $Al(i\text{-}C_4H_9)_2Cl$ and $Al(C_2H_5)Cl_2$. The cocatalysts help to activate the organometallic component ($TiCl_x$), thereby creating the so-called active centers or sites – where polymerization takes place. None of these components can function alone to effect polymerization. Polymerization using the Ziegler-Natta

catalysts is usually carried out in an inert hydrocarbon diluent such as hexane or heptane.

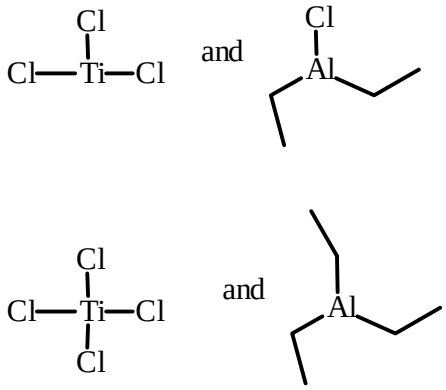

Figure 2.3: Typical Ziegler-Natta catalyst systems for α-olefin polymerization

The active sites of these catalyst systems are heterogeneous in nature and during polymerization do not all behave in the same manner. Due to the non-uniform active sites, Ziegler-Natta catalysts are normally referred to as multi-site catalyst systems. Consequently, they produce polymers with non-uniform or heterogeneous properties. Polyolefins produced with Ziegler-Natta catalysts are characterized by broad molecular weight distribution or broad short chain branching distribution (SCBD) in the case of copolymers. In the case of polypropylene, stereospecific polymerization using Ziegler-Natta catalysts could be achieved by carefully selecting a combination of a transition metal complex and a co-catalyst. The introduction of support such as $MgCl_2$ to Ziegler-Natta catalysts, in the 1970's, offered even much greater control over polymer properties and an improvement to the industrial production process in general[22,23]. The activities of the supported catalyst systems were two orders of magnitude greater than the original catalysts. The supported catalysts made a

significant breakthrough with regard to the industrial production of polyethylene and propylene. For polyethylene, the supported catalysts circumvented the need to de-ash. Furthermore, neither de-ashing nor removal of atactic-polypropylene was required during the production of polypropylene. High catalyst efficiency of the supported catalysts allows the production of very high isospecific polypropylene ([*mmmm*]>98%)[24]

2.2.2 Metallocene catalysts

Generally, metallocene catalysts are bi-components consisting of group four transition metal compounds and cocatalysts. The transition metal is usually sandwiched between two cyclopentadienyl (Cp) ligands or derivatives such as indenyl (Ind) or fluorenyl, (Flu) ligands (Figure 2.4). Since the discovery of early metallocene catalyst systems in the 1950's[5], much effort went into improving all the components of metallocene catalyst system structures, i.e modifying the Cp ligands, varying transition metals and using other types of activators. Co-catalysts such as $B(C_6F_5)_3$ or $Al(C_6F_5)_3$ have been used successfully[25].

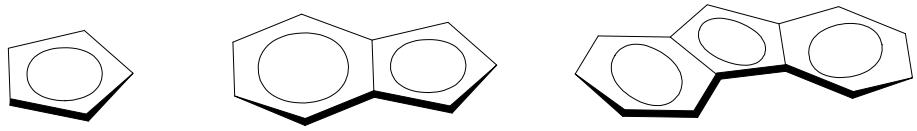

Cyclopentadienyl (Cp) Indenyl (Ind) Fluorenyl (Flu)

Figure 2.4: Typical Cp-based ligands for metallocene catalysts

Today, the metallocene catalysts (complexes **2.1** to **2.7** in Figure 2.5), by definition, include half-sandwich (complex **2.5**) or constrained geometry compounds (complex **2.6**) and bridged metallocenes (complexes **2.2** and **2.7**). As a result of such improvements of the metallocene catalysts, the polymers and copolymers produced have more uniform properties than obtained with Ziegler-Natta catalysts. Such properties of as well as different metallocene catalyst system will be discussed in more detail later in this chapter.

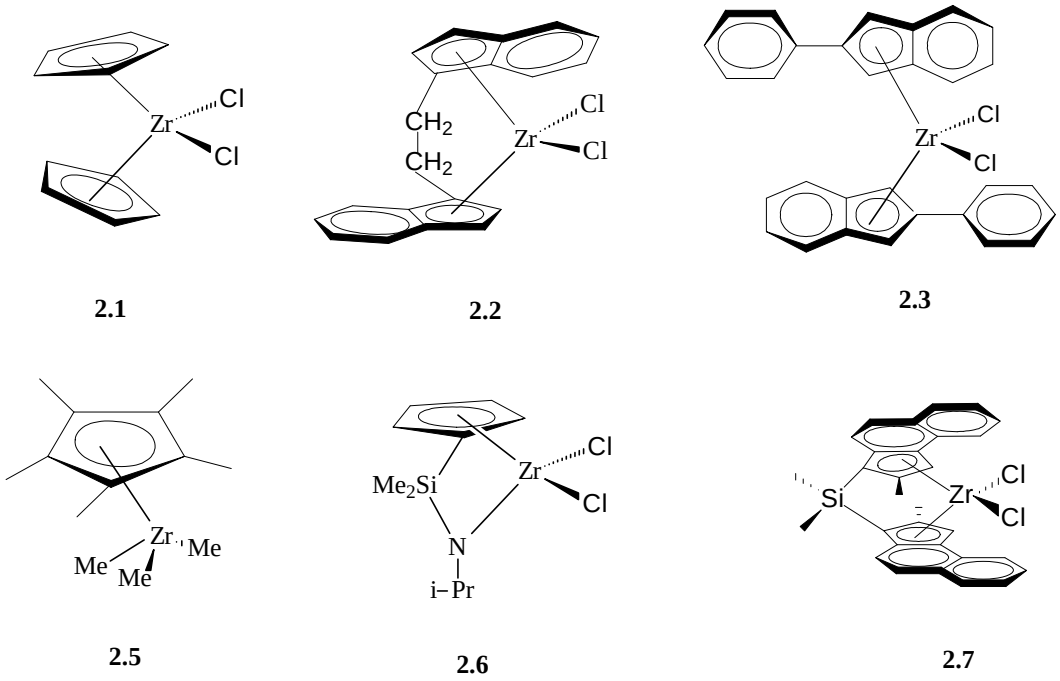

2.1 **2.2** **2.3**

2.5 **2.6** **2.7**

Figure 2.5: Examples of metallocene precursors for α-olefin polymerization

Metallocenes generally act as single-site catalysts. They produce polymers with more well defined structures i.e. uniform short chain branching distribution, controlled stereochemistry as well as narrow molecular weight distribution ($M_w/M_n \approx 2$). In addition, they are claimed to produce copolymers with uniform short chain branching

distribution. The so-called *ansa*-metallocenes or bridged metallocenes discovered by Brintzinger and coworkers (complexes **2.2** and **2.7** in Figure 2.5) offer a greater control in polymer properties than the unbridged analogues[26]. Metallocenes contributed significantly to the understanding of stereospecific polymerization of α-olefins (catalyst structure–polymer property relations). By knowing the molecular symmetry of the metallocene complex, it is now possible to predict the stereochemistry of the resultant polymers as shown by Ewen[27].

Despite very good progress made in the development of metallocene catalyst systems, complete control of molecular weight and effective polymerization of polar monomers have not been successful. Moreover, chain transfer and termination reactions associated with metallocenes prohibit the synthesis of block copolymers by sequential monomer addition as mentioned previously.

2.2.3 Non-Metallocene catalysts

Non-metallocene catalysts (complexes **2.8** to **2.13** in Figure 2.6) are single-site catalyst systems which do not contain cyclopentadienyl ligands. Examples of selected non-metallocene complexes are shown in Figure 2.6. They are also known as post-metallocene catalysts and are generally capable of performing living polymerization of α-olefins. Living polymerization techniques allow the synthesis of polymers with predictable (controlled) molecular weight and narrow molecular weight distribution ($M_w/M_n \approx 1$). In addition, living polymerization lead to the production of block

copolymers block copolymers (e.g. A-A-A-B-B-B,etc.) and end-functionalized or polar materials which would otherwise be inaccessible using conventional polymerization methods such as metallocene and Ziegler-Natta catalysts. The early non-metallocene catalyst systems could only oligomerize ethylene due to competing β-hydride elimination reactions[28,29]. However, subsequent studies showed that these catalyst systems can polymerize ethylene and propylene in a living fashion[11,16].

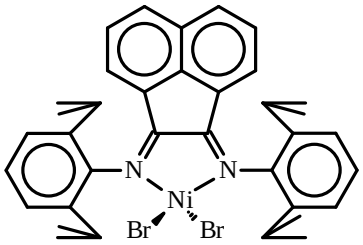

2.8

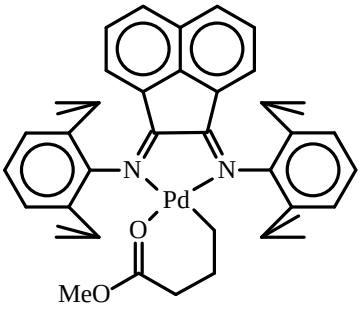

2.9

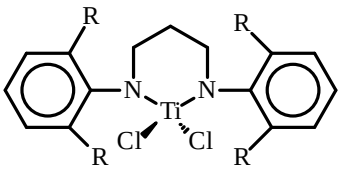

2.10 R = iPR or Me

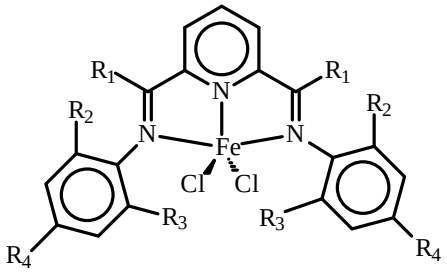

2.11

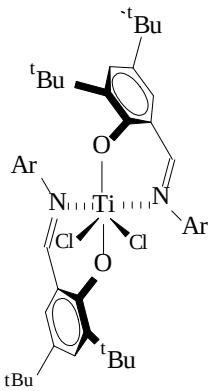

2.12 Ar = C_6H_5 or Ar = C_6F_6

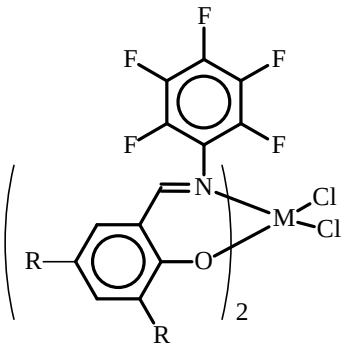

2.13

Figure 2.6: Examples of non-metallocene precursors for α-olefin polymerization

Brookhart reported that late transition metal complexes (complexes **2.8** and **2.9** in Figure 2.6) with diimine ligands were also active in the living polymerization of ethylene[30,31]. Scollard et al.[13] reported the living polymerization of α-olefins (1-hexene, 1-octene and 1-decene) using amide complexes **2.10**, $[RN(CH_2)_3NR]TiMe_2$. Coates and coworkers designed a highly syndiotactic living polymerization of propylene with high percentage syndiospecific content of 99% ([*rrrr*] = 96%) using the complex **2.12**. This catalyst could also produce syndiotactic poly(propylene)-block-poly(ethylene-co-propylene)[16]. Recently Fujita's group reported highly active phenoxy imine (complex **2.13** in Figure 2.6) catalyst systems based on early transition metals (Ti and Zr) and MAO. They showed that these systems afford polyethylene with high molecular weight and very narrow M_w/M_n at room temperature. Other polymeric materials produced with these catalysts include highly syndiotactic polypropylene in a living manner and subsequent block copolymer formation of ethylene and propylene.

Non-metallocene systems have been shown to also effect living polymerization when activated with tris(perfluorophenyl)boron instead of MAO[11-13,16].

2.2.4 Fischer-type carbene complexes

In 1964 Fischer and Maasböl prepared the first isolable metal carbene complexes[32]. Since their discovery, a large number of Fischer-type carbene complexes and other

carbene complexes in general have been made[33-41]. In the present study (Chapter 3) we describe new anionic Fischer-type carbene complexes and how they behave in α-olefin polymerization. The general structure or formula of an anionic Fischer carbene complex is shown in Figure 2.7. Such complexes are readily formed from the reaction between a group 6 transition metal hexacarbonyl and an alkyllithium reagent, followed by alkylation. Recently a number of reviews on carbene complexes and their applications in organic synthesis and catalysis have appeared[42-45].

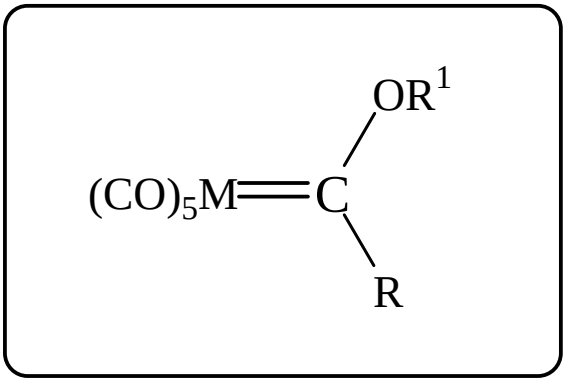

Figure 2.7: General structure of a group 6 metal Fischer carbene complexes

It is noteworthy that carbene complexes play a particularly important role in the synthesis of organic molecules via metathesis reactions. Although catalyzed metathesis reactions had already been discovered in the 1950's by Ziegler during ethylene polymerization, their mechanism was not properly understood. It is Chauvin who proposed the first correct mechanism for metathesis in 1971. After Chauvin's proposal, numerous attempts were made to design catalysts which could effect metathesis[46]. Major breakthroughs were made in the 1990's by Schrock and Grubbs who respectively prepared very reactive molybdenum (Figure 2.8) and ruthenium

carbene (Figure 2.9) catalysts for metathesis[47-51]. The Nobel Prize in Chemistry for 2005 was awarded to Chauvin, Schrock and Grubbs for these achievements.

Our laboratory has been active in using both anionic and neutral Fischer-type[52,53] as well as other classes of carbene complexes in general[54-60]. We are not aware of any study involving the use of anionic carbene complexes as potential catalyst systems earlier, except by us[58]. It is one of the main aims of the present study to explore the potential of these complexes as catalyst systems for α-olefin polymerization.

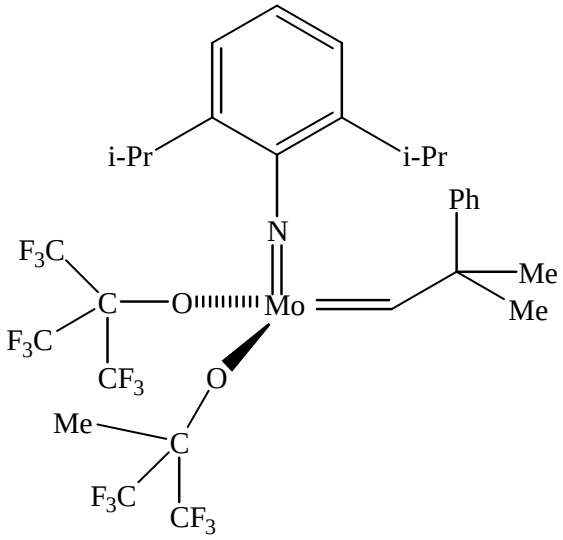

Figure 2.8: Molybdenum catalyst developed by Schrock

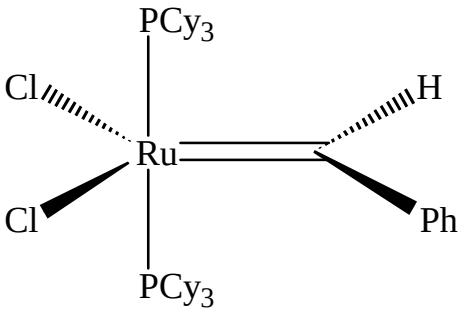

Figure 2.9: Ruthenium catalyst developed by Grubbs

2.3 Polymerization and termination mechanisms

2.3.1 The formation of the active center for polymerization

The structure of the active centers in metallocene and non-metallocene halide compounds activated with MAO are ion pairs consisting of cationic species Cp_2MR^{+}[61,62]. These species are formed during the reaction between metallocenes or related complexes of the type L_2MCl_2 (where L = ligand e.g. Cp, indenyl, etc.) and MAO. The working mechanism illustrating the formation of the Cp_2MR^{+} active species during the reaction between zirconocene and MAO is shown in Scheme 2.1.

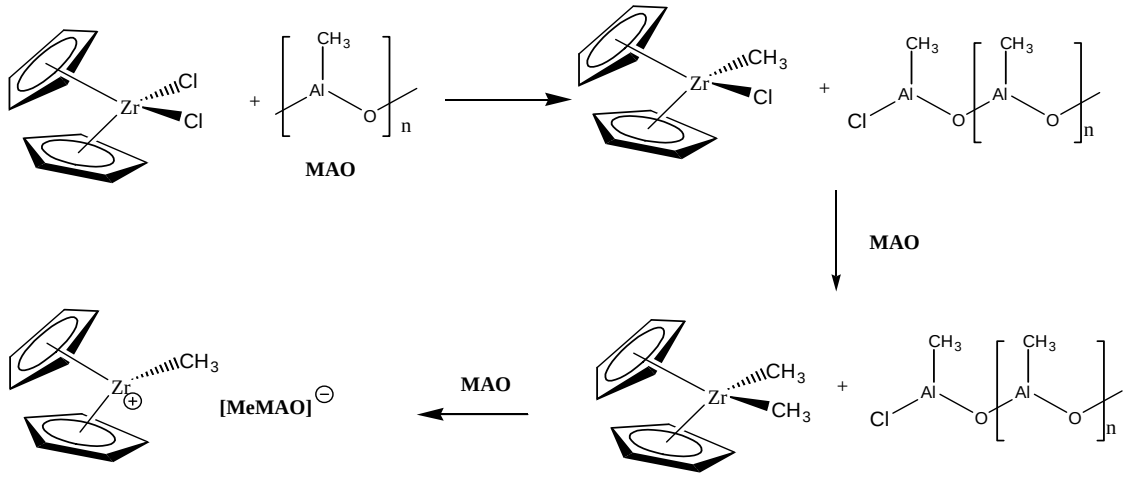

Scheme 2.1: Formation of the first active cationic species during olefin polymerization

As shown in Scheme 2.1, the primary function of MAO is to activate the metallocene catalyst precursor by alkylating the transition metal. Furthermore, MAO enhances the

formation of cationic metallocenes by reaccepting the methyl group. In this manner an anionic counterion is produced that interacts only weakly with the active catalyst cationic unit. It is also believed that a large excess number of moles of MAO compared to catalyst precursor is needed to increase the number of the active cationic metallocene species as well as to remove or complex any impurities present in the reactor. It should be mentioned in passing that the function of MAO is not precisely known.

As mentioned before, other cocatalysts such as tetraphenylborate $(C_6H_5)_4B^-$, carborane ($C_2H_9H_{12}^-$) or fluorinated borate can also be used as a counterion to the cationic catalytic centre [5,63-65]. The main advantage of borate cocatalysts is that they are more economical with a ratio of 1:1 of borate to metallocene. The disadvantage of using borate cocatalysts is that they are very sensitive to poisons, decompose easily and must be stabilized by addition of aluminiumalkyls such as tri-isobutylaluminium[66-68]

2.3.2 Initiation, propagation and termination steps

The polymerization starts when an α-olefin monomer inserts into the M^+-R bond. The reaction is very fast and as a result, the mechanistic details of this initiation step are not readily available. However, it is assumed that the reaction usually proceeds in two steps, coordination of the olefin molecule at the positively charged metal atom

followed by the insertion step itself[69]. The polymerization mechanism applicable in this study is

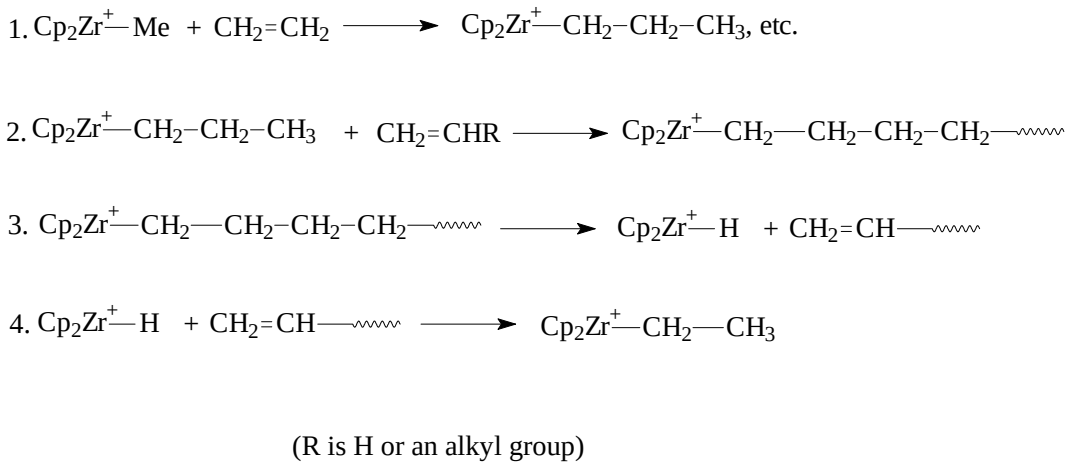

(R is H or an alkyl group)

Scheme 2.2: Initiation for coordination (1) and propagation (2), termination and active center regeneration, steps (3) and (4)

Chain initiation involves the insertion of an olefin into the Zr^+-Me bond (Step 1) while propagation (Step 2) takes place as a result of repetition of Step 1 in Scheme 2.2 i.e a large number of consecutive α-olefin insertion reactions. The polymerization reaction is terminated by a β-hydride elimination (Step 3) and followed by regeneration of a new hydride active species (Step 4). Chain termination reactions may result in the formation of various kinds of vinyl endgroups as shown in Scheme 2.3. Scheme 2.3 shows possible termination mechanisms and the resulting endgroups of propylene monomer. As shown, the chain propagation occurring via 1,2-insertion followed by β-hydride elimination yields to vinylidene endgroups. On the other hand, if the last monomer is misinserted (2,1 misinsertion) and then followed by β-hydride

elimination, the resulting endgroup is a 1,2-disubstituted alkene. Chain migration always leads to the formation of 1,1,2-trisubstituted endgroups. The typical endgroups during coordination homopolymerization of ethylene are vinyl since ethylene is symmetrical. However, during copolymerization of ethylene with other α-olefins, e.g. 1-pentene, 1,2-disubstituted endgroups are formed if the last monomer inserted is 1-pentene followed by β-hydride elimination.

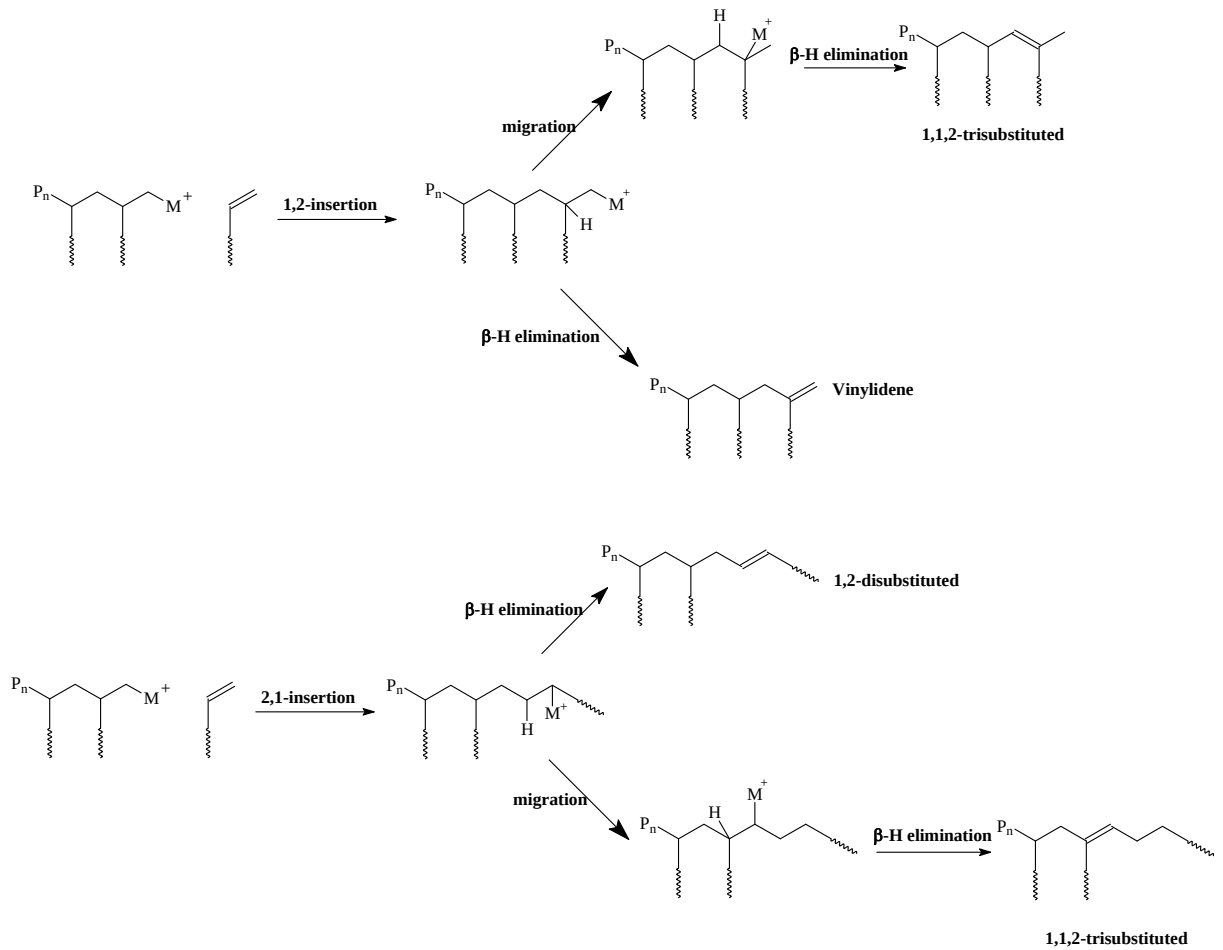

Scheme 2.3: Different termination mechanisms and the resulting endgroups

2.4 Polymer properties and characterization techniques

2.4.1 Molecular weight distributions

The chains resulting from the polymerization process are not identical either in terms of the size of polymer chain or its composition in the case of a copolymer. The molecular weight of a given polymer is represented by mean values such as number-average molecular weight (M_n) and weighted-average molecular weight (M_w). Analytical techniques for the absolute determination of these values are light scattering and osmometry while size exclusion chromatography (SEC), also referred to as gel permeation chromatography (GPC), gives relative values as it depends on the hydrodynamic size of the molecules in solution. For polyolefins, high temperature SEC, i.e. HT-SEC is needed since these polymers are semi-crystalline materials.

2.4.2 Chemical structure and microstructures

Chemical structure and different functional groups within the polymer chains can be fairly accurately characterized by nuclear magnetic resonance (NMR) and infrared (IR) studies. Of these, NMR yields more information than IR. ^{13}C and ^{1}H-NMR provide information about regularity, comonomer content as well as sequence and endgroups. Information about the mechanism of polymerization can also sometimes be deduced from such NMR data.

2.4.3 Chemical composition distribution

In addition to molecular weight distribution, copolymers possess chemical composition distribution (CCD) (also known as short chain branching distribution (SCBD). Temperature rising elution fractionation (TREF) has been used to study the CCD of polymers[70,71]. The drawback of TREF is long analysis time (one sample per day). However, recent advances in TREF technology have managed to reduce analysis time significantly as will be shown in Chapter 5[71]. Crystallization analysis fractionation (CRYSTAF), which is a relatively new technique compared to TREF, has also been used extensively to study SCBD[72]. CRYSTAF has short analysis time (five samples in about 6h). Recently, the coupling of SEC and Fourier transform infrared (FTIR) spectroscopy has enabled polymer chemists to study SCBD along the molecular weight axis in a very short analysis time using small sample weights. The principles surrounding CRYSTAF and SEC-FTIR are explained in more detail in Chapter 4.

2.4.4 Thermal and mechanical properties

Thermal transitions such as glass transition temperature (T_g), crystallization and melting temperatures can be studied using differential scanning calorimetry (DSC) while information about thermal stability of a polymer can be obtained using thermogravimetric analysis (TGA). Dynamic mechanical analysis (DMA) and dielectric analysis (DEA) measure changes in mechanical behaviour such as modulus

and damping as a function of temperature, time, frequency, stress or a combination of these parameters. In addition, linear or volumetric changes in dimensions of a sample as a function of force and temperature can be obtained from thermomechanical analysis (TMA). The most common thermal analysis techniques are DSC and TGA. In this study both conventional and a special type of DSC which is known as High performance DSc (HPer DSC) is used to study the thermal properties of ethylene/1-pentene along the molecular weight axis[73-76]. Details of HPer DSC are discussed in Chapter 5.

2.5 References

1. Mülhaupt, R. *Macromol. Chem. Phys.* **2003**, 204, 289.

2. Krentsel, B. A.; Kissin, Y. V.; Kleiner, V. J.; Stotskaya, L. L. in *Polymers and Copolymers of Higher α-Olefins*, Carl Hansa Verlag, Munich, **1997**, p. 109.

3. Mülhaupt, R. *Novel polyolefin materials and processes: Overview and prospects* in *Ziegler Catalysts*, Eds, Fink, G.; Mülhaupt, R.; Brintzinger, H. H. Springer-Verlag Berlin, **1995**, p. 35.

4. Moore, E. P, Jr. *Polypropylene Handbook*, Ed, Moore, E. P, Jr, Carl Hanser Verlag, Munich **1996**, Chapter 1.

5. Kaminsky, W.; Arndt, M. *Adv.Polym. Sci.* **1997**, 127, 143.

6. Breslow, D. S.; Newburg, N. R. *J. Am. Chem. Soc.* **1957**, 79, 5072.

7. Natta, G.; Pinno, P.; Mazzanti, G.; Giannini, U.; Montica, E.; Peralto, M. *J. Polym. Sci.* **1957**, 26, 120.

8. Sinn, H.; Kaminsky, W. *Adv. Organomet. Chem.* **1980**, 18, 99.

9. Mecking, S.; Johnson, L. K.; Wang, L.; Brookhart, M. *J. Am. Chem. Soc.* **1998**, 120, 888.

10. Tian, J.; Hustad, P. D.; Coates, G. W. *J. Am. Chem. Soc.* **2001**, 123, 5134.

11. Gibson, V. C.; Spitzmesser, S. K. *Chem. Rev.* **2003**, 103, 283.

12. Johnson, L. K.; Killian, C. M.; Brookhart, M. *J. Am. Chem. Soc.* **1995**, 117, 6414.

13. Scollard, J. D.; McConville, D. H. *J. Am. Chem. Soc.* **1996**, 118, 10008.

14. Ittel, S. D.; Johnson, L. K. *Chem. Rev.* **2000**. 100, 1169.

15. Jenkins, J. C.; Brookhart, M. *Organometallics* **2003**, 22, 250.

16. Coates, G. W.; Hustad, P. D.; Reinartz, S. *Angew. Chem. Int. Ed. Engl.* **2002**, 41, 2236.

17. *Anionic Polymerization:Principles and Practical Applications* (Ed's.: Hsieh, L.; Quirk, R. P.),Marcel Dekker,New York, **1996** .

18. *Cationic Polymerizations:Mechanisms,Synthesis, and Applications* , (Ed.:K. Matyjaszewski), Marcel Dekker, New York, **1996** .

19. Hawker, C. J.; Bosman, A.W.; Harth, E. *Chem. Rev.* **2001**, 101, 3661.

20. Kamigaito, M.; Ando, T.; Sawamoto, M. *Chem. Rev.* **2001**, 101, 3689.

21. Matyjaszewski, K.; Xia, J. H. *Chem. Rev.* **2001**, 101, 2921.

22. Kashiwa, T.; Tokumizu, T.; Fujimura, H. *Chem. Abstr*. **1970**, 72, 101227.

23. Bajgur, C. S.; Sivaram, S. Current Science, **2000**, 78, 1325.

24. Makio, H.; Kashiwa, N.; Fujita, T. *Adv. Synth. Catal.* **2002**, 344, 477.

25. Chen, E. Y.; Marks, T. J. *Chem. Rev.* **2000**. 100, 1391.

26. Wild, F. R. W. P.; Wasincionek, M.; Huttener, G.; Brintzinger, H. H. *J. Organomet. Chem.* **1985**, 288, 63.

27. Ewen, J. A.; Jones, R. L.; Razavi, A.; Ferrara, J. P. *J. Am. Chem. Soc.* **1988**, 110, 6255.

28. Peuckert, M.; Keim, W. *Organometallics* **1983,** 2, 594.

29. Rix, F.; Brookhart, M. *J. Am. Chem. Soc.* **1995,** 217**,** 1137.

30. Gottfried, A. C.; Brookhart, M. *Macromolecules* **2001**, 34, 1140.

31. McCord, E. F.; McLain, S. J.; Nelson, L. T. J.; Urther, S. D.; Coughlin, E. B; Ittel, S. D.; Johnson, L. K.; Tempel, D.; Killian, C. M.; Brookhart, M. *Macromolecules* **2001**, 34, 362.

32. Fischer, E. O.; Maasböl, A. *Ange*w. *Chem*., *Int. Ed*. *Engl.* **196**4, 3, 580.

33. Erker, G.; Dorf, U.; Lecht, R.; Ashby, M.T.; Aulbach, M.; Schlund, R.; Kruger, C.; Mynott, R. *Organometallics* **1989**, 8, 2037.

34. Erker, G.; Pfaff, R.; Kruger, C.; Werner, S. *Organometallics* **1991**, 10, 3559.

35. Sabat, M.; Gross, M. F.; Finn, M.G. *Organometallics* **1992**, 11, 745.

36. Hegedus, L. S. *Tetrahedron* **1997**, 53, 4105.

37. Rawat, M.; Wulff, W. *Org. Lett.* **2004**, 6, 329.

38. Dötz, K. H. *Angew. Chem. Int. Ed. Engl.* **1975**, 14, 644.

39. Bos, M. E.; Wulff, W. D.; Miller, R. A.; Chamberlin, S.; Brandvold, T. A. *J. Am. Chem. Soc.* **1993**, 115, 10671.

40. Dötz, K. H.; Pruskil, I.; Mühlemeier, J. *J. Chem. Ber.* **1982**, 115, 1278.

41. Wu, Y.T.; Kurahashi, T.; de Meijere, A. *J. Org. Chem.* **2005**, 690, 5900.

42. Barluenga, J.; Fernández-Rodríguez, M. A.; Aguilar, E. *J. Org. Chem.* **2005**, 690, 539.

43. Barluenga, J.; Santamaría, J.; Tomás, M. *Chem. Rev.* **2004**, 104, 2259.

44. Herndon, J. W. *Tetrahedron*, **2000**, 56, 1257.

45. Barluenga, J.; Fañanás, F. J. *Tetrahedron*, **2000**, 56, 4597.

46. Hérisson, J.-L.; Chauvin, Y. *Macromol. Chem*., **1971**, 141, 161.

47 Schrock, R. R.; Murdzek, J. S.; Barzan, G. C.; Robbins, J.; DiMare, M.; O`Regan, M. *J. Am. Chem. Soc*., **1990**, 112, 3875.

48 Bazan, C. G.; Oskam, J. H.; Cho, H. -N.; Park. L. Y.; Schrock, R. R. *J. Am. Chem. Soc.* **1991**,113, 6899.

49 Nguyen, S. T.; Johnsson, L. K.; Grubbs, R. H.; Ziller, J. W. *J. Am. Chem. Soc*., **1992**, 114, 3974.

50 Wu, Z.; Nguyen, S.T.; Grubbs, R. H.; Ziller, J.W. *J. Am. Chem. Soc*., **1995**.117, 5503.

51. Nguyen, S.T.; Grubbs, R. H.; Ziller, J. W. *J. Am. Chem. Soc*., **1993**,115, 9858.

52. Neveling A. *MSc Thesis*, University of Stellenbosch, Stellenbosch, South Africa. **1999**.

53. Nel J. *MSc Thesis*, University of Stellenbosch, Stellenbosch, South Africa. **2002**.

54 Raubenheimer, H. G.; Kruger, G. J.; Lombard, A.; Linford, L.; Viljoen, J. C. *Organometallics* **1985,** 4, 275.

55. Raubenheimer, H. G.; Cronje, S. *J. Organomet. Chem.* **2001**, 617-618, 170.

56. Raubenheimer, H. G.; Esterhuysen, M. W.; Timoshkin, A.; Chen, Y.; Frenking, G. *Organometallics* **2002,** 21, 3173.

57. Raubenheimer, H. G.; Du Toit, A.; Du Toit, M.; Jin, A.; Van Niekerk, L.; Cronje, S.; Esterhuysen, C.; Crouch, A. M. *Dalton Trans.* **2004**, 8, 1173.

58. Luruli, N.; Grumel, V.; Brüll, R.; Du Toit, A.; Pasch, H.; van Reenen, A. J; Raubenheimer, H. G. *J. Polym. Sci. Part A: Polym. Chem.* **2004**, 42, 5121.

59. Raubenheimer, H. G.; Stander, Y.; Marais, E. K.; Thompson, C.; Kruger, G. J.; Cronje, S.; Deetlefs, M. *J. Organomet. Chem.* **1999**, 590, 158.

60. Cronje, S.; Julius, G. R.; Stander, E.; Esterhuysen, C.; Raubenheimer, H. G. *Inorg. Chim. Acta*. **2005**, 358, 1581.

61. Tritto, I.; Li, S.X.; Sacchi, M. C.; Locatelli, P.; Zannoni, G. *Macromolecules* **1995**, 28, 5358.

62. Shishta, C.; Hathorn, R. M.; Marks, T. J. *J. Am. Chem. Soc.* **1992**, 114, 1112.

63. Hlatky, G. G.; Upton, D. J.; Tuner, H. W. *Chem. Abstr.* **1991**, 115, 256897v.

64. Yang, X.; Stern, C. L.; Marks, T. J. *Organometallics* **1991**, 10, 840.

65. Zambelli, A.; Grassi, A.; Luongo, P. *Macromolecules* **1989**, 22, 2186.

66. Chien, J. C. W.; Tsai, W. M.; Rausch, M. D. *J. Am. Chem. Soc.* **1991**, 113, 8570.

67. Bochmann M.; Lancaster, S. J. *Organometallics* **1993**, 12, 633.

68. Bochmann M.; Lancaster, S. J. *Angew. Chem. Int. Ed. Engl.* **1994**, 33, 1634.

69. Krentsel, B. A.; Kissin, Y.V.; Kleiner, V. I.; Stotskaya, L.L. *Polymers and copolymers of higher a-olefins*, Chapter 1, page 14 and Chapter 8, page 292.

70. Soares, J. B. P.; Hamielec, A. E. *Polymer*, **1995**, 36, 1639.

71. Monrabal, B.; *Temperature rising elution fractionation and crystallization analysis fractionation*. In *Encyclopedia of Analytical Chemistry*, Ed, Mayers, R.A. **2000**, 14, page 1-20.

72. Monrabal, B. *J. Appl. Polym. Sci.* **1994**, 52, 491.

73. Mathot, V. B. F. *J. Therm. Anal. Cal.* **2001**, 64, 15.

74. Pijpers, M. F. J.; Mathot, V. B. F.; Goderis, B.; Scherrenberg, R.; van der Vegte, E. *Macromolecules* **2002**, 35, 3601.

75. McGregor, C.; Saunders, H. M.; Buckton, G.; Saklatvala, R. D. *Thermochim. Acta* **2004**, 417, 231.

76. Abdulkarim, S. M, Long, K.; Lai, O. M.; Muhammad, S. K. S.; Ghazali, H. M. *Food Chemistry* **2005**, 93, 253.

3 Synthesis of metalloxycarbene complexes and their use in α-olefin polymerization*

* Based on: Luruli, N.; Stander, E.; Esterhuysen, C.; du Toit, A.; Neveling, A.; Nel, J.; Grumel, V.; Brüll, R.; Pasch, P.; van Reenen, A. J.; Raubenheimer, H. G. *J. Mol. Catal*. **2005**, to be submitted.

ABSTRACT

Metalloxycarbene complexes were synthesized by reacting an anionic Fischer-type carbene complex with zirconocene - or hafnocene dichloride. The molecular and crystal structures of selected metalloxycarbene complexes were determined by X-ray methods. The complex $[(CO)_5W=C(Me)OZr(Cp)_2Cl]$ has short $C_{carbene}$-O and relatively long O-Zr separations. Other complexes whose structures were determined using X-ray diffraction are $[(CO)_5Cr=C(Me)OZr(Cp)_2Cl]$ and $[(CO)_5W=C(Ph)OHf(Cp_2)Cl]$. When metalloxycarbene complexes were activated with MAO, oligomers of 1-pentene and polyethylene with polydispersity indices (PDI's) ranging from 6 to 15 were obtained. Polyethylene synthesized with some of these catalyst precursors showed small amounts of branching as determined by ^{13}C NMR and CRYSTAF.

3.1 INTRODUCTION

Metallocenes, when activated with MAO, are well known to produce polyolefins with narrow molecular weight distribution and controlled stereoregularity that could not be achieved using Ziegler-Natta catalysts. Despite these advantages, metallocene catalyst systems have limitations. Such limitations include the inability to tolerance towards functionalized monomers and polar solvents. Furthermore, polymers with narrow molecular weight distributions cause problems during processing because of their high shear viscosity and low melt flow index.[1,2] In view of this, development of new catalyst systems for both homo- and copolymerization remains important in the context of polymer design. Many authors have shown that catalyst activity and selectivity can be altered significantly by changing the coordination site or modifying the ligand structure-type or its configuration. The relationship between catalyst structure, polymerization behaviour and polymer properties has been extensively investigated and excellent reviews have appeared recently[3]. In this chapter we discuss the synthesis of metallocene derivatives that contain anionic carbene complexes as well as their use as catalyst precursors in the oligomerization and polymerization of α-olefins.

While polyethylene and polypropylene have many commercial applications, oligomers and homo-polymers of higher α-olefins ($>C_4$) are still of less commercial importance. Some of the applications of polyethylene and polypropylene as well as homopolymers of higher α-olefins have been highlighted in the previous chapter.

We have indicated in Chapter 2 that we have been investigating on anionic Fischer carbene complexes of the type $[(CO)_nM^1=C(R)OM^2L_n]$. These are complexes with the Fischer-type carbene complex bonded to a second organometallic unit, M^2L_n, through the carbene oxygen atom. These complexes with M^2 = Cp_2ZrCl, i.e. containing a metallocene, are referred to as metalloxycarbenes. When such metalloxycarbenes are activated with MAO, they oligomerize of 1-pentene. We further indicated that the metalloxycarbene complex, $[(CO)_5W=C(Me)OZr(Cp_2)Cl]$, in the presence of MAO shows much higher catalytic activity for the oligomerization 1-pentene than the related compounds Cp_2ZrCl_2 and $Cp_2Zr(Cl)OMe$[4]. This shows a huge potential in metalloxycarbene complexes as catalysts for olefin polymerization.

Although a large variety of metalloxycarbene complexes are known[5-7], no member of the zirconoxycarbene family mentioned above, has been investigated by X-ray diffraction or used in homogeneous catalysis. We describe here the preparation of the metalloxycarbene complexes of tungsten and chromium involving zirconocene and hafnocene as the second metal centre and their characterization by single crystal X-ray diffraction. Furthermore, first polymerization results of ethylene and of 1-pentene oligomerization utilizing selected metalloxycarbene complexes as catalyst precursors, are presented. Finally, the thermal properties of the polymers, measured by differential scanning calorimetry (DSC) and crystallization analysis fractionation (CRYSTAF) [8,9] are discussed.

3.2 EXPERIMENTAL

3.2.1 Materials

All materials used for the preparation of metalloxycarbenes were supplied by SIGMA-Aldrich. Polymerization grade ethylene was purchased from Fedgas. The preparation of the carbene complexes were performed under an inert atmosphere with standard vacuum and Schlenk tube techniques[10]. All the glassware used for the preparations of metalloxycarbenes were dried at 110ºC and cooled down under vacuum before it was used. All the solvents were dried by distilling in sodium metals under argon.

1-Pentene, obtained from SASOL, was dried by refluxing over $LiAlH_4$, distilled and then stored under nitrogen. Methylaluminoxane (10% w/v solution in toluene) and toluene was purchased from SIGMA-Aldrich and used as received. Toluene was dried by refluxing over sodium/benzophenone and distilled under inert atmosphere.

3.2.2 The synthesis of metalloxycarbenes

3.2.2.1 General synthetic procedures

The metalloxycarbene complexes were prepared according to experimental procedures illustrated in Scheme 3.1. The first step involves the attack on the electrophilic carbon of the metal carbonyl unit with methyllithium using diethyl ether as solvent. Route A shows that the lithium carbene complex was first converted to a tetraethyl ammonium carbene complexes salt.

The addition of $AgBF_4$ to a mixture of the ammonium salt, $[(CO)_5M^1{=}O(R)][NEt_4]$ (M^1 = Cr, W) and Cp_2ZrCl_2 in CH_2Cl_2 facilitated the removal of a chloride from the metallocene centre and subsequent formation of the Zr-O bond. By-products of this reaction are AgCl and $[Et_4N]BF_4$ precipitates that can be removed by filtration. Concentration and subsequent layering with pentane afforded crystals of $[(CO)_5M^1{=}O(R)Zr(Cp_2)Cl]$ (M^1 = Cr , W). Route A furnished better yields of the product than Route B. Usually the unreacted hexacarbonyl should be removed using column chromatography. However, the complete removal of unreacted metal hexacarbonyl in this study was not feasible because these complexes decompose on a silica-gel-column.

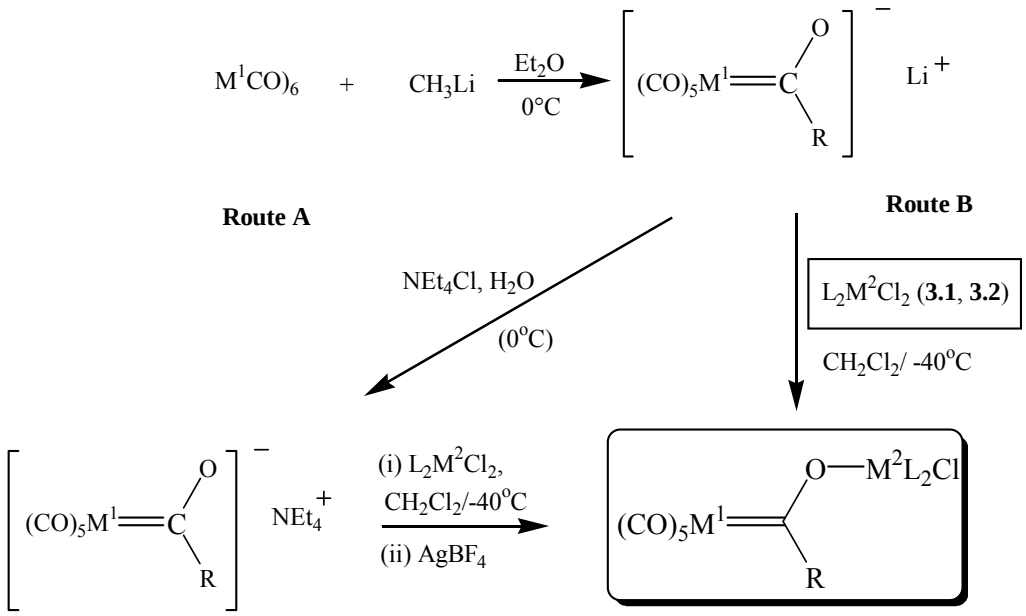

3.3. M^1 = W, R = Me, M^2 = Zr, L=Cp
3.4. M^1 = W, R = Me, M^2 = Zr, L=Cp*

3.5. M^1 = Cr, R = Me, M^2 = Zr, L=Cp
3.6. M^1 = Cr, R = Me, M^2 = Zr, L=Cp*
3.7. M^1 = W, R = Ph, M^2 = Hf, L=Cp

Scheme 3.1: General reaction scheme for the preparation of complex **3.3** to **3.7** using **3.1** and **3.2**

3.2.2.2 Synthesis of the carbene complex ligand, $[(CO)_5W=C(Me)O][NEt_4]$

The procedure followed for the synthesis of the $[(CO)_5W=C(Me)O][NEt_4]$ carbene ligand was based on that of Mayer[11]. In a two-neck round bottomed 250 ml flask with nitrogen inlet, methyl lithium (9.0 ml, 12.4 mmol, 1.4 M) in 50 ml diethyl ether was added (over a period of 60 minutes) to a well-stirred suspension of 4.0 g (11.3 mmol)

of $W(CO)_6$ by means of a dropping funnel. During the addition of the base, the colour of the solution changed to yellow. After the addition of the methyl lithium was complete, the solution was stirred for an additional 60 minutes followed by the removal of the solvent *in vacuo.* The residue was dissolved in 100 ml deoxygenated cold (4 ºC) water saturated with nitrogen and filtered over Celite to remove unreacted $W(CO)_6$. A solution of Et_4NCl (3.7 g, 22.5 mmol), dissolved in chilled water pre-saturated with nitrogen, was added to the filtrate. A light yellow precipitate immediately formed. The solution was stirred for 30 minutes and filtered. The product was dissolved in CH_2Cl_2 and dried by filtration over $MgSO_4$. The solvent was removed *in vacuo* to give 6.0 g, (85 %) of the yellow, microcrystalline material, $[(CO)_5W{=}C(Me)O][NEt_4]$.

*3.2.2.3 Synthesis of the metalloxycarbene complex, [(CO)5W=C(Me)OZr(Cp2)Cl] (**3.3**)*

In a two-neck, round-bottomed 250 ml flask equipped with a nitrogen inlet and a pressure equalizing funnel, a solution of crystalline Cp_2ZrCl_2 (1.7 g, 5.9 mmol) in 60 ml CH_2Cl_2 was stirred at -40 ºC. To this solution was added the ammonium salt of the acyl complex, $[(CO)_5W{=}C(Me)O][NEt_4]$ (3.0 g, 6.0 mmol), dissolved in 30 ml CH_2Cl_2. The resulting reaction mixture was stirred for 80 minutes at -40ºC after which, $AgBF_4$ (1.2 g, 6.0 mmol) was added. The solution was stirred for an additional 60 minutes at -40 ºC and then allowed to reach room temperature after which it was evaporated to dryness *in vacuo*. The precipitate was extracted 10 times with 20 ml

toluene and filtered through $MgSO_4$. The solution was concentrated under vacuum, layered with pentane and then cooled to -15ºC to afford yellow crystals of $[(CO)_5W=C(Me)OZr(Cp_2)Cl]$ (**3.3**).

Yield 2.1 g (57%). Mp ≈140 ºC - 143 ºC (decompose) ^{1}H NMR (δ, acetone-d_6): 6.4, 6.6, 6.7 [s, Cp, 10H]; 2.8, 2.9, 2.9 [br, CH_3, 3H]. ^{13}C {H} NMR (δ, acetone-d_6): 340.8 [$C_{carbene}$]; 199.5 [CO_{trans}]; 192.3 [t, J_{W-C} 63.2 Hz, CO_{cis}]; 117.1, 116.62, 115.0 [Cp]; 56.4 [CH_3]. IR (cm^{-1}, ATR, ν_{CO}): 2059.7; 1926.6; 1880.6. IR (cm^{-1}, CH_2Cl_2, ν_{CO}): 2063.6; 1930.5. MS (FAB) *m/z*: 623 $[M]^+$; 595 $[M\text{-}CO]^+$; 567 $[M\text{-}2CO]^+$; 558 $[M\text{-}Cp]^+$; 539 $[M\text{-}3CO]^+$; 511 $[M\text{-}4CO]^+$; 493 $[M\text{-}2Cp]^+$; 483 $[M\text{-}5CO]^+$; 446 $[(CO)W=C(Me)OZrCpCl]^+$; 255 $[(CO)W=C(Me)O]^+$; 256 $[Cp_2ZrCl]^+$.

*3.2.2.4 Synthesis of the metalloxycarbene complex, $[(CO)_5W=C(Me)OZr(Cp^*_2)Cl]$ (**3.4**)*

The synthetic procedure for complex **3.4** is similar to that of complex **4.3**. However, $ZrCp_2Cl_2$ (0.4 g, 1.2 mmol); $[(CO)_5W=C(Me)O][NEt_4]$ (0.6 g, 1.2 mmol)] and $AgBF_4$ (0.2 g, 1.2 mmol).

Yield 0.429 g (63 %). Mp ≈ 239.1 – 240.4 °C (decomposition) ^{1}H NMR (δ, $CDCl_3$) 2.7 (s, 3H, CH_3); 2.0 (m, 30H, Cp*). ^{13}C {H} NMR (δ, $CDCl_3$): 336.9 [$C_{carbene}$); 199.6 [CO_{cis}]; 198.8 [CO_{trans}]; 123.6 [Cp*]; 55.6 [CH_3]; 12.0 [Cp* ($10CH_3$)]. IR (cm^{-1}, CH_2Cl_2, ν_{CO}): 2060 (C=O); 1922 (C=O). MS (EI) *m/z*: 764 $[M]^+$; 736 $[M\text{-}CO]^+$; 708

$[M\text{-}2CO]^+$; 680 $[M\text{-}3CO]^+$; 652 $[M\text{-}4CO]^+$; 624 $[M\text{-}5CO]^+$; 489 $[M\text{-}5CO\text{-}Cp^*]^+$; 454 $[M\text{-}5CO\text{-}Cp^*\text{-}Cl]^+$; 432 $[Cp^*_2ZrCl_2]^+$; 395 $[Cp^*_2ZrCl]^+$; 295 $[Cp^*ZrCl_2]^+$; 255 $[(CO)W{=}C(Me)O]^+$ and/or $[Cp^*ZrCl]^+$; 136 $[Cp^*]^+$.

3.2.2.5 Synthesis of the carbene complex ligand, $[(CO)_5Cr{=}C(Me)O][NEt_4]$

The same procedure described for the preparation of complex **3.3** was followed. Methyl lithium (8.0 ml, 11.0 mmol, 1.4 M) in 50 ml diethyl ether, 2.2 g (10.0 mmol) $Cr(CO)_6$ and 3.7 g (22.5 mmol) Et_4NCl were used to yield 2.8 g (73%) of the yellow microcrystalline material, $[(CO)_5Cr{=}C(Me)O][NEt_4]$.

*3.2.2.6 Synthesis of the carbene complex, $[(CO)_5Cr{=}C(Me)OZr(Cp_2)Cl]$ (**3.5**)*

This complex was previously prepared by a different method and only characterized by NMR and elemental analysis[12]. Complex **3.5** was synthesized using the procedure described for complex **3.3**. The ammonium salt of the acyl complex, $[(CO)_5Cr{=}C(Me)O][NEt_4]$ (1.4 g, 3.8 mmol), dissolved in 30 ml CH_2Cl_2, was added to a well-stirred solution of Cp_2ZrCl_2 (1.1 g, 3.7 mmol) over 60 minutes. The resulting reaction mixture was stirred for 30 minutes at -40 ºC after which, $AgBF_4$ (1.2 g, 6.0 mmol) was added. The solution was stirred for an additional 60 minutes at -40 ºC and then allowed to reach room temperature. The resulting reaction mixture

was evaporated to dryness *in vacuo*. The precipitate was extracted 5 times with 15 ml toluene and filtered through $MgSO_4$. The solvent was removed to yield 1.3 g (2.6 mmol) of yellow, microcrystalline $[(CO)_5Cr=C(Me)OZr(Cp_2)Cl]$. Some of the product was dissolved in a minimum amount of CH_2Cl_2, layered with pentane and cooled to -15 ºC to afford yellow crystals of $[(CO)_5Cr=C(Me)OZr(Cp_2)Cl]$.

Yield 1.3 g (70 %). Mp ≈ 113 – 115 ºC (Decompose) ^{1}H NMR (δ, acetone-d_6): 6.7, 6.6, 6.4 [s, Cp]; 2.9 [br, CH_3]. ^{13}C {H} NMR (δ, acetone-d_6): 364.3 [$C_{carbene}$]; 225.4 [CO_{trans}]; 218.2 [CO_{cis}]; 117.1, 116.6, 115.0 [Cp]; 53.0 [br, CH_3]. IR (cm^{-1}, ATR, ν_{CO}): 2053.9; 1924.7; 1880.4. IR (cm^{-1}, CH_2Cl_2, ν_{CO}): 2053.9; 1930.5. MS (FAB) *m/z*: 492 $[M]^+$; 464 $[M\text{-}CO]^+$; 441 $[(CO)_5Cr\text{-}CO\text{-}ZrCp_2]^+$; 255 $[Cp_2ZrCl]^+$; 235 $[(CO)Cr=C(Me)O]^+$; 123 $[(CO)_2Cr=C(Me)O]^+$.

*3.2.2.7 Synthesis of the carbene complex, $[(CO)_5Cr=C(Me)OZr(Cp^*_2)Cl]$ (**3.6**)*

The synthetic procedure of complex **3.6** is similar to that of complex **3.4**. However, $[(CO)_5Cr=C(Me)OLi]$ (0.5 g, 2.1 mmol) and $Cp^*_2ZrCl_2$ (0.6 g, 1.4 mmol) were used.

Yield 0.245 g (28 %). Mp ≈ 117 - 120 °C (Decomposition) ^{1}H-NMR (δ, $CDCl_3$): 2.73 (s, 3H, CH_3); 1.96 (m, 30H, Cp*). ^{13}C {H} NMR (δ, $CDCl_3$): 362.9 [$C_{carbene}$]; 218.6 [CO_{cis}]; 218.0 [CO_{trans}]; 123.8 [Cp* (ring)]; 53.0 [CH_3]; 11.8 [Cp* ($10CH_3$)].
IR (cm^{-1}, CH_2Cl_2, ν_{CO}): 2052 (C=O); 1925 (C=O).

MS (EI) *m/z*: 547 $[M\text{-}CO\text{-}Cl]^+$; 519 $[M\text{-}2CO\text{-}Cl]^+$; 491 $[M\text{-}3CO\text{-}Cl]^+$; 463 $[M\text{-}4CO\text{-}Cl]^+$; 435 $[M\text{-}5CO\text{-}Cl]^+$; 432 $[Cp^*_2ZrCl_2]^+$; 395 $[Cp^*_2ZrCl]^+$; 295 $[Cp^*ZrCl_2]^+$; 255 $[Cp^*ZrCl]^+$; 136 $[Cp^*]^+$.

*3.2.2.8 Synthesis of the carbene complex, $[(CO)_5W=C(Ph)OHf(Cp_2)Cl]$ (**3.7**)*

$[(CO)_5W=C(Ph)O][NEt_4]$ was synthesized using a similar method as employed for the synthesis of the methyl analogue amino carbene salt of complexes **3.3** and **3.5**. $W(CO)_6$ (17.8 g, 50.6 mmol), LiC_6H_5 (31 ml, 1.6 M, 50.2 mmol) and Et_4NCl (8.7 g, 52.6 mmol) were used. Orange-yellow microcrystalline material was stored in a refrigerator at -6ºC. The procedure for the preparation of $[(CO)_5W=C(Ph)OHf(Cp_2)Cl]$ (**3.7**) is similar to that of $[(CO)_5W=C(Me)OZr(Cp_2)Cl]$ (**3.3**). $[(CO)_5W=C(Ph)O][NEt_4]$ (0.74 g, 1.3 mmol), Cp_2HfCl_2 (0.50 g, 1.3 mmol) and $AgBF_4$ (0.3 g, 1.4 mmol) were used. Cp_2HfCl_2 was dissolved in dichloromethane before the addition to the carbene salt solution. After purification, red crystals were removed and washed with cold pentane and stored in the refrigerator at -6ºC.

Yield 0.2 g (19 %). Mp ≈ 119 – 123 ºC ^{1}H NMR (δ, acetone-d_6): 7.45 [m, 5H, Ph]; 6.4 – 6.5 [m, 10H, Cp]. ^{13}C {H} NMR (δ, acetone-d_6): 333.1 [$C_{carbene}$]; 205.6 [CO_{trans}]; 199.0 [CO_{cis}]; 127.4, 128.7, 132.9, 156.4 [Ph], 113.5, 114.7, 115.4, 116.3 [Cp]. IR (cm^{-1}, CH_2Cl_2, ν_{CO}): 2067.0; 1938.0. MS (EI) *m/z*: 773 $[M]^+$; 717 $[M\text{-}2CO]^+$; 661 $[M\text{-}4CO]^+$; 596

$[M\text{-}4CO\text{-}Cp]^+$; 532 $[W\text{-}C(Ph)OHfCp]^+$; 449 $[C(Ph)OHfCp_2Cl]^+$; 446 $[(CO)_2W\text{-}COHf]^+$; 418 $[(CO)W\text{-}COHf]^+$; $[(CO)_4W\text{-}C(Ph)O]^+$; 390 $[W\text{-}COHf]^+$; 385 $[(CO)_2W\text{-}COHf]^+$.

3.2.3 Synthesis of 1-pentene oligomers and polyethylenes

3.2.3.1 The oligomerization of 1-pentene

The catalyst (5.5 x 10^{-3} mmol), was dissolved in 10 ml toluene in a 100 ml Schlenk tube equipped with Teflon screw cap together with nonane (1 ml) as an internal standard. The co-catalyst MAO (≈ 4 mmol) was also added to the reaction mixture. Finally, after addition of 15 ml of 1-pentene the reaction mixture was stirred for 24 hours. Excess MAO was then destroyed with methanol/HCl.

3.2.3.2 Ethylene polymerization

All reactions were carried out under inert gas atmosphere using standard Schlenk techniques. Polymerization reactions were performed in a 350 ml stainless steel batch reactor fitted with a glass liner, an inlet valve and a pressure gauge. The catalyst was prepared by reacting 5.5 x 10^{-3} mmol of metalloxycarbene complex and 2.5 ml of MAO. Thereafter, the reactor was saturated with ethylene gas, kept constant at ca. 5 g for each run. The catalyst/MAO ratio was kept at 1: 1 000 throughout. All the

reactions were carried out at room temperature for 3 h. The polymer was isolated by precipitation in acidic methanol, washed thoroughly with methanol and subsequently dried in vacuum at 65 °C for 10 h.

3.2.4 Characterization procedures

3.2.4.1 Characterization of metalloxycarbenes

Melting points were determined on a Stuart SMP3 apparatus and are uncorrected. NMR spectra were recorded Varian 300, 400 or 600 MHz spectrometers (^{1}H NMR at 300/400/600 MHz and $^{13}C\{^{1}H\}$ NMR at 75/100/151 MHz; δ reported relative to the solvent resonance), the infrared spectra on either a Perkin Elmer 1600 Series or a Nicolet Avatar 330 FTIR spectrometer and FAB mass spectra on a VGA70-70E mass spectrometer at 70 eV with xenon as bombardment gas and *m*-nitrobenzylalcohol as matrix and EI mass spectra on a Finnigan Matt 8200 at *ca* 70 eV.

3.2.4.2 X-ray experiments

The crystal data collection and refinement details for complexes **3.3**, **3.5** and **3.7** are summarised in Table 3.1. Data sets were collected on a Bruker SMART Apex CCD diffractometer[13] or Enraf-Nonius Kappa CCD diffractometer[14] with graphite monochromated Mo-K_α radiation (λ = 0.71073 Å). Data reductions were carried out with standard methods using the software packages DENZO-SMN[15] and Bruker

SAINT[16] respectively. Empirical absorption corrections were performed using SCALEPACK[17] and SMART data were treated with SADABS[18]. The structures were solved by direct methods. All non-hydrogen atoms were refined anisotropically by full-matrix least squares calculations on F^2 using SHELXL-97[19] within the X-Seed environment[20]. The hydrogen atoms were fixed in calculated positions. ORTEP-III for Windows[21] was used to generate the various figures of the three complexes at the 50% probability level.

3.2.4.3 Characterization of 1-pentene oligomers and polyethylene

1-Pentene oligomers were characterized by gas chromatography using pre-isolated oligomers (dimers, trimers and tetramers) of 1-pentene as standards. As mentioned before, nonane was used as an additional standard.

The polymer structures were determined using ^{13}C NMR spectroscopy measured in 1,2,4-trichlorobenzene/C_6D_6 (9:1) at 100 °C at 75 MHz on a Varian VXR-300 NMR spectrometer.

The molecular weight of the polymers was determined at 140 ^oC using a PL 220 chromatograph from Polymer Laboratories packed with five Waters Styragel columns (HT 2 – 6). Polystyrene standards were used for calibration. The solvent used was 1,2,4-trichlorobenzene at a flow rate of 1 ml/min.

Thermal analyses were done on a Perkin Elmer DSC 7 at a heating and cooling rate of 10 °C/min using between 5-6 mg of the polymer. Two heating and one cooling

cycles were carried out. The maxima and minima of the second heating and cooling curves were recorded as melting and crystallization temperatures respectively.

A CRYSTAF apparatus model 200 from Polymer Char S.A (Valencia, Spain) was used for fractionation, at a cooling rate of 0.1 °C/min. The sample (20 mg) was dissolved in 30 ml 1,2,4-trichlorobenzene.

3.3 RESULTS AND DISCUSSION

3.3.1 Metalloxycarbene complexes

3.3.1.1 Spectroscopic and structural characterization

The results of physical measurements are reported in the experimental section. Due to the existence of more than one isotope for W, Zr and Hf, the FAB MS spectra have many peaks. The theoretical isotopic distribution compares well with the distribution obtained for the three complexes. Molecular ions were observed for complexes **3.3**, **3.5** and **3.7**. Typical stepwise fragmentation of carbonyl groups takes place.

Three infrared active carbonyl frequencies are expected for a pentacarbonyl compound with C_{4v} symmetry, but due to overlap, only two carbonyl frequencies are observed ($A_1^{(1)}$ and E) for complexes **3.3**, **3.5** and **3.7.** More than one chemical shift per compound are generally observed for the cyclopentadienyl groups and broad

methyl resonances occur in both the ^{1}H and ^{13}C spectra of complexes **3.3**, **3.5** and **3.7**. A possible explanation could be the formation of rotational isomers due to the various configurations of these complexes arising from rotation around the $C_{carbene}$-O and Zr-O bonds. The differences in relative intensities are due to the fact that some configurations are sterically less hindered and, therefore, preferred. As a result of the isomers, the methyl resonances appear as broad signals in the ^{1}H-NMR spectra for complexes **3.3** and **3.5**. The phenyl group in complex **3.7** shows a chemical shift at 7.45 ppm (average of multiplet). Although additional resonances were not identified, it cannot be ruled out as they might overlap, due to the complexity of the multiplet observed. The low intensity and absence of additional methyl resonances in ^{1}H and ^{13}C NMR spectra can be attributed to spin-rotational relaxation which leads to low intensity chemical shifts for unhindered methyl groups[22]. A broadening of the methyl group resonance was also observed by Grubbs et al. who prepared complex **3.5** *via* a different route[12]. Chromium(0) is slightly more electronegative than tungsten(0), it decreases the electron density on the carbene carbon more and hence it appears at a lower field in the chromium complex (δ 364.3 in **3.5** vs δ 340.8 in **3.5**). The presence of the phenyl group in complex **3.7** increases the electron density on the carbene carbon more (by π-effect) than the methyl (σ-indicative) group in complex **3.3** and hence the resonance at a higher field of 333.1 ppm. The carbonyls (*cis* and *trans* to the carbene ligand) have chemical shifts as expected for the different metals, with the carbonyls in the W-complex being less deshielded due to its lower electronegativity.

3.3.1.2 Single crystal X-ray diffraction

Crystallization of complex **3.3** from toluene/pentane gave yellow crystals in the orthorhombic space group P*nma,* while crystallization of **3.7** from a saturated solution of toluene afforded red crystals whereas yellow crystals of **3.5** formed from CH_2Cl_2/pentane. The latter two complexes crystallized in the monoclinic space group $P2_1/c$.

The molecular structures and numbering schemes of **3.3, 3.5** and **3.7** are shown in Figures 3.1, 3.2 and 3.3. Selected bond lengths and angles are listed in Table 3.2. All three structures contain an $M(CO)_5$ (M = W or Cr) moiety that is linked to either Cp_2ZrCl or Cp_2HfCl through a carbenoxyl group.

The most significant aspect of all these structures is the very large, almost linear, $C_{carbene}$-O-M angle, with the C4-O4-Zr1 angle 169.33(13)º in **3.5** and 177.3(6)º in **3.3**, the latter being the largest angle yet identified for this type of complex[6]. The corresponding angle in **3.7** has a value of 171.4(3)º, which is similar to the hafnium metallacycles prepared by Erker and co-workers having C-O-Hf angles of 173.95(5)[6] and 172.25(0)°[23]. In addition, the W- and Cr- $C_{carbene}$ separations are fairly long, while the $C_{carbene}$-O bond lengths, on the other hand, are short compared to alkoxycarbene complexes [1.321, 1.323(2), 1.299 and 1.311(8) Å][24-26] and similar to a 1.265(3) Å separation in the metallacyclic complex prepared by Erker et al.[23] The Hf-O bond length of 2.006(3) Å is longer than the Hf-O bond lengths found for the metallacycles prepared by Erker (1.904 Å[6] and 1.900 Å[23]). The Zr-O bond lengths of 2.032(5) and

2.048(2) Å in **3.3** and **3.5** respectively, are of the same order as other metalloxycarbene complexes[27-29].

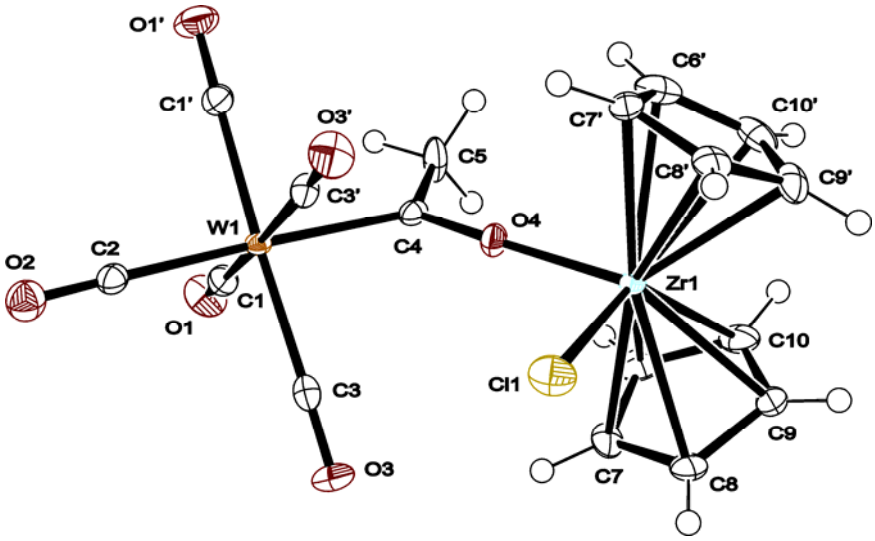

Figure 3.1: Molecular structure and numbering scheme of $[(CO)_5W{=}C(Me)OZr(Cp)_2Cl]$ (**3.3**); ellipsoids are shown at the 50% probability level

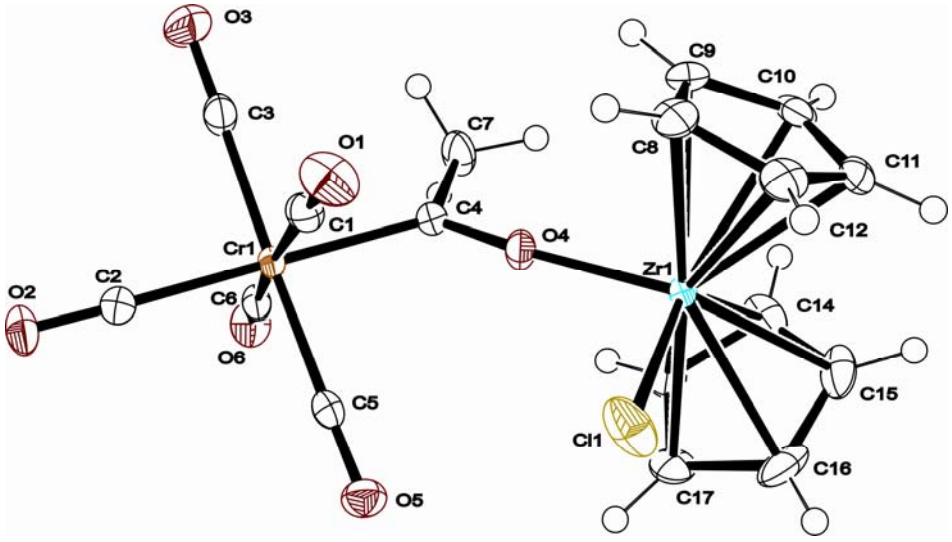

Figure 3.2: Molecular structure and numbering scheme of $[(CO)_5Cr{=}C(Me)OZr(Cp)_2Cl]$ (**3.5**); ellipsoids are shown at the 50% probability level

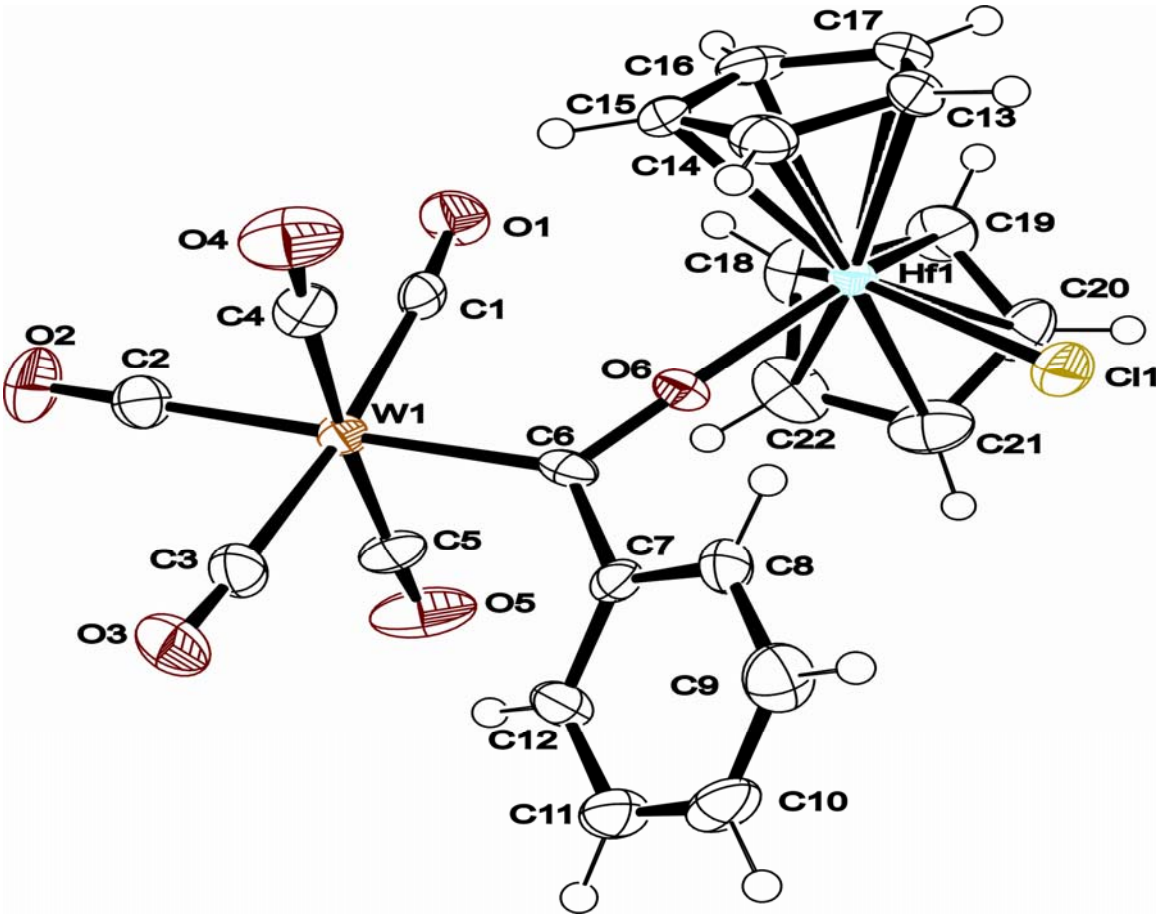

Figure 3.3: Molecular structure and numbering scheme of;

$[(CO)_5W{=}C(Ph)OHf(Cp)_2Cl]$ (**3.7**); ellipsoids are shown at the 50% probability level.

Table 3.1: Crystal data and structure refinements for the compounds **3.3**, **3.5** and **3.7**

Compound	**3.3**	**3.5**	**3.7**
Empirical formula	$C_{17}H_{13}ClO_6WZr$	$C_{17}H_{13}ClO_6CrZr$	$C_{17}H_{13}ClO_6WHf$
Formula weight	623.79	491.94	773.13
Space group	*Pnma*	$P2_1/c$	$P2_1/c$
a (Å)	21.986(2)	12.467(2)	8.5422(2)
b (Å)	12.1603(11)	12.0495(19)	12.5546(3)
c (Å)	7.1088(7)	12.5041(19)	21.0237(7)
α (º)	90	90	90
β (º)	90	100.502(4)	96.1520(10)
γ (º)	90	90	90
V (Å^3)	1900.5(3)	1846.9(5)	2241.68(11)
Z	4	4	4
$D_{calc.}$ (g.cm^{-3})	2.18	1.769	2.291
Adsorption coefficient (mm^{-1})	6.766	1.327	9.910
$F_{(000)}$	1176	976	1432
θ (min – max) (°)	2.50-25.68	1.66-26.37	1.89-27.49
Index ranges, *h k l*	-26 – 25, -14 – 14, -5 – 8	-14 – 15, -13 – 15, -10 – 15	-11 – 8, -16 – 15, -26 – 27
Temperature (K)	173(2)	100(2)	173(2)
Reflections collected	9804	10487	12410
Independent reflections [R_{int}]	1894 [0.0425]	3764 [0.0172]	5106 [0.0487]
Data/restraints/parameters	1747/0/131	3548/0/236	4234/0/280
Final *R* indices [$I>2\sigma(I)$]	$R_1 = 0.0352$, $wR_2 = 0.0850$	$R_1 = 0.0232$, $wR_2 = 0.0579$	$R_1 = 0.0320$, $wR_2 = 0.0743$
R indices (all data)	$R_1 = 0.0386$, $wR_2 = 0.0869$	$R_1 = 0.0250$, $wR_2 = 0.0589$	$R_1 = 0.0443$, $wR_2 = 0.0788$
Goodness-of-fit on F^2	1.108	1.053	1.01
Largest shift estimated S.D.	0	0.001	0.002
Largest peak (e Å^{-3})	3.284	0.533	2.608

Table 3.2: Selected bond lengths (Å) and angles (°)

	Complex 3.3	**Complex 3.5**	**Complex 3.7**
W1-C1	2.181(8)	2.044(2)	2.177(6)
C1-O1	1.273(9)	1.280(2)	1.291(6)
Zr/Hf1-O1	2.032(5)	2.048(2)	2.006(3)
C1-O1-Zr/Hf1	177.3(6)	169.3(3)	171.4(3)
O1-C1-W1	122.6(6)	123.0(14)	123.3(4)
C2-C1-W1	125.0(5)	124.7(3)	126.1(4)

In **3.3** the complex lies on a crystallographic mirror plane defined by O11, C11, W1, C1, C2, O1, Zr1 and Cl1. Complex **3.5** is isostructural to **3.3**, although it only has a pseudo-mirror plane through the two metals, the metalloxy bridge and *trans*-CO group, with the greatest deviation from planarity of the pseudo-mirror by O4 [0.0640(13) Å]. In **3.7** this pseudo-symmetry is broken by the twisting of the phenyl ring by 40.1(2)° with respect to the molecular plane through O11, C11, W1, C1, C2, O1, Hf1 and Cl1. The molecular plane is, nevertheless, nearly flat, with the largest deviation from planarity by Hf1 [0.082(2) Å]. Furthermore, the Cp rings are no longer symmetrically arranged around the molecular plane as found in **3.3** and **3.5**

(oriented at 25.32(14) and 26.09(6)° for **3.3** and **3.5** respectively), but are oriented at 31.2(2) and 18.8(2)° respectively.

Complex **3.3** exhibits no significant intermolecular interactions, with the molecules packing in columns along the *a*-axis with alternating head-to-tail orientations parallel to the *c*-axis. No significant intermolecular interactions are observed for complex **3.5** either. The molecules pack in layers of alternating orientation parallel to the *ab* plane. In complex **3.7**, non-bonded π-π intermolecular interactions link pairs of Cp ligands in neighbouring molecules. In this packing arrangement, the Cp_2HfCl groups align in layers parallel to the *bc* plane, with the $W(CO)_5$ moieties located between these layers. As a result of these interactions between Cp ligands, the Cp_2HfCl moiety is oriented differently to Cp_2ZrCl in **3.3** and **3.5** where the Cl ligand is on the opposite side of the molecule to the methyl group on the carbenoxy group, as indicated by the improper torsion angle Cl1-Zr-C1-C2 of 180º in both cases. The equivalent improper torsion angle in **3.7** is -4.4(4)º, showing that the Cl and phenyl group are on the same side of the molecule.

The large variations found in the $C_{carbene}$-O-Zr angle for **3.3** and **3.5** (177.3 and 169.3°) can be explained by the presence of resonance structures indicated in Scheme 3.2[12]. Consider the two contributing structures for our metalloxycarbene catalyst precursor, for example $[(CO)_5W{=}C(Me)OZr(Cp_2)Cl]$. [M] and [Zr] represent the two complex units within the metalloxycarbene catalyst precursor.

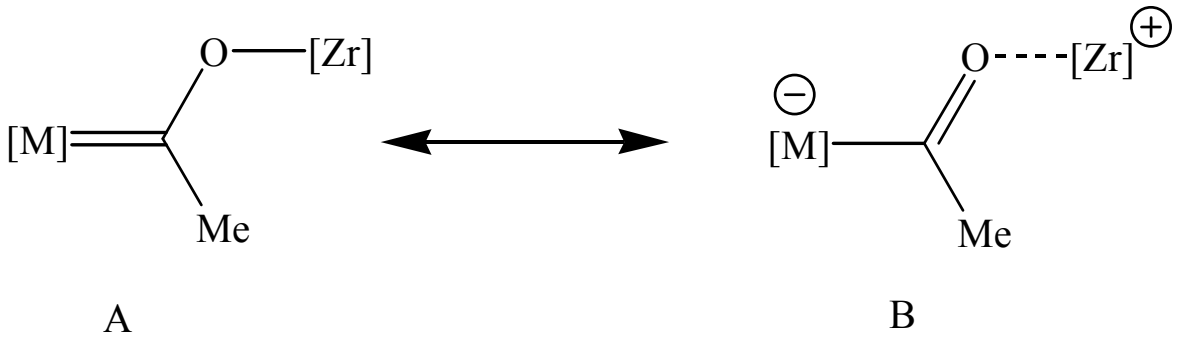

A B

Scheme 3.2 Possible isomers of metalloxycarbene complexes

The structure A is the standard representation of a carbene complex, whereas B is an electrosratically-bonded isomer. One could also consider a delocalized π-system represented by C and D in Scheme 3.3.

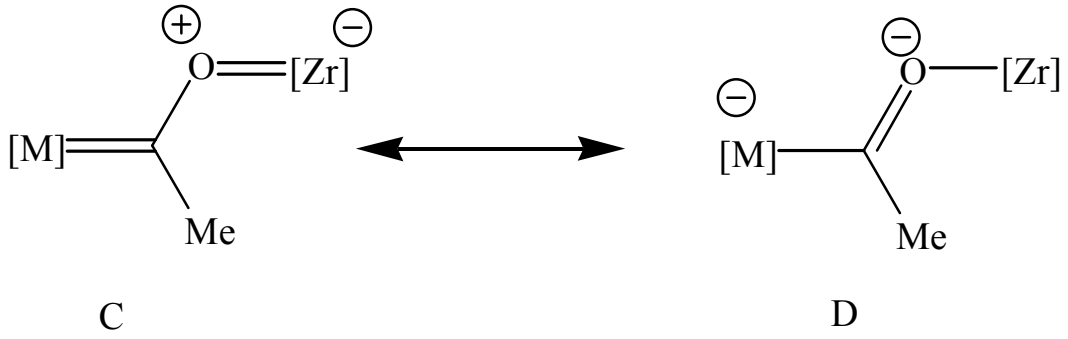

C D

Scheme 3.3: Other possible isomers of metalloxycarbene complexes

Relatively long M-C bond lengths, an almost linear $C_{carbene}$-O-M angle and short $C_{carbene}$-O bond distances suggest that resonance structure B is the most important in the stabilization of **3.3** and **3.5.** In terms of the linearity observation (and structure C and D) the oxygen atom could have almost *sp* hybridization in order to make both other *p* orbitals available for π-delocalization to the M-C(carbene) and O-M systems.

We prefer to argue, however, on the basis of the relative importance of B in Scheme 3.2, and one is tempted to speculate that the observed catalytic activity is at least partly due to the relative facile abstraction of the anionic acyl adduct by MAO to afford an ion pair with the active cationic zirconium centre. Due to its thermodynamic instability the hafnium compound could not be used in catalysis.

3.3.1.3 1-Pentene oligomerization

The yields of 1-pentene oligomers, synthesized according to Scheme 3.4, were analyzed with gas chromatographic (GC) techniques and the results are displayed in Table 3.3.

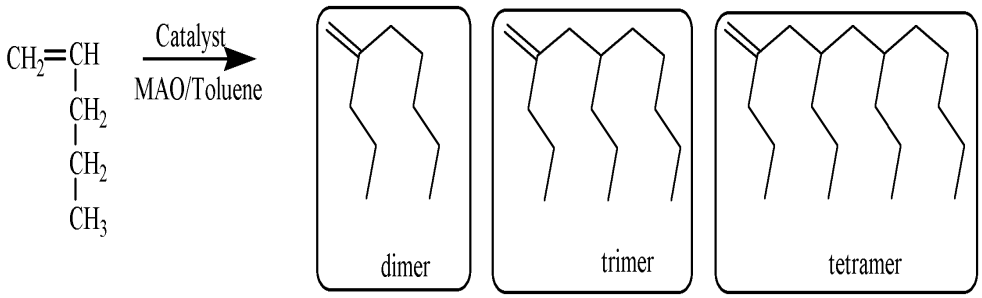

Scheme 3.4: Reaction scheme for the oligomerization of 1-pentene

Determination of 1-pentene oligomer yields by GC requires standards. Dimers were isolated via distillation over a Vigreux column whereas the trimers and tetramers were collected in vacuum (≈2 mbar) between 90-100 ^{o}C and 115-130 ^{o}C respectively[30]. The products were subsequently used as standards for GC measurements. Generally metalloxycarbene complexes **3.3**, **3.4** and **3.6** produced low overall yields of 1-pentene oligomers (dimers, trimers and tetramers) compared to the oligomers produced with Cp_2ZrCl_2 (**3.1**)(see Table 3.3).

Table 3.3: Percentage yields and molecular weight results for the oligomerization of 1-pentene

Catalyst No.	Sample Code	Dimer Yield (%)	Trimer Yield (%)	Tetramer Yield (%)	Total Yield (%)	M_n (g/mol)	M_w (g/mol)	PDI
3.1	PO1A	25.7	24.2	14.9	64.8	nd	nd	nd
	PO1B	28.4	70.9	6.8	100.0	430	460	1.1
3.2	PO2A	4.3	3.4	2.8	10.5	1200	2100	1.8
	PO2B	4.9	1.7	1.5	7.9	1400	2300	1.6
3.3	PO3A	10.5	12.2	8.8	38.5	460	530	1.2
3.4	PO4A	1.4	1.5	0.8	3.6	1300	2200	1.7
	PO4B	1.5	1.4	1.7	4.6	1400	2600	1.9
3.6	PO5A	2.6	2.3	0.7	5.5	1400	2400	1.7
	PO5B	1.9	1.8	1.1	4.8	1400	2400	1.7

The yields of dimmers, trimers and tetramers of 1-pentene obtained with $(CO)_5W{=}C(Me)OZr(Cp)_2Cl$ (**3.3**) were significantly higher than those synthesized with $Cp^*_2ZrCl_2$ (**3.2**) and other carbene complexes. This could be attributed to superior stability of complex **3.3** compared to other carbene complexes **3.4** and **3.6**. These results differ significantly compare to those of previous study. Previously it was shown that $[(CO)_5W{=}C(Me)OZr(Cp)_2Cl]$ (**3.3**) higher overall yields of 1-pentene

oligomers (dimers, trimers and tetramers) than those produced with **3.1** and $MeOZr(Cp)_2Cl/MAO$[4]. However, higher molecular weight oligomers were not analyzed. As shown in Table 3.3, higher molecular weight oligomers, with weight average molecular weight (M_w) ranging from 460 to 2600 g/mol, were also present in all the runs. Figure 3.4 shows a typical ^{13}C NMR spectrum of these oligomers. Only major peaks of poly 1-pentene were resolved. Additional minor peaks could be due to 2,1 mis-insertion. These peaks appear to be common for homopolymers of α-olefins with five and more carbons and above [31-33].

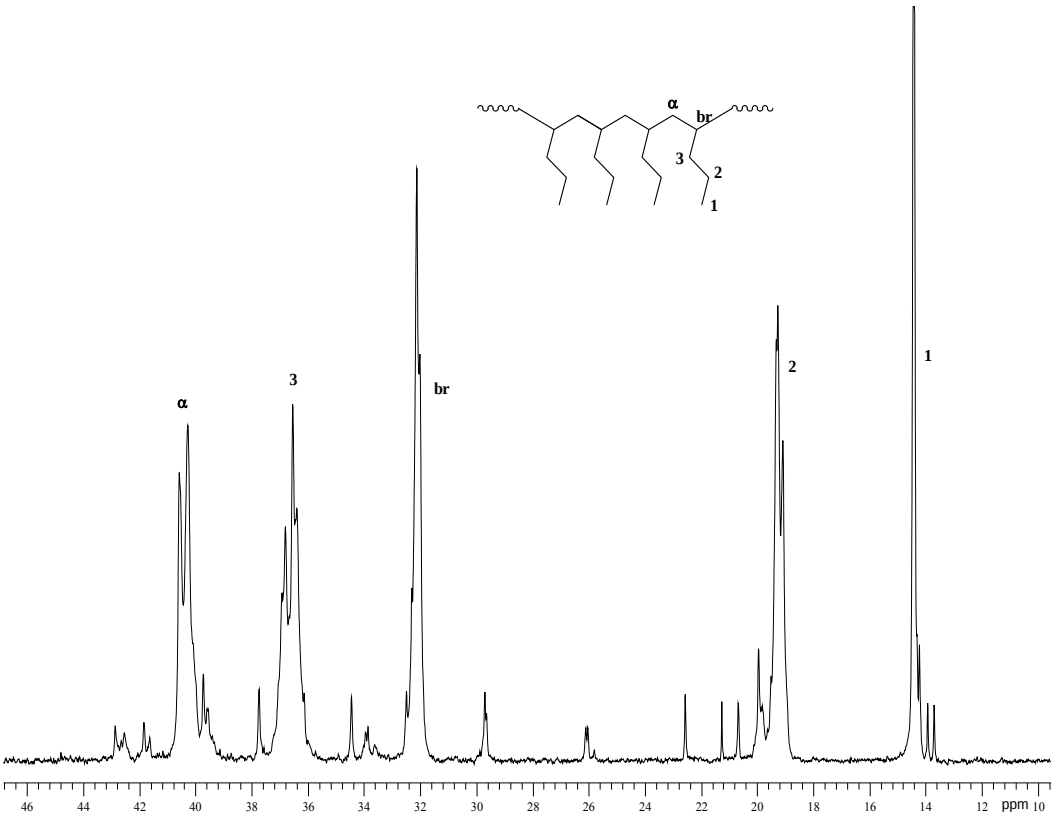

Figure 3.4: ^{13}C NMR spectrum of higher molecular weight oligomer PO3 produced with **3.3**/AMO

3.3.2 Ethylene polymerization

Thermal and molecular weight properties of polyethylenes are displayed in Table 3.4. The polymerization activities of metalloxycarbene **3.3**, **3.4** and **3.6**/MAO are significantly higher than those of metallocenes catalyst systems. Polyethylenes produced with Cp_2ZrCl_2 (**3.1**) and $Cp^*_2ZrCl_2$ (**3.2**) have narrow polydispersities which is characteristic of metallocene catalyzed polymer. In contrast, ethylene polymers obtained using metalloxycarbene complexes as precursors possess broad polydispersities ranging from 6 to about 15. In addition molecular weight distribution curves shown in Figure 3.5 also exhibit bimodal distributions in the form of shoulders.

Table 3.4: DSC, GPC and CRYSTAF characterization data for polyethylene

Catalyst No.	Sample Code	$T_{c\ CRYSTAF}$ (^oC)	$T_{c\ DSC}$ (^oC)	$T_{m\ DSC}$ (^oC)	M_n (g/mol)	M_w (g/mol)	PDI	Activity (kg/(mol.h)
3.1	ZRA	87.7	119.5	132.4	41 700	96 000	2.3	133.3
	E1B	nd	118.2	138.3	67 800	260 000	2.8	97.0
3.2	E2C	86.1	117.8	130.8	8 600	48 000	2.5	102.8
	E2D	87.8	118.1	133.5	23 200	136 700	2.2	126.9
3.3	E3A	87.5	117.0	135.7	44 900	225 900	5.0	373.3
3.4	E4A	87.4	118.0	132.5	8 000	149 800	18.9	353.3
	E4B	86.9	118.3	131.5	7 300	64 300	8.8	292.1
3.6	E5A	86.9	118.3	132.2	9 200	215 800	23.5	343.6
	E5B	86.6	118.9	131.1	6 000	171 600	28.7	271.5

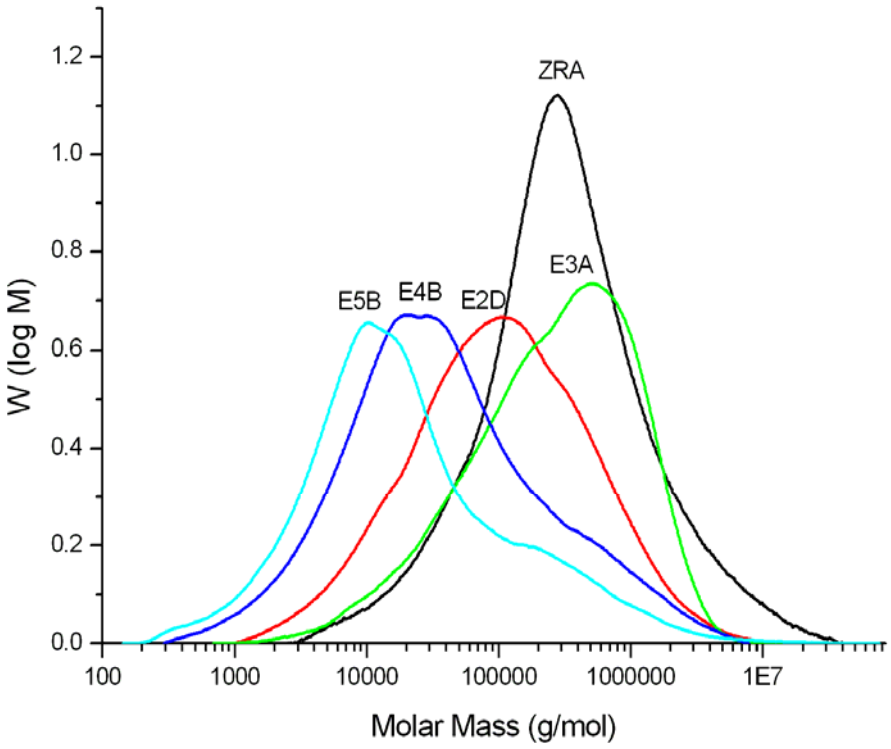

Figure 3.5: Molecular weight distribution curves of polyethylene

Polyethylenes produced with the Cp* containing ligands display the presence of additional resonances at δ ≈ 13.86, 22.67, 29.38 and 31.98 ppm (Figure 3.6) which were not expected since this were pure homopolymerization reactions i.e. there was no α-olefin comonomer present in the reaction. These additional peaks show that short chain α-olefins, acting as comonomers, exist in the reaction mixture. Additional peaks indicate that carbene catalyst with Cp* forms short chain ethylene oligomers which then act as comonomers during polymerization resulting in the formation of slightly branched polyethylenes.

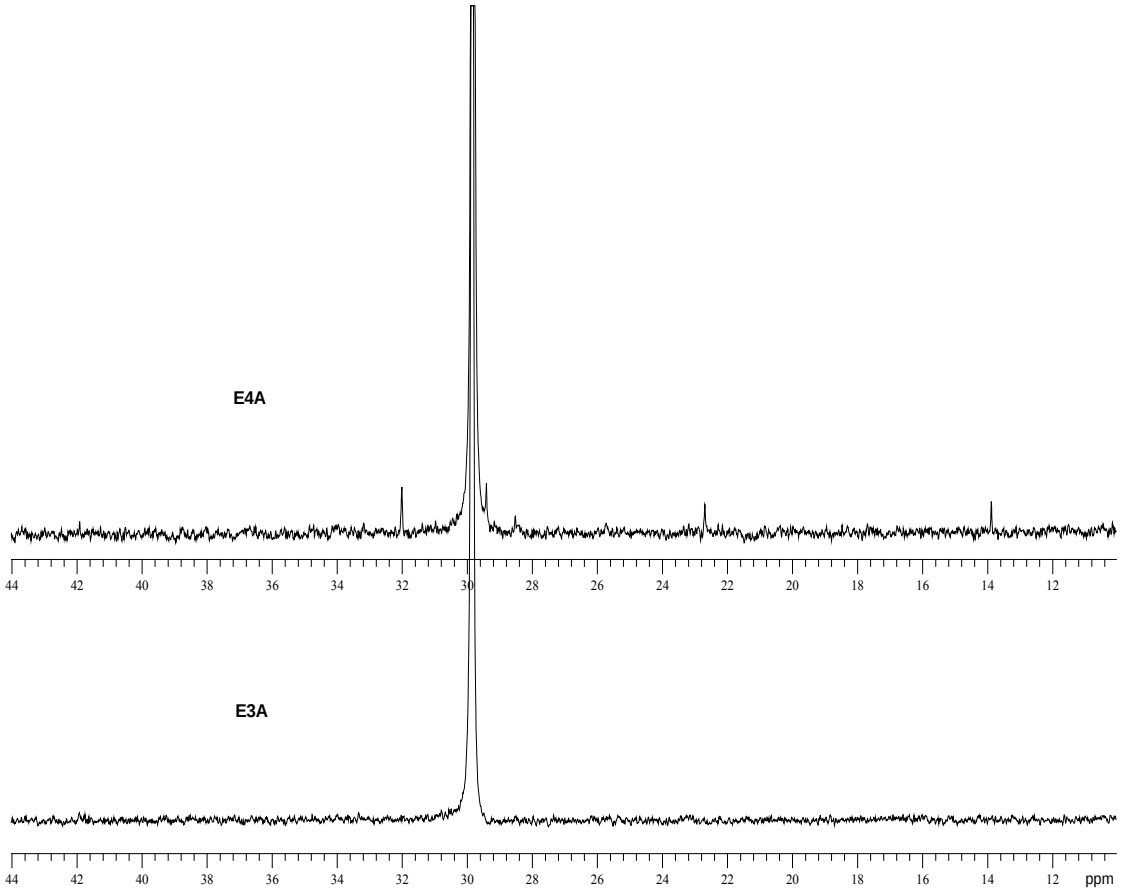

Figure 3.6: The ^{13}C NMR spectra of linear and slightly branched polyethylene

The branching was probed further using CRYSTAF. The principle about CRYSTAF as an analytical technique will be discussed in Chapter 4. Figure 3.7 shows the CRYSTAF plots of both linear (E3A) and branched (E4A) produced with **3.3** and **3.4**/MAO respectively. As clearly shown, the branching (peaks indicated by arrows) was also observed in CRYSTAF plots confirming the observation already made with ^{13}C NMR.

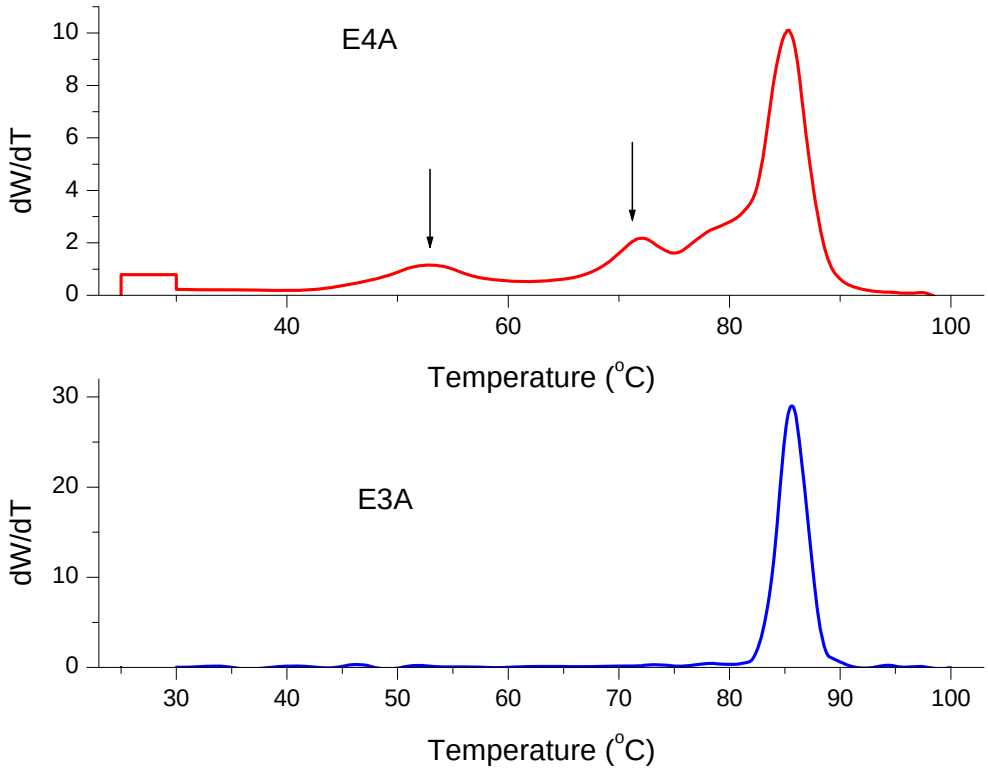

Figure 3.7: The short chain branching distribution of linear and slightly branched polyethylene

The melting and crystallization temperatures (Figures 3.8 and 3.9) investigated by DSC did not show significant shifts implying that the contribution of these branches to thermal properties is negligible. The formation of branched polyethylenes without a comonomer is not unusual. This kind of phenomenon has been observed before particularly in polyethylenes synthesized with late transition non-metallocene catalysts systems[34].

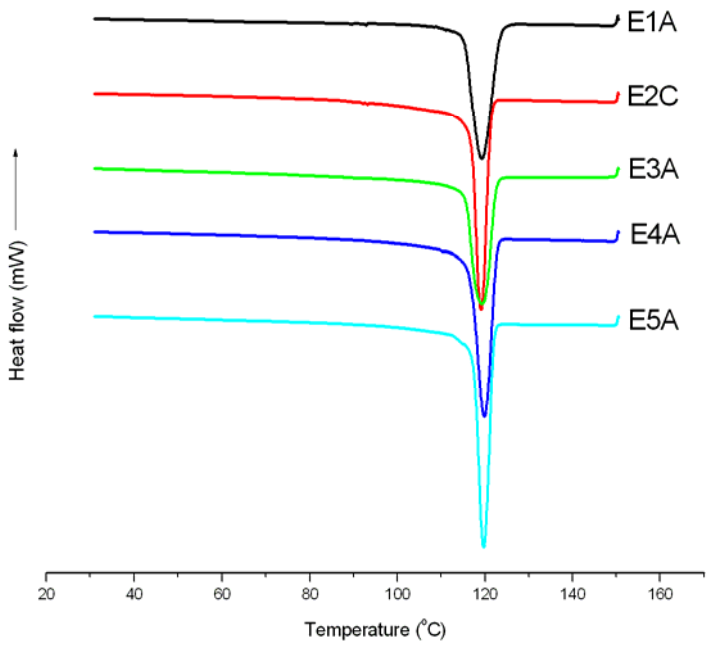

Figure 3.8: The crystallization curves of polyethylenes

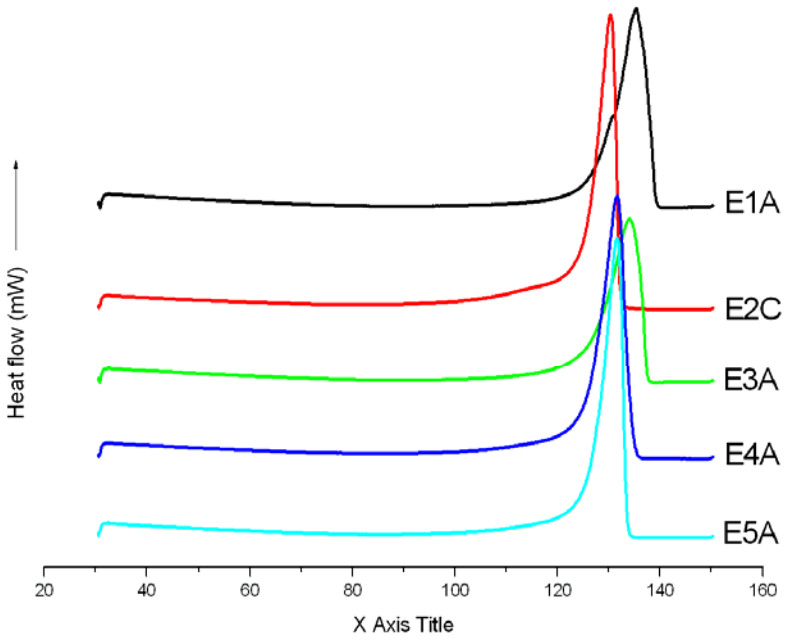

Figure 3.9: The melting curves of polyethylenes

The role of carbene ligand and particularly the first metal (M_1) during polymerization is not yet clear but will receive further attention. The mechanism explaining the formation of the active species after the activation of metalloxycarbenes by MAO is discussed in Chapter 4. It is sufficient to say at this stage that exactly like in our preceding investigation, the zirconoxycarbene differ significantly from single site Cp_2ZrCl_2, and probably also from $Cp_2ZrCl(OR)$. By definition, metallocene catalysts are bi-components consisting of group four transition metal compounds and cocatalysts (usually MAO). The transition metal of metallocene catalysts bears two

η^5 cyclopentedienyl-type (cyclopentadiene (Cp), alkylated cyclopenteniene (Cp*), indenyl (Ind) or fluorenyl, (Flu) ligands and two σ-donor ligands[35,36]. Although the structures of metalloxycarbenes would partly fit this definition, the broad polydispersities of polymers produced with these precursors suggest that they are most probably not single site type catalysts but behave more like multi-sited Ziegler-Natta catalyst types. Metalloxyarbene complexes are less stable than metallocenes. We speculate that the high PDI of polymers and copolymers produced with metalloxycarbenes is probably due to the presence of other catalytically active species present during polymerization reactions.

3.4 CONCLUSIONS

The structural modification of metallocenes by mono-substitution of chlorine with a Fischer-type complex anion carbene salt resulted in the formation of bi-metallic complexes **3.3** – **3.7**. The tungsten (**3.3**) and chromium (**3.4** and **3.6**) metalloxycarbenes complexes when activated MAO are capable of oligomerizing 1-pentene and homopolymerizing ethylene. The broad molar mass and bimodal distribution of polymers obtained using **3.3**, **3.4** and **3.6**/MAO lead to the conclusion that metalloxycarbene catalyst precursors behave like Ziegler-Natta catalyst types.

3.5 REFERENCES

1. Zhu, F.; Yang, Y.; Huang, Y.; Lin, S. *Macromol. Phys.* **2001**, 202, 1935.

2. Carella, J. M.; Gotro, J.T.; Graessley, W.W. *Macromolecules* **1986**, 19, 659.

3. Bajgur, C. S.; Sivaram, S. *Curr. Sci.* **2000**, 78, 1325.

4. Brüll, R.; Kgosane, D.; Nevelling, A.; Pasch, H.; Raubenheimer, H.G.; Sanderson, R.D.; Wahner, U.M. *Macromol. Symp*. **2001**, 16, 511.

5. Erker, G.; Dorf, U.; Lecht, R.; Ashby, M.T.; Aulbach, M.; Schlund, R.; Kruger, C.; Mynott, R. *Organometallics* **1989**, 8, 2037.

6. Erker, G.; Pfaff, R.; Kruger, C.; Werner, S. *Organometallics* **1991**, 10, 3559.

7. Sabat, M.; Gross, M. F.; Finn, M.G. *Organometallics* **1992**, 11, 745.

8. Monrabal, B. *J. Appl. Pol. Sci.* **1994**, 52, 491.

9. Monrabal, B. *Macromol. Symp*. **1996**, 110, 81.

10. Errington, R. J. *Advanced Practical Inorganic and Metalorganic Chemistry,* Chapman & Hall, London, **1997**, pp. 26-52, 97.

11. Mayr, A. in *Synthetic Methods of Organometallic and Inorganic Chemistry. Vol.7,* (W. A. Herrman, red.), Georg Tieme Verlag, Stuttgart, **1997**, 156.

12. Anslyn, E. V.; Santarsiero, B. D.; Grubbs, R. H. *Organometallics,* **1988**, 7, 2137.

13. SMART *Data collection software* (version 5.629), Bruker AXS Inc., Madison, WI, **2003**.

14. COLLECT, Data Collection Software, Nonius BV Delft, The Netherlands, **1998**.

15. Otwinowski, Z.; Minor, W. *Methods Enzymol.* **1997**, 276, 307.

16. SAINT, *Data reduction software* (version 6.45) Bruker AXS Inc., Madison, WI, **2003**

17. Ferrugia, L. J. *J. Appl. Crystallogr*. **1999**, 32, 837.

18. Blessing, R.H. *Acta Crystallogr*., *Sect. A* **1995**, 51, 33; SADABS (version 2.05) Bruker AXS Inc., Madison, WI, **2002**.

19. Sheldrick, G. M. SHELX-97. *Program for crystal structure analysis*, University of Göttingen, Germany, **1997**.

20. Barbour, L. J. *J. Supramol. Chem*. 2001, 1, 189.

21. Farrugia, J. *J. Appl. Cryst.* **1997**, 30, 565.

22. Neuhaus, D.; Williamson, M.; in *The steady state NOE for spins,* Chapter 2, VCH Publishers, New York, **1989**, p51.

23. M. Berlekamp, G. Erker and J. L. Peterson, *J. Organomet. Chem.,* 1993, **456**, 97.

24. Toledano, C. A.; Paelier, A.; Rudler, H.; Daran, J. C.; Jeanin, Y. *J. Chem. Soc. Chem. Commun.,* **1984**, 576.

25. Staples, R. J.; Potts, D. M.; Yoder, J. C. *Z. Kristallogr.* **1995**, 210, 381.

26. Albrecht, T.; Sauer, J. *Tetrahedron Letters,* **1994**, 35, 561.

27. Erker, G.; Sosna, F.; Petersen, J. L.; Benn, R.; Grondey, H. *Organometallics,* **1990**, 9, 5462.

28. Erker, G.; Dorf, U.; Kruger, C.; Tsay, Y. H. *Organometallics,* **1987**, 6, 680.

29. M. Berlekamp, G. Erker, B. Schönecker, R. Krieg and A. Rheingold, *Chem. Ber.,* **1993**, 126, 2119.

30. Wahner, U. M.; Brull, R.; Pasch, H.; Raubenheimer, H. G.; Randerson, R. *Angew. Makromol. Chem.* **1999**, 270, 49.

31. Grumel, V.; Pasch, P.; Raubenheimer, H.G.; Sanderson, R.; Wahner, U.M. *Macromol. Mat. Eng.* **2001**, 286, 480.

32. Zhao, X.; Odian, G.; Rossi, A. *J. Polym. Sci., Part A: Polym. Chem.* **2000**, 38, 3802.

33. Kim, I.; Zhou, J.; Chung, H. *J. Polym. Sci., Part A: Polym. Chem.* **2000**, 38, 1687.

34. Johnson, L. K.; Killian, C. M.; Brookhart, M. *J. Am. Chem. Soc*. **1995**, 117, 6414.

35. Alt, H.G.; Köppl, A.*Chem. Rev.* **2000**, 100, 1205.

36. Resconi, L.; Cavallo, L.; Fait, A.; Piemontesi, F. *Chem. Rev*. **2000**, 100, 1253.

4 Copolymerization behaviour of metallocene and metalloxycarbene catalyst systems: A comparative study on ethylene/1-pentene copolymers*

* Based on: **1**. Luruli, N.; Grumel, V.; Brüll, R.; Du Toit, A.; Pasch, H.; van Reenen, A.J.; Raubenheimer, H.G. *J. Polym. Sci. Part A: Polym. Chem.* **2004**, 42, 5121. **2**. Luruli, N.; Heinz, L.; Grumel, V.; Brüll, R.; Pasch, H.; Raubenheimer, H.G. *Polymer* **2006,** 47, 56. The SEC-FTIR fractionation was done at Deutsches Kunststoff-Institut (German Institute for Polymers), Germany under the supervision of Dr. R. Brüll and Prof. H. Pasch.

ABSTRACT

Ethylene/1-pentene copolymers were synthesized using Cp_2ZrCl_2 (**4.1**), $[(CO)_5W{=}C(Me)OZr(Cp)_2Cl]$ (**4.2**), $[(CO)_5Cr{=}C(Me)OZr(Cp)_2Cl]$ (**4.3**)/MAO and selected Cp^* analogue catalyst systems. The resulting copolymers were characterized using standard analytical techniques such as SEC, DSC, FTIR and ^{13}C NMR spectroscopy. In addition, the chemical heterogeneity was investigated by SEC-FTIR and fractionation techniques. The copolymers synthesized with metalloxycarbenes **4.2** and **4.3**/MAO had higher average molecular weights and broader polydispersities compared to those produced with Cp_2ZrCl_2 (**4.1**)/MAO. All copolymers showed heterogeneous comonomer incorporation as displayed by SEC-FTIR. Crystallization analysis fractionation (CRYSTAF) showed a broad chemical composition distribution (CCD) for all the copolymers synthesized with all three **4.1**, **4.2**, and **4.3**/MAO catalyst systems. The copolymers obtained using $Cp^*_2ZrCl_2$ (**4.4**) and $[(CO)_5W{=}C(Me)OZr(Cp^*)_2Cl]$ (**4.5**)/MAO had low comonomer incorporation.

4.1 INTRODUCTION

The macroscopic properties of a polymer are largely influenced by morphology, molecular weight and molecular weight distribution. In the case of copolymers, the amount (and sometimes nature) of the selected comonomer as well as the average distribution of the comonomer throughout the material (often expressed as the chemical composition distribution or CCD) are additional factors that influence its final properties. During the synthesis, these individual molecular parameters are influenced by, *inter alia*, the chosen metal in the polymerization catalyst as well as the ligands surrounding it. Changing the position of the available coordination site or modifying the type of ligand structure or configuration, usually significantly affect catalyst activity and selectivity.

The copolymerization of α-olefins is one of the most important approaches for improving the properties of polyolefins. Studies investigating properties of olefin copolymers that contain even-numbered α-olefin comonomers are readily available[1-11]. However, very little interest has been shown in copolymers with odd-numbered α-olefins (1-pentene, 1-heptene and 1-nonene). This is due to the fact that the world's α-olefin market is saturated with even-numbered monomers while South Africa has a monopoly on odd-numbered monomers from Sasol's Fischer-Tropsch processes[12-16] .

Using metallocene/MAO catalyst systems for the copolymerization of α-olefins, we recently carried out in-depth studies of the melting and crystallization behaviour of copolymers derived from propene or ethylene and both odd and even-numbered α-olefins[17-20]. Copolymerization as well as homopolymerization of α-olefins using a wide variety of catalyst systems has been reviewed[21-24]. As indicated in Chapter 2, a large number of metalloxycarbenes complexes are known, however we are not aware of any copolymerization study using such complexes as catalyst precursors for α-olefin polymerization. It has been shown in Chapter 3 that metalloxycarbenes can effect polymerization of α-olefins. Understanding the copolymerization behaviour of these catalyst precursors is, therefore, important for further studies involving both catalyst design and polymerization. The development of new catalyst systems for both homopolymerization and copolymerization remains important in the context of polymer design. Simultaneously, more accurate polymer characterization methods are required to enable a better understanding of polymer formation and complete structural resolution.

In this chapter we compare the copolymerization behaviour of Cp_2ZrCl_2 (**4.1**), $[(CO)_5W{=}C(Me)OZr(Cp)_2Cl]$ (**4.2**), and $[(CO)_5Cr{=}C(Me)OZr(Cp)_2Cl]$ (**4.3**)/MAO towards ethylene/1-pentene copolymers. Particular emphasis has been given to the chemical heterogeneity, investigated by hyphenated SEC-FTIR and fractionation techniques. The results of the copolymers obtained using Cp* (**4.4** and **4.5**) analogue catalyst systems are briefly discussed and also compared to those obtained using Cp-

containing compounds. The structures of all these catalyst precursors are shown in Scheme 4.1.

4.2 EXPERIMENTAL

4.2.1 Materials

All materials (tungsten- and chromiumhexacarbonyl, methyllithium, Et_4NCl and $AgBF_4$) used in the preparation of complex $[(CO)_5W{=}C(Me)OZr(Cp)_2Cl]$ (**4.2**), $[(CO)_5Cr{=}C(Me)OZr(Cp)_2Cl]$ (**4.3**) and $[(CO)_5W{=}C(Me)OZr(Cp^*)_2Cl]$ (**4.5**) were obtained from SIGMA-Aldrich and used as received. Ethylene, polymerization grade, was purchased from Fedgas and used without further purification. 1-Pentene was obtained from SASOL. It was dried by refluxing over $LiAlH_4$ and then distilled under nitrogen. Methylaluminoxane (10% w/v solution in toluene), Cp_2ZrCl_2 and $Cp^*_2ZrCl_2$, were purchased from SIGMA-Aldrich and used as received. Toluene (SIGMA-Aldrich) was dried by refluxing over sodium/benzophenone and then distilled under an inert gas atmosphere.

4.2.2 The synthesis of metalloxycarbene complexes

The metalloxycarbene catalyst precursors were again prepared according to Scheme 4.1 where, M = metal; L = Cp ligand; R = alkyl. Details of the synthesis of metalloxycarbenes have already been discussed in Chapter 3 and elsewhere[25-27].

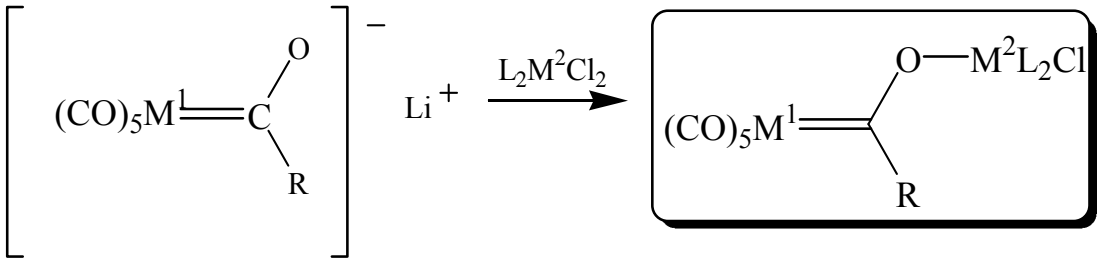

4.1. M^2 = Zr, L = Cp
4.2. M^1 = W, R = Me, M^2 = Zr, L=Cp
4.3. M^1 = Cr, R = Me, M^2 = Zr, L=Cp
4.4. M^2 = Zr, L = Cp*
4.5. M^1 = W, R = Me, M^2 = Zr, L=Cp*

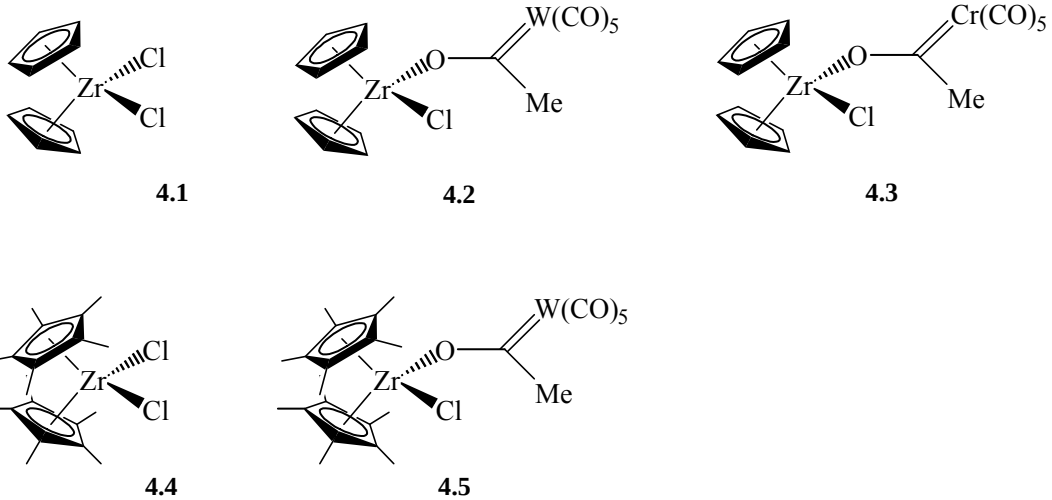

4.1 **4.2** **4.3**

4.4 **4.5**

Scheme 4.1: General reaction scheme showing the synthesis of metalloxycarbene complexes

4.2.3 General polymerization procedure

All the catalyst preparations for polymerization reactions were carried out under an inert gas atmosphere using standard Schlenk techniques. Polymerization reactions were performed in a 350 ml stainless steel batch reactor (Parr) fitted with an inlet valve and pressure gauge. A glass liner was used in the reactor. Generally, the reagents were introduced into the reactor in the following order: catalyst, MAO and the comonomer (Scheme 4.3). For each catalyst, ca. 5.5 x 10^{-3} mmol in 30 ml of toluene were used per run. Amounts of 1-pentene in the feed were varied from ≈ 10 to 60 mol% (Table 4.1) relative to the total number of moles of monomers. Thereafter, the reactor was saturated with ethylene gas, kept constant at about 5 g for each run. The catalyst/MAO ratio was kept at 1:1 000 throughout. All the reactions were carried out at room temperature over a period of 3 h. The polymers were isolated by precipitation in acidic methanol, washed thoroughly with methanol and subsequently dried in vacuum at 65 °C for 10 h.

4.2.4 Characterization of the polymers

The structures of the copolymers were determined using ^{13}C NMR spectroscopy, in 1,2,4-trichlorobenzene/C_6D_6 (9:1) as solvent and measured at 100 °C on a Varian VXR-300 (75 MHz) NMR spectrometer.

Molecular weights of the polymers were determined using a PL 220 chromatograph from Polymer Laboratories fitted with five Waters Styragel columns (HT 2 – 6), at a

flow rate of 1 ml/min in 1,2,4-trichlorobenzene at 140 ºC, relative to narrowly distributed polystyrene standards. The eluent was stabilized with Irganox 1010 to prevent degradation.

Thermal analyses were conducted under nitrogen on a Mettler Toledo DSC 822, at a heating and cooling rate of 10 °C/min, using about 6 mg of the samples. Two heating cycles and one cooling cycle were run. The maxima and minima of the second heating and cooling curves were analyzed and recorded as melting and crystallization temperatures respectively.

A CRYSTAF apparatus, model 200 from PolymerChar S.A (Valencia, Spain), was used for fractionation. Samples (20 mg) were dissolved in 30 ml of distilled 1,2,4-trichlorobenzene at 160 ^{o}C. After dissolution, the temperature was decreased at a rate of 0.1 °C/min.

Infrared spectra were acquired using a Nicolet Nexus spectrometer in ATR-Mode and Omnic 5.2 software for interpretation. Typically 60 scans at a resolution of 2 cm^{-1} were accumulated for each sample.

An LC-transform Model 300 from LabConnections, coupled to a Waters 150C chromatograph (columns HT 2 – 6) was used for the SEC-FTIR analyses. The stage temperature was 160 °C, the temperature of the nozzle 125 °C and the transfer line was operated at 150 °C. The rotating speed of the Germanium disc was 10 °/min.

4.3 RESULTS AND DISCUSSION

Ethylene/1-pentene copolymers were synthesized using two sets of catalyst systems. The first set contained two cyclopentadienyl (Cp) ligands and the second set methyl substituted cyclopentadienyl, Cp^* ligands. The first catalysts were Cp_2ZrCl_2 (**4.1**), $[(CO)_5W{=}C(Me)OZr(Cp)_2Cl]$ (**4.2**) and $[(CO)_5Cr{=}C(Me)OZr(Cp)_2Cl]$ (**3**) while the Cp* analogues comprised of $Cp^*{}_2ZrCl_2$ (**4.4**) , $[(CO)_5W{=}C(Me)OZr(Cp^*)_2Cl]$ (**4.5**). Section 4.3.1 outlines results of the copolymers produced with Cp-containing catalyst systems, the results of the copolymers synthesized using Cp* analogues are discussed in Section 4.3.2.

4.3.1 Copolymers synthesized using Cp-containing catalyst systems

4.3.2.1 Molecular weight and molecular weight distribution

Ethylene/1-pentene copolymers were synthesized using catalyst precursors shown in Scheme 4.2. The catalytic results and molecular characterization data are summarized in Table 4.1. The molecular weight distribution profiles of the copolymers synthesized with **4.1**, **4.2** and **4.3**/MAO are shown in Figures 4.1, 4.2, and 4.3, respectively.

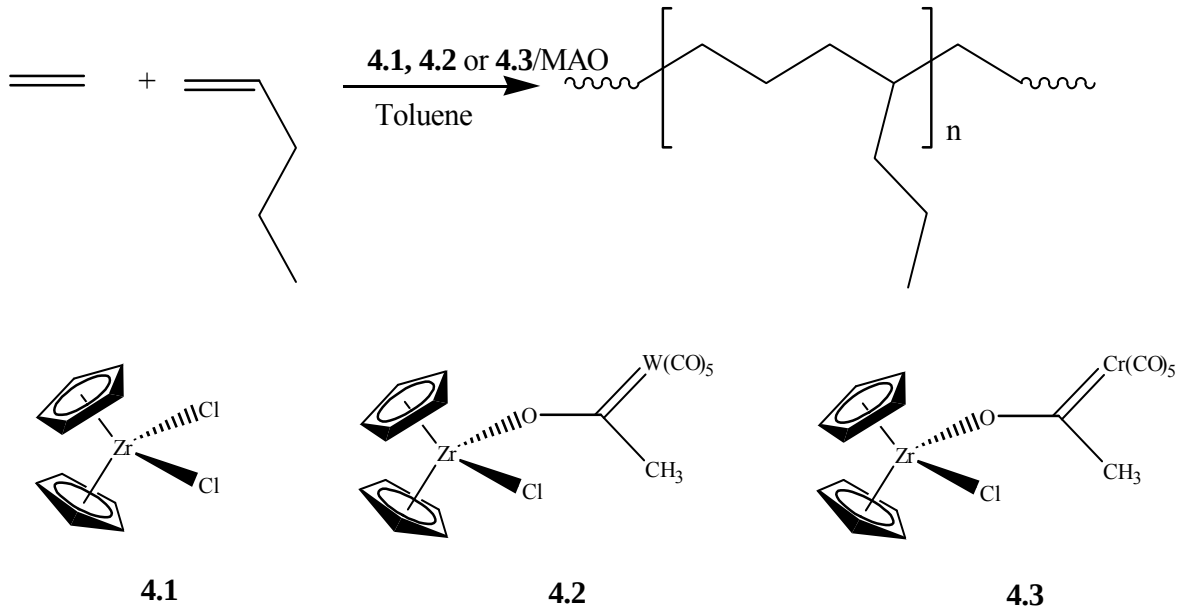

4.1 **4.2** **4.3**

Scheme 4.2: Polymerization reaction scheme for ethylene/1-pentene copolymers

The homopolymerization activities of all three catalyst systems are comparable. The copolymerization activities of **4.2** and **4.3**/MAO were generally above 200 kg/(mol.h) while those of **4.1**/MAO dropped significantly below 100 kg/(mol.h) when the comonomer in the feed was increased. The influence of the anionic carbene ligand on catalysis can clearly be seen when comparing the molecular weights of the copolymers produced with metalloxycarbenes and metallocenes.

Table 4.1: The NMR, GPC, DSC and CRYSTAF results as well as polymerization parameters for ethylene/1-pentene copolymers obtained using **4.1** and **4.2**/MAO

Sample code	Catalyst No	1-pentene in feed [mol-%]	1-pentene in the copolymer [mol-%]	CRYSTAF Sol. fraction (%)	$T_{c\ CRYSTAF}$[a] (°C)	$T_{c\ DSC}$[b] (°C)	$T_{m\ DSC}$[c] (°C)	M_n[d] (g/mol)	M_w[d] (g/mol)	PDI[d]	Activity (kg/(mol.h))
ZrA	4.1	0	0	0	87.7	119.5	132.4	41 700	119 000	2.8	133.3
Zr1	4.1	29.1	9.0	31.7	78.7	106.2	114.7	7 000	26 000	3.8	503.0
Zr2	4.1	60.6	14.9	58.2	54.7	95.3	102.2	6 300	15 700	2.5	67.9
Zr3	4.1	29.1	4.5	5.6	73.2	104.4	116.8	14 200	39 400	2.8	64.2
Zr4	4.1	16.1	7.0	15.6	78.3	108.6	118.1	13 000	46 500	3.6	84.8
Zr5	4.1	33.9	8.6	22.7	76.8	96.0	105.2	17 400	40 000	2.3	84.2
Zr6	4.1	47.3	16.1	60.1	non	92.8	100.9	8 500	20 000	2.4	109.1
Zr7	4.1	55.2	5.2	8.6	76.4	104.5	116.8	29 600	87 000	2.9	46.5
WA	4.2	0	0	0	87.5	116.9	134.1	44 900	225 900	5.0	266.7
W1	4.2	9.3	0.2	0	86.2	114.8	133.8	235 600	772 900	3.3	176.4
W3	4.2	29.1	2.3	7.4	85.3	113.8	130.0	47 500	245 100	5.2	283.0
W4	4.2	45.1	2.0	8.3	83.9	110.6	129.9	18 700	156 200	8.4	357.6
W5	4.2	55.2	3.9	10	82.3	111.0	124.6	18 300	218 400	11.9	262.4
W6	4.2	60.6	7.0	35.9	80.3	107.0	119.4	2 500	126 600	50.5	285.5
W7	4.2	43.5	2.0	10.7	84.3	114.1	127.3	26 500	185 500	7.0	254.5
W8	4.2	50.6	5.3	12.3	81.8	110.4	122.9	81 700	317 300	3.9	309.1
W9	4.2	64.2	3.9	14.6	82.7	112.0	125.0	20 000	321 100	16.0	280.6

[a] crystallization temperature determined using CRYSTAF; [b] crystallization temperature determined using DSC; [c] melting temperature determined using DSC ; [d] molecular weight property determined using SEC

Table 4.2: The NMR, GPC, DSC and CRYSTAF results as well as polymerization parameters for ethylene/1-pentene copolymers obtained using **4.3**/MAO

Sample code	Catalyst No.	1-pentene in feed [mol-%]	1-pentene in the copolymer [mol-%]	CRYSTAF Sol. fraction (%)	$T_{c\ CRYSTAF}$[a] (^oC)	$T_{c\ DSC}$[b] (^oC)	$T_{m\ DSC}$[c] (^oC)	M_n[d] (g/mol)	M_w[d] (g/mol)	PDI[d]	Activity (kg/(mol.h))
CRB	4.3	0.0	0.0	3.4	86.0	118.2	132.9	19 800	168 000	8.5	260.6
Cr1	4.3	17.0	9.10	27.2	79.2	107.2	115.9	7 600	35 000	4.7	280.0
Cr2	4.3	20.4	12.48	51.2	73.4	102.0	111.9	4 100	57 600	14.2	254.5
Cr3	4.3	38.1	4.89	16.3	79.6	114.4	119.1	60 300	390 000	6.4	207.3
Cr4	4.3	45.1	10.99	nd[e]	nd	101.6	110.4	8 900	39 800	4.5	195.8
Cr5	4.3	39.1	4.81	12.9	85.5	106.7	116.4	25 000	106 000	4.3	115.2
Cr6	4.3	23.5	9.16	nd	nd	102.3	110.9	27 700	174 000	6.3	68.5
CR13	4.3	33.9	7.5	nd	nd	102.4	105.6	10 200	28 400	2.8	200.0
Cr14	4.3	33.9	4.8	10.8	82.7	108.2	118.2	34 000	96 400	2.8	261.8
Cr15	4.3	41.8	8.3	5.2	80.4	104.8	109.8	15 200	43 100	2.8	60.6

[a] crystallization temperature determined using CRYSTAF; [b] crystallization temperature determined using DSC; [c] melting temperature determined using DSC ; [d] molecular weight property determined using SEC; [e] nd = not detemined

Generally, ethylene/1-pentene copolymers synthesized with metalloxycarbene catalyst systems (**4.2** and **4.3**/MAO) have high weight average molecular weights (M_w's) – above 100 000 g/mol - and broad polydispersities. In contrast, copolymers with Cp_2ZrCl_2 (**4.1**)/MAO had low M_w's - below 100 000 g/mol - and relatively narrow polydispersities. Broad MWD's are consistent with the homopolymerization results discussed earlier in Chapter 3. Narrow molecular weight distributions for polymers produced with **4.1**/MAO were expected since metallocenes are known to produce polymers with PDI's of about 2[11,28,29].

The majority of the polymers synthesized with $[(CO)_5Cr=C(Me)OZr(Cp)_2Cl]$ (**4.3**)]/MAO have lower M_w and relatively narrower polydispersity indices compared to those synthesized with $[(CO)_5W=C(Me)OZr(Cp)_2Cl]$ (**4.2**)]/MAO (see Table 4.2). However, as in the case of **4.2**/MAO, most of the samples displayed bimodal molecular weight distributions (Figure 4.3). The reason could be differences in electronic distributions within the carbene ligands arising from differences in the electronegativities between tungsten and chromium.

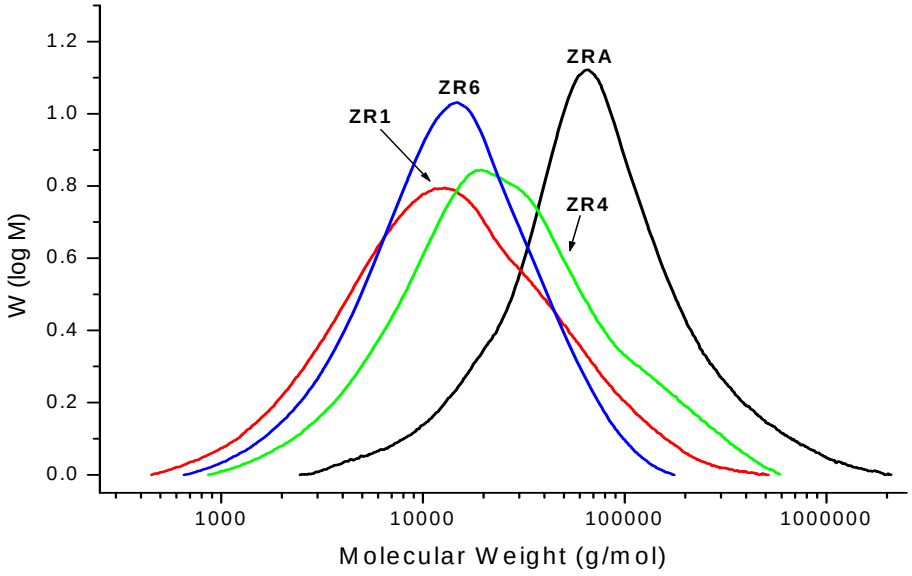

Figure 4.1: Molecular weight distribution curves of ethylene/1-pentene copolymers prepared with Cp_2ZrCl_2 (**4.1**)/MAO

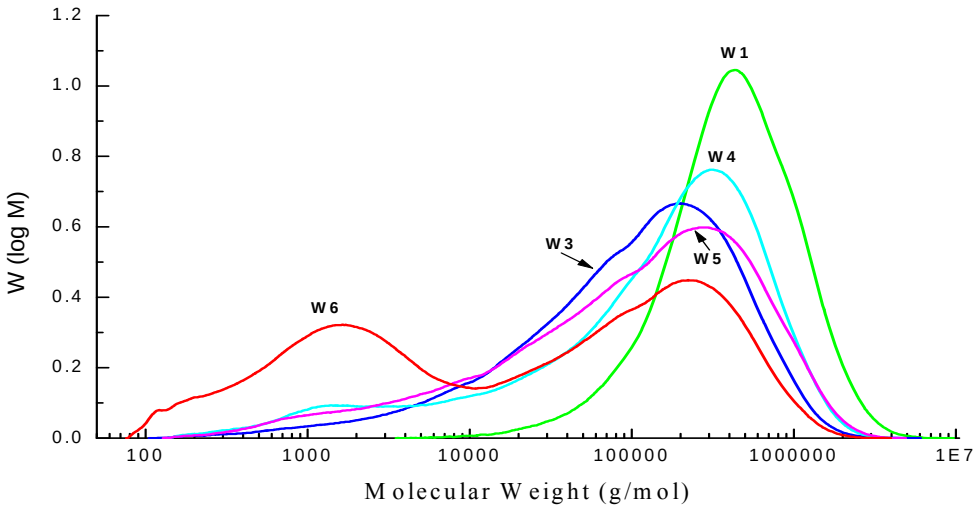

Figure 4.2: Molecular weight distribution curves of ethylene/1-pentene copolymers obtained with **4.2**/MAO

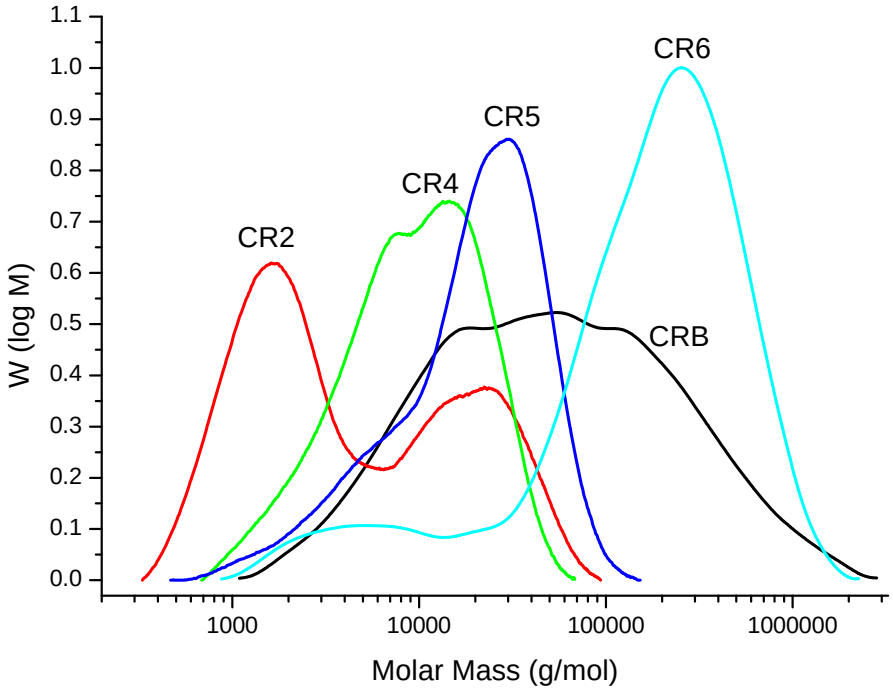

Figure 4.3: Molecular weight distribution curves of ethylene/1-pentene copolymers obtained with **4.3**/MAO

The average molecular weight of ethylene/1-pentene copolymers produced by all three catalyst systems decrease with increasing comonomer content in the copolymers (Table 4.1 and 4.2). The influence of comonomer on the molecular weight properties of the copolymers is detailed in the following section.

We still can't explain the higher average molecular weight of ethylene/1-pentene copolymers produced with metalloxycarbenes in comparison to those obtained with

Cp_2ZrCl_2 (**4.1**)/MAO. It is not impossible that steric factors (but not directly at the active centre, *vide infra*) could be involved. Usually, an increase in the steric factors around the active site or coordination center brought about by a bulky ligand retards β-hydride elimination, making chain transfer to the monomer more difficult and resulting in the formation of high molecular weight polymers or copolymers [28-30]. Ko et al investigated the copolymerization of ethylene with propylene using Cp_2ZrCl_2 and the same catalyst supported with NaY[28]. The results they obtained showed that copolymers produced using a catalyst with high steric factors - Cp_2ZrCl_2/NaY/MAO – have high molecular weights. A similar behaviour was observed by Czaja et al. when they investigated the copolymerization of ethylene with 1-hexene using Cp_2ZrCl_2(**4.1**) supported with $MgCl_2$[39]. The examples, however, differ from the present situation.

It is known that ionic pair formation is extremely important in determining catalytic activity. Due to the relatively long Zr-O bond (2.034 Å) in the complex $[(CO)_5W{=}C(Me)OZr(Cp)_2Cl]$ (**4.2**)/MAO (refer to Chapter 3 for molecular structure), we assume that this bond would be heterolytically cleaved in the formation of the active cationic catalyst just as one Cl would be replaced by CH_3 from MAO. This would result in the formation of a Cp_2ZrMe^+ species (as in the case of **4.1**/MAO) and adduct formation between $(CO)_5W{=}C(Me)O^-$ and MAO. The consequent weak ion pair interaction could be responsible for both the high molecular weights of the ethylene/1-pentene copolymers, as a result of hindered β-H elimination reactions, as well as the higher catalytic activity exhibited by **4.2**/MAO compared to **4.1**/MAO.

However, other types of ion pair interactions could also be responsible for the generation of different types of active species producing bimodal and multimodal copolymers.

4.3.2.2 The compositional and structural analysis of ethylene/1-pentene copolymers using ^{13}C NMR

Typical ethylene/1-pentene ^{13}C NMR spectra with resonance assignments are shown in Figures 4.4 and 4.5. Such spectra were used to determine the amount of comonomer incorporation[31]. The copolymers synthesized with **4.1**/MAO have higher amount of 1-pentene (Table 4.1) than copolymers produced with metalloxycarbenes when comparable feed stream compositions were used.

In order to fully understand the comonomer incorporation behaviour, the amount of 1-pentene content was not limited in this study. The comonomer incorporation for copolymers produced with **4.2**/MAO could not exceed 7% even after increasing the 1-pentene in the feed stream to more than 60% but decreased instead (for example W9) (refer to Table 4.1). However, copolymers produced with $[(CO)_5Cr=C(Me)OZr(Cp)_2Cl]$ (**4.3**)]/MAO display superior comonomer incorporation in comparison to those produced with **4.2**/MAO.

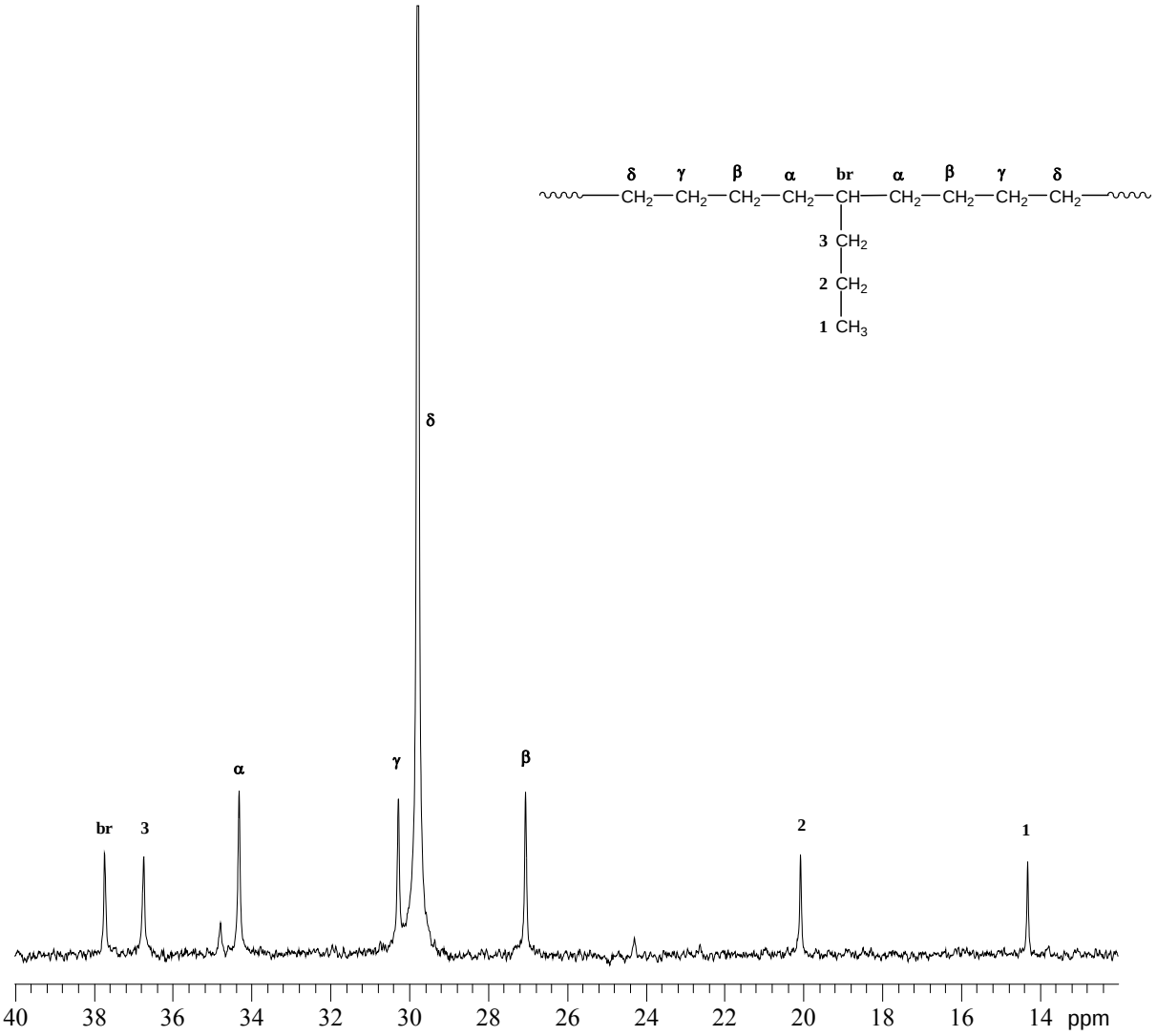

Figure 4.4: ^{13}C NMR spectrum of ethylene/1-pentene (ZR6) copolymer with resonance assignments

As shown in Table 4.2 several samples synthesized using **4.3**/MAO have comonomer contents of between 7 and 12%. The low comonomer incorporation in copolymers produced with metalloxycarbenes could be due to the chain length of 1-pentene and increased chain transfer reactions to the comonomer.

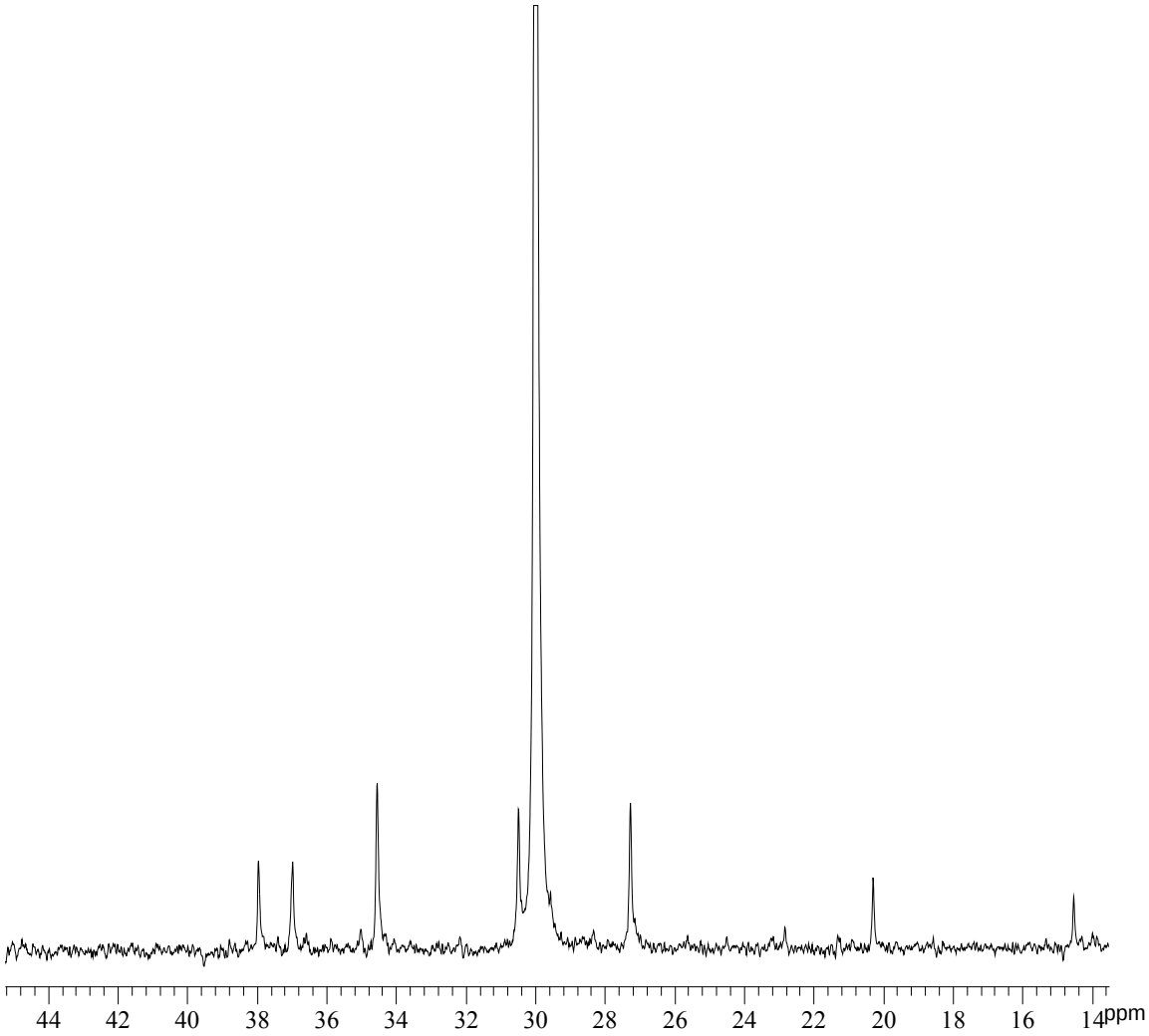

Figure 4.5: ^{13}C NMR spectrum of ethylene/1-pentene (W6) copolymer (compare with Figure 4.4 for resonance assignments)

During polymerization chain propagation competes with chain termination reactions. High comonomer and cocatalyst ratios, among others, promote chain transfer reactions which could lead to chain termination[32-36]. While steric hindrance in **4.2**/MAO helps to increase the molecular weight by suppressing chain termination

reactions, increasing comonomer concentration reaches a point where chain transfer to the monomer overcomes chain propagation, ultimately leading to lower average molecular weight and finally, low comonomer incorporation[28,37,38]. As already mentioned in the previous section, a closer look at the molecular weights of copolymers especially those produced with **4.2** and **4.3** indicate that increasing 1-pentene in the feed generally leads to a decrease in the weight average molecular weight. Since the comonomer ratio was kept constant at 1000 throughout the study, it could be speculated that higher 1-pentene concentration enhances chain transfer reactions to the comonomer resulting in low comonomer incorporation and reduced molecular weight. This phenomenon has been previously observed with various catalyst systems during α-olefin copolymerizations[28,33,39]. It has been widely proposed that α-olefins in high concentrations act as chain transfer agents, resulting in low incorporation and low molecular weight. Although the chemical structure of $(CO)_5W{=}C(Me)OZr(Cp)_2Cl$ (**4.2**) would fit metallocene definition[40-42], the molecular weight distributions of polymers or copolymers produced with this catalyst system at ambient temperature strengthen the conclusion we made earlier in Chapter 3 that such catalyst systems are not metallocene catalysts but rather behave somewhat like Ziegler-Natta-type catalysts.

4.3.2.3 Thermal (melting and crystallization) properties

The melting and crystallization temperatures for copolymers synthesized with **4.1** and **4.2**/MAO, respectively, were plotted as a function of comonomer content and the

results are shown in Figures 4.6 and 4.7. For a similar plot of copolymers produced with **4.3**/MAO please refer to Appendix A (Figure A1). Most of the copolymers synthesized with **4.1** and **4.3**/MAO show broad and multiple (two or three) melting and crystallisation transitions as measured by DSC while those produced with **4.2**/MAO only show a single transition during both heating and cooling. The melting and crystallization temperatures reported in Table 4.1 are values corresponding to the highly crystalline materials only. As clearly shown in these figures, the melting and crystallization temperatures of all copolymers generally decrease with increasing comonomer content. The melting and crystallization temperatures of copolymers produced with $[(CO)_5W{=}C(Me)OZr(Cp)_2Cl]$ (**4.2**)]/MAO follow a more linear decrease while those synthesized with **4.1** and **4.3**/MAO are scattered. Furthermore, when comparing samples with similar amounts of 1-pentene, comonomer incorporation has a significant impact on reduction of melting and crystallization temperatures in copolymers synthesized with **4.1**/MAO compared to those produced with metalloxycarbenes. For example, sample ZR12 with 5.2 [mol-%] has crystallization and melting temperatures of 104.5 and 116.8 ^{o}C, respectively while W8 with 5.3 [mol-%] crystallizes at 110.4 ^{o}C and melts at 122.9 ^{o}C.

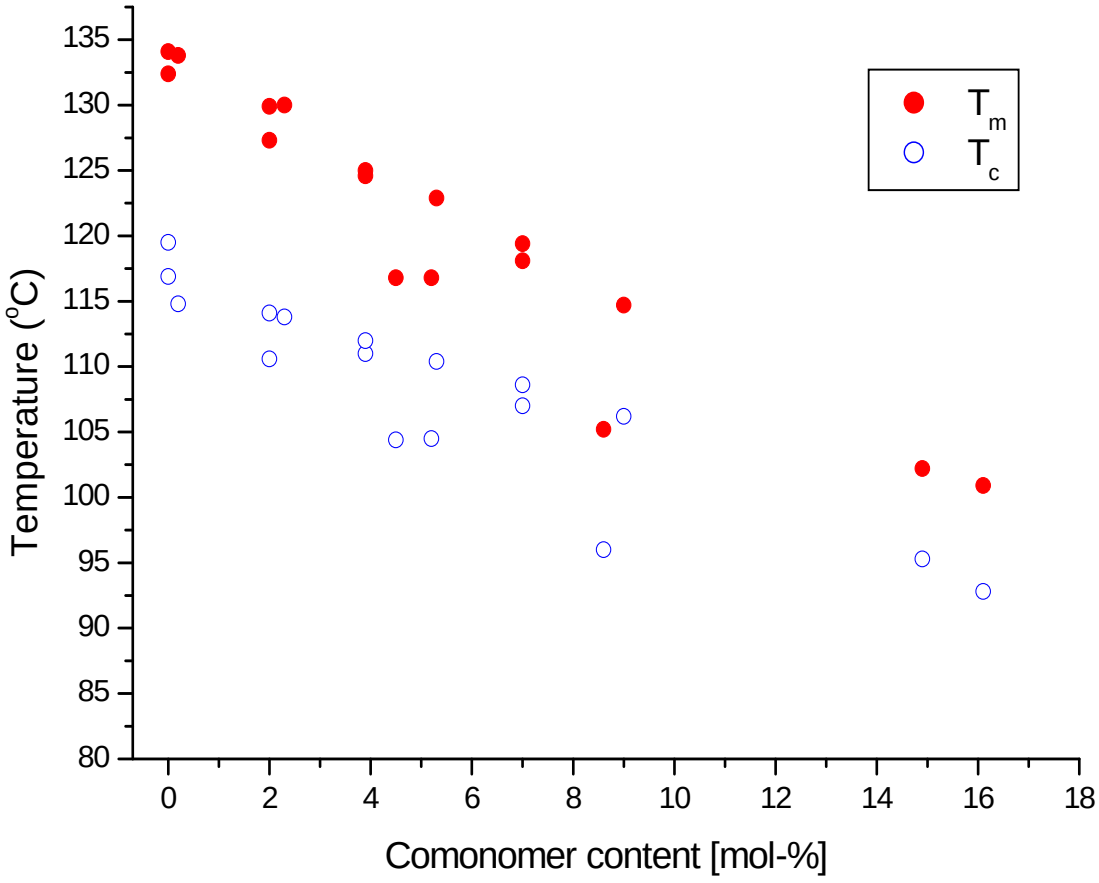

Figure 4.6: Melting (T_m) and crystallization (T_c) temperatures vs. comonomer content of copolymers produced with **4.1**/MAO

The multiple DSC transitions could indicate that the copolymers have broad CCD's. Alternatively, these can result from a combination of melting and crystallization processes. Multiple transitions can be separated by applying different heating rates as shown in Figure 4.8. For example, three distinct melting peaks are observed for sample ZR2 (Figure 4.8) during slow heating.

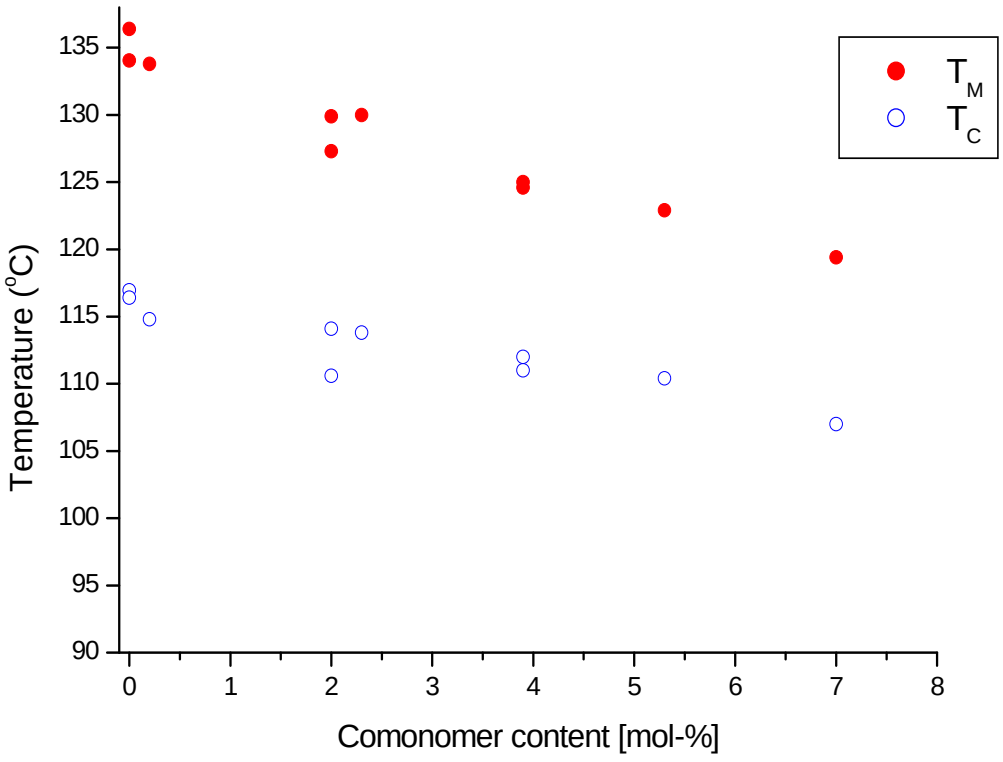

Figure 4.7: Melting (T_m) and crystallization (T_c) temperatures vs. comonomer content of copolymers produced with **4.2**/MAO

However, when fast heating rates are applied (Figure 4.8), a re-crystallization peak (indicated by an arrow) disappear owing to the fact that the chains are not given enough time to re-crystallize. Nevertheless, two melting peaks remain even after applying fast heating scans.

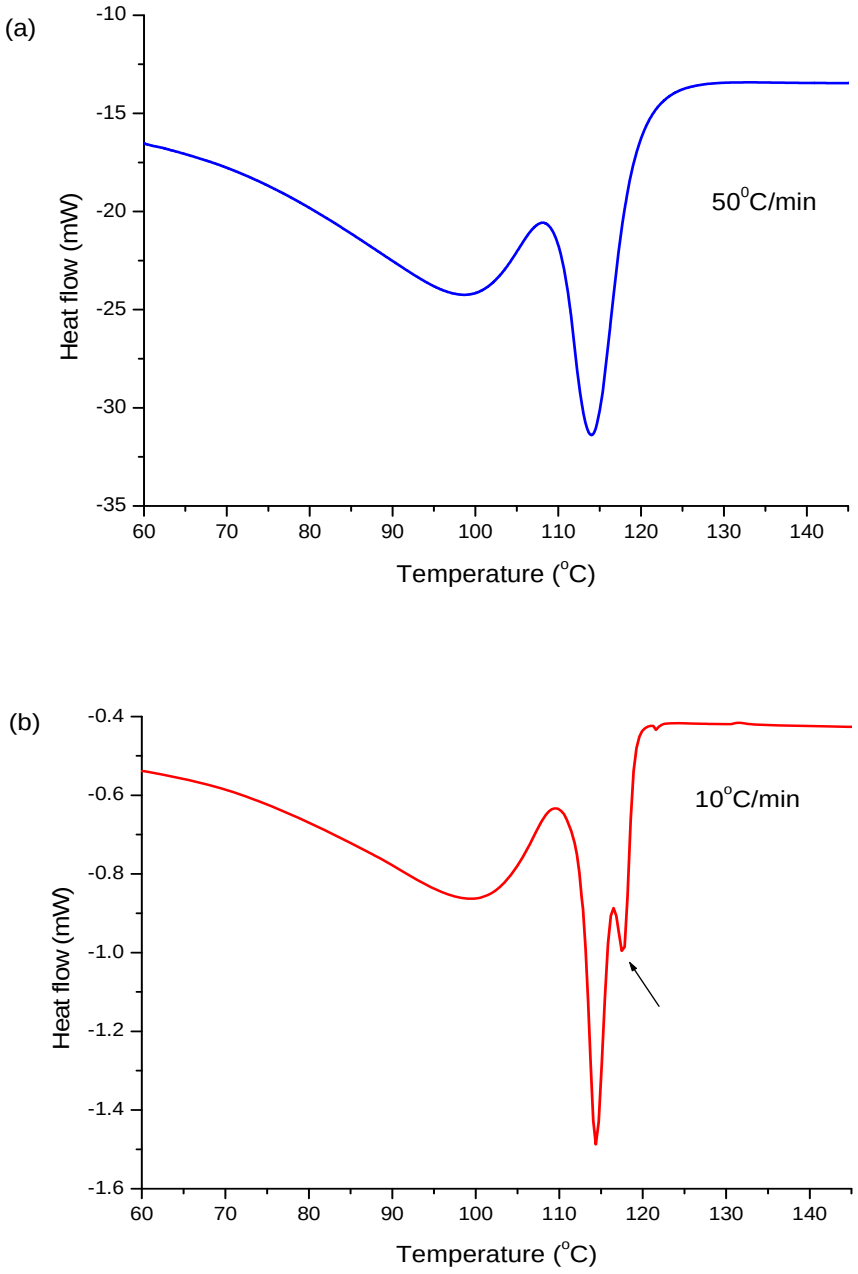

Figure 4.8: DSC heating curves of sample ZR2 measured using a heating rate of 50 ^{o}C/min (a) and 10 ^{o}C/min (b)

Multiple DSC transitions for metallocene catalyzed polymers have previously been associated with broader CCD of the copolymers[43]. Other studies have shown that the active sites in metallocene catalyst systems in general, are not all homogeneous resulting in the formation of polymers with multiple thermal transitions or broad CCD or high degree of chemical heterogeneity[44,45].

Although all the copolymers are generally characterized by heterogeneous comonomer incorporation or broad CCD's, the different behaviour observed in the melting and crystallization temperature vs. comonomer incorporation plots, could indicate that each of these three catalyst systems behave in a different manner during copolymerization which affect 1-pentene incorporation. It is important to interpret DSC results with other fractionation techniques, especially SEC-FTIR, which will be explained in detail later in this chapter. Furthermore, advanced molecular weight fractionation techniques were carried out in Chapter 5 to further study the polymerization behaviour of these catalyst systems especially the SCBD along the M_w axis.

The chemical heterogeneity describes the distribution of comonomers, endgroups and microstructural parameters along and perpendicular to the molecular weight axis. These microstructural parameters determine the end-properties of the polymers and also indicate how a particular catalyst system behaves during polymerization. The knowledge of such parameters is crucial for catalyst design. Typically, chemical

heterogeneity or CCD of semi-crystalline polymers is studied using fractionation techniques. These techniques involve polymer fractionation according to composition or molecular weight coupled with spectroscopic detection. As already observed in DSC analyses of ethylene/1-pentene copolymers, a slight variation in composition significantly shifts crystallization and melting properties of the resulting copolymer. Recently, the crystallization analysis fractionation (CRYSTAF) technique has been used extensively to study the composition of polyolefins copolymers[46].

CRYSTAF fractionates semi-crystalline materials according to their crystallizability or composition in solution. Typically, a sample is dissolved at a temperature above crystallization. After complete dissolution, the polymer is allowed to crystallize by reducing the temperature at a slow rate. Aliquots of the polymer solution are filtered and the concentration of the polymer in solution analyzed by an infrared detector. Details of this technique have been published earlier[47,48]. A typical CRYSTAF profile (Figure 4.9) consists of a cumulative curve and its first derivative.

The first derivative is generally associated with the CCD of the polymer and will be referred to as CRYSTAF profile or curve in this study. Figures 4.10 and 4.11 show the overlay of the CRYSTAF profiles of ethylene/1-pentene copolymers synthesized with **4.1** and **4.2**/MAO, respectively.

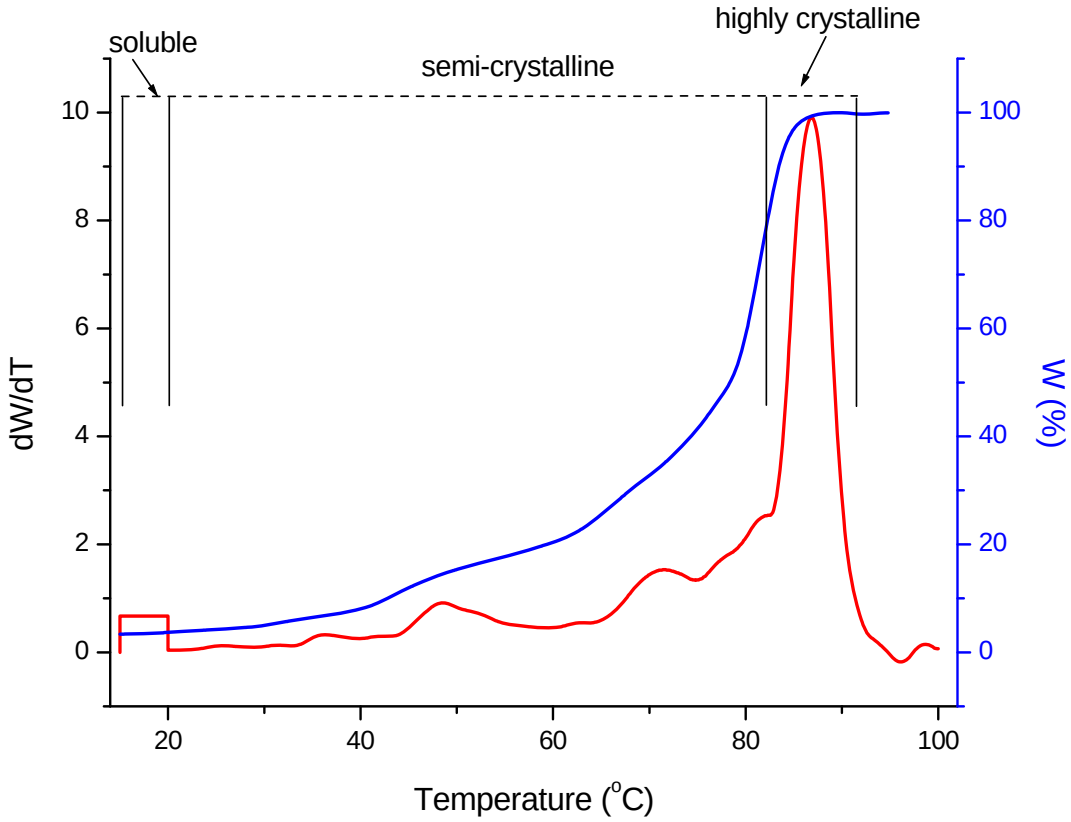

Figure 4.9: Typical CRYSTAF profile for semi-crystalline polymers

In general, the crystallization profiles for all series slightly broaden relative to the homopolymers with increasing comonomer content and simultaneously the amount of soluble fraction increases. These trends are in agreement with CRYSTAF results which have been obtained for copolymers synthesized with *rac*-Et(Ind)$_2$ZrCl$_2$/MAO[49,50] and elsewhere[46]. For both series, the peak crystallization temperatures decrease with an increase in comonomer content as already observed in DSC analysis.

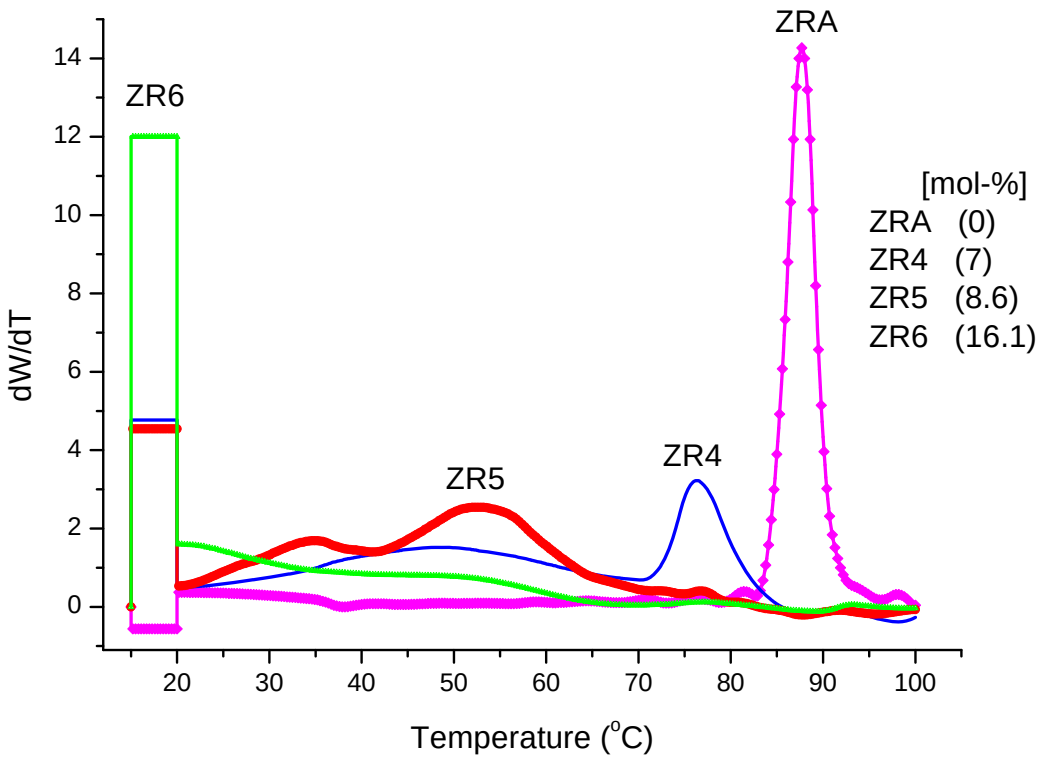

Figure 4.10: CRYSTAF profiles of ethylene/1-pentene copolymers synthesized with **4.1**/MAO

The crystallization peak finally disappears for copolymers with high comonomer content, e.g. ZR6. Comparing the CRYSTAF profiles of the copolymers with similar amounts or percentages of comonomer from both series, it is clear that copolymers synthesized with **4.1**/MAO show crystallization below the main peak, whereas the same behaviour is not observed for copolymers produced with **4.2**/MAO.

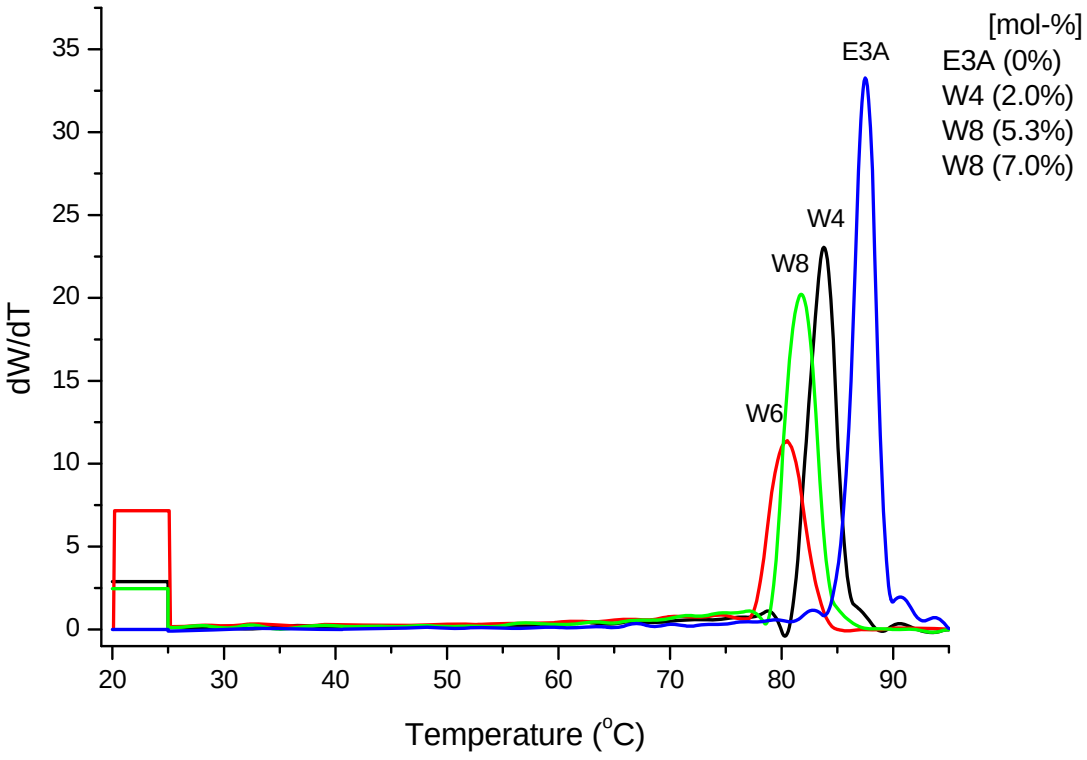

Figure 4.11: CRYSTAF profiles of ethylene/1-pentene copolymers synthesized with **4.2**/MAO

The behaviour of the copolymers produced with **4.3**/MAO is intermediate between the two. Again, we see different crystallization behaviour of the copolymers synthesized with these three catalysts similar to the observation made in DSC analyses. In order to study the distribution of 1-pentene along the molecular weight axis, the copolymers were further analyzed using FTIR and SEC-FTIR via LC-Transform and the results are discussed in the following section.

4.3.2.4 The short chain branching distribution (SCBD) analysis of ethylene/1-pentene copolymers

The compositional analysis of ethylene copolymers by FTIR is well established and very good papers in this area are available[51-55]. McRae and Maddams used infrared spectroscopic methods to study types of alkyl branches in low-branched polyethylene and ethylene-alkene copolymers[51]. Neves et al. fractionated ethylene/1-butene copolymers using preparative temperature rising elution fractionation (TREF) and used FTIR to study chemical composition of the resulting fractions[52]. Blitz et al. quantitatively and qualitatively characterized methyl, ethyl, propyl, butyl, isobutyl and hexyl branches in LLDPE using transmission FTIR[53]. A typical IR spectrum of an ethylene/1-pentene copolymer with signal assignments is shown in Figure 4.12.

The absorption bands at 1379 cm^{-1} and 1460 cm^{-1} correspond to the methyl and methylene groups, respectively. Figure 4.13 depicts the enlargement of the unsaturated endgroup region in the FTIR spectrum. The absorption bands at 886 cm^{-1}, 908 cm^{-1} and 966 cm^{-1}correspond to vinylidene ($R_2C=CH_2$),vinyl ($RCH=CH_2$) and to trans-vinylene, respectively. FTIR, however, only gives information about the average composition. The distribution of different functional groups can be profiled along the molecular weight axis using the SEC-FTIR technique.

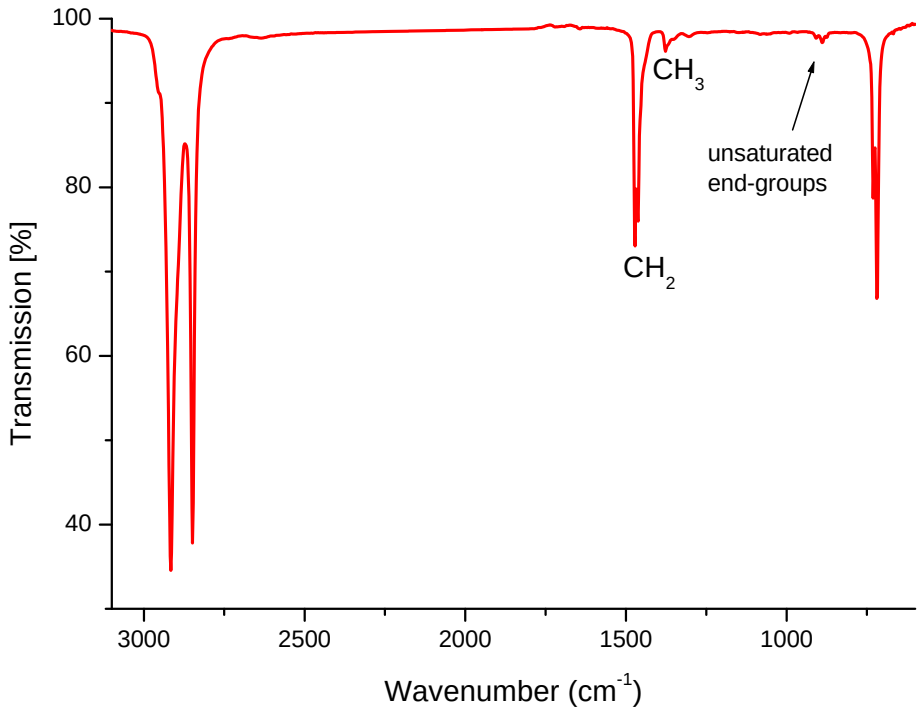

Figure 4.12: Typical FTIR spectrum of ethylene/1-pentene copolymer

In the LC-Transform approach, the polymer in the eluent is deposited on a rotating Germanium disc via nebulization of eluent. The trace on the polymer sample carrier, in this case a Germanium disc, is then analyzed off-line using FTIR (Scheme 4.3). From the spectra taken around the disc, the software re-constructs the Gram-Schmidt plot which gives concentration profiles that resemble refractive index signals (or molecular weight distribution curves) of high temperature SEC. Chemigrams are then generated to show the intensity of a particular chosen absorption along the molecular weight axis[56,57].

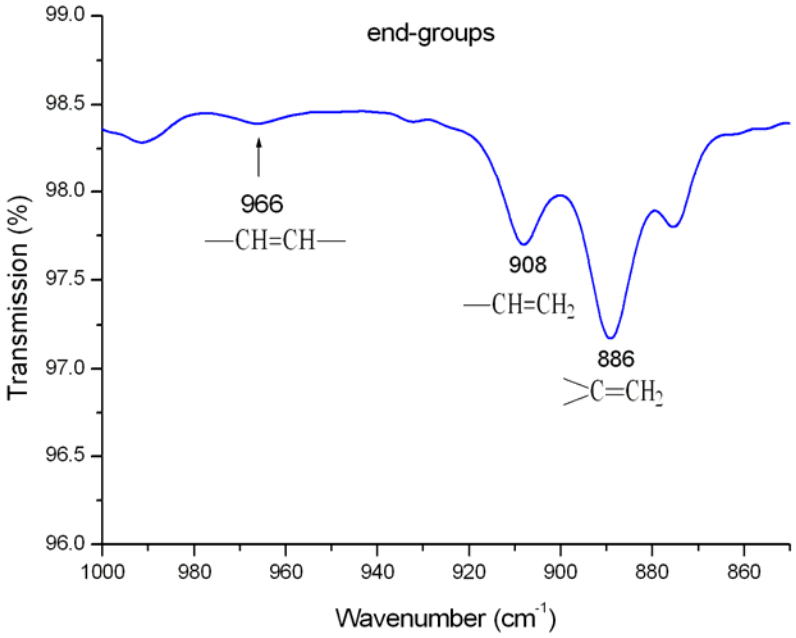

Figure 4.13: Unsaturated end-group region of the FTIR spectrum of ethylene/1-pentene copolymers

A chemigram at 1376 cm^{-1} was constructed for the methyl groups of the comonomer, and at 1465 cm^{-1} for the methylene units of the main chain. A ratio of these chemigrams, i.e. a chemigram of $CH_3/(CH_3 + CH_2)$ then reflects the relative comonomer concentration over the molecular weight distribution. The SEC-FTIR analyses of the copolymers obtained using **4.1**, **4.2** and **4.3**/MAO are shown in Figures 4.14, 4.15 and 4.16. All copolymers investigated, regardless of the catalyst used, show an increase in the 1-pentene concentration (CH_3 concentration) towards the low molecular weight fraction (Figures 4.15 and 4.16).

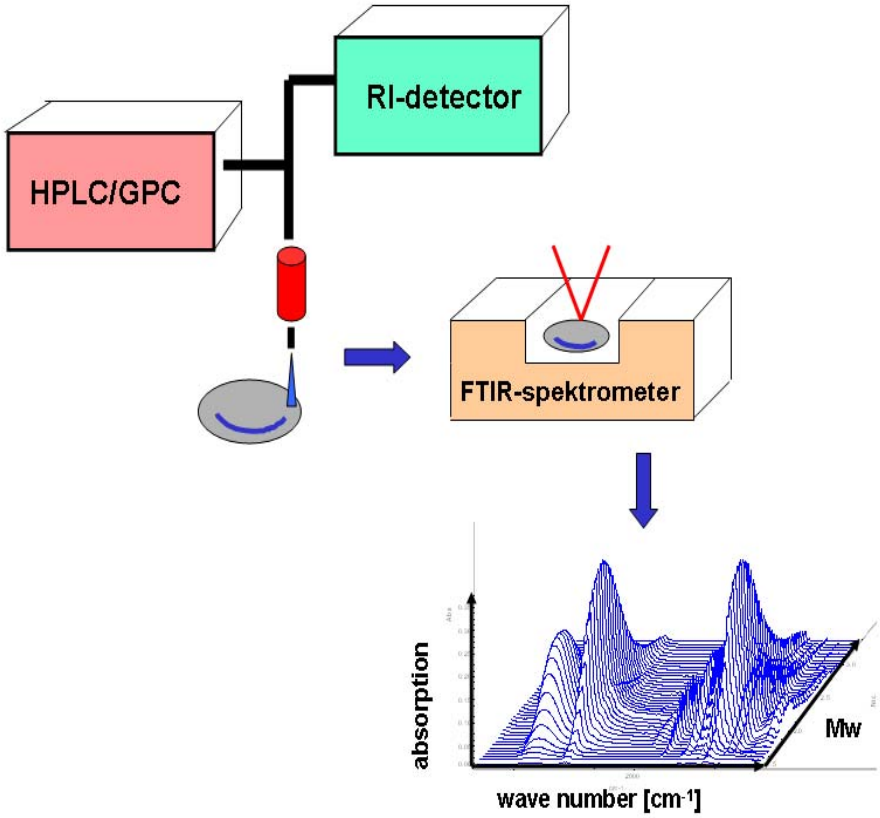

Scheme 4.3: Schematic representation of fractionation of polyolefins using SEC-FTIR

However, copolymers synthesized with metalloxycarbenes (W5, W6, CR2 and CR6) indicate a sharper increase compared to those synthesized with Cp_2ZrCl_2 (**4.1**)/MAO (ZR3 and ZR5). The heterogeneous comonomer distribution on copolymers obtained by both **4.2** and **4.3**/MAO catalyst systems, can be explained by the lack of a bridging ligand which would have restricted the rotation or movements of the Cp-ligands during polymerization.

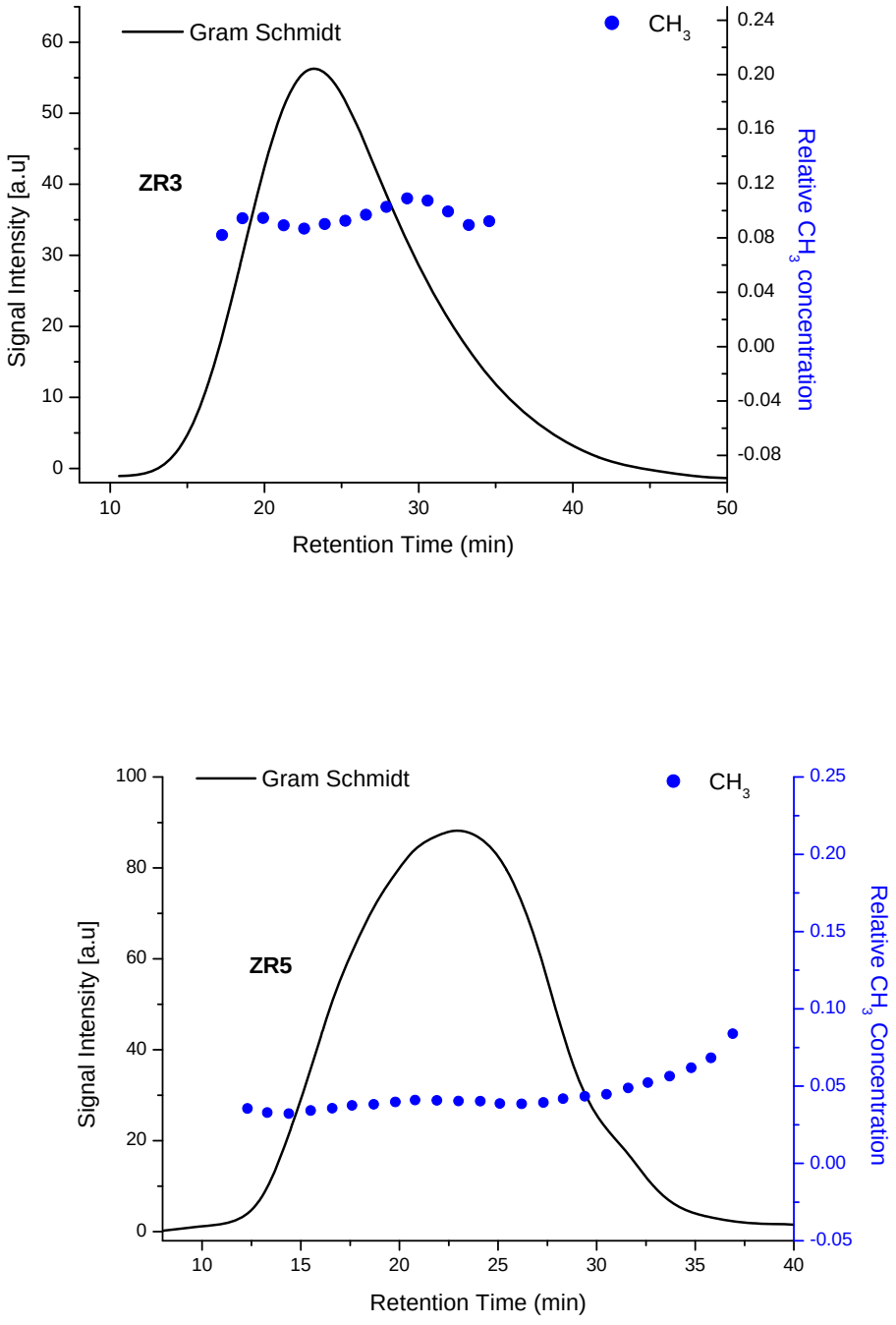

Figure 4.14: SEC-FTIR results of ethylene 1-pentene copolymers synthesized by **4.1**/MAO

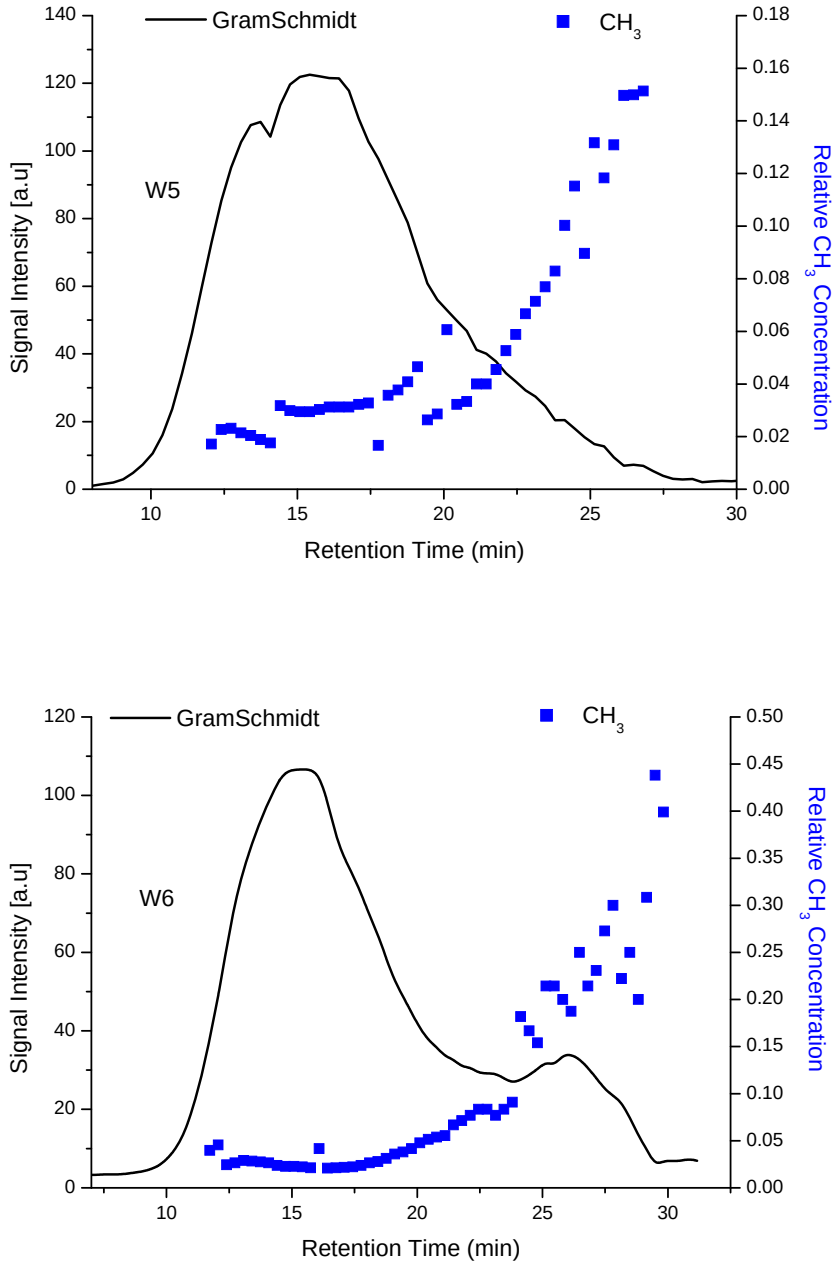

Figure 4.15: SEC-FTIR results of ethylene 1-pentene copolymers synthesized by **4.2**/MAO

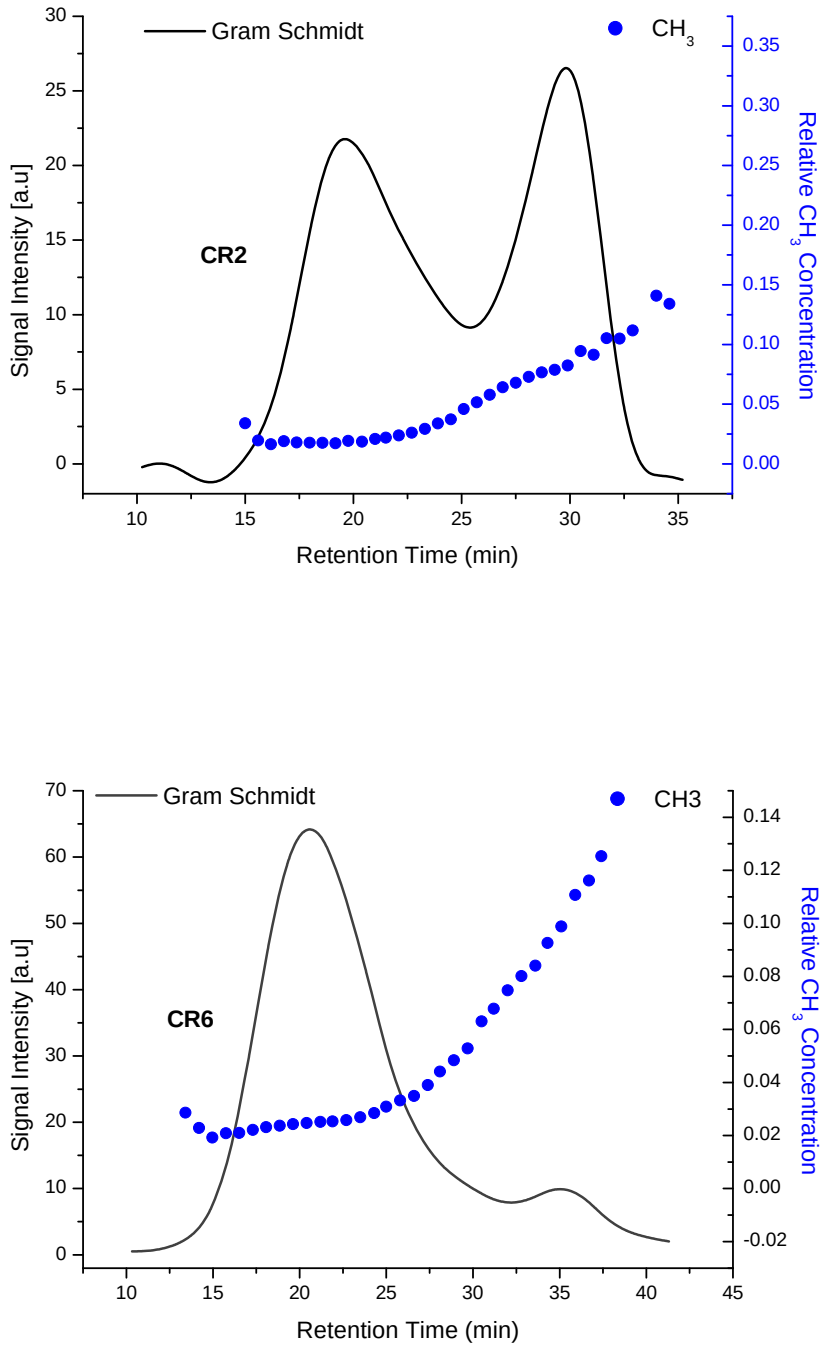

Figure 4.16: SEC-FTIR results of ethylene 1-pentene copolymers synthesized by **4.3**/MAO

Although we are not aware of a study involving SEC-FTIR analysis of polyolefin copolymers synthesized with Cp_2ZrCl_2/MAO, non-*ansa* metallocene catalyst systems have previously shown a heterogeneous comonomer distribution[58]. On the other hand, ethylene/α-olefin copolymers, synthesized using the bridged catalyst system *rac*Et[Ind]$_2$ZrCl$_2$/MAO, which were investigated by us using SEC-FTIR[59], show a more homogeneous comonomer distribution than that observed with the catalysts **4.1**, **4.2** or **4.3**/MAO.

The high degree of heterogeneity of samples synthesized with metalloxycarbenes prompted us to fractionate the samples into soluble and crystallizable fractions in order to further our understanding of CCD and its influence on thermal properties. A simple fractionation experiment (i.e. simple solvent extraction) was conducted for sample W6. This sample was chosen because of its broad crystallization peak, high amount of soluble fraction as observed in CRYSTAF analyses, high comonomer content in this particular series and bimodal distribution. The fractionation was done by refluxing a sample of the copolymer in hexane for 8 hours. The sample was placed in a 25 x 80 mm extraction thimble in a standard Soxhlet apparatus. The soluble fraction remained in the thimble. The soluble fraction was recovered by removing the solvent under vacuum and precipitation in acetone. Both fractions were dried in a vacuum oven and subsequently analyzed. Figure 4.17 shows the ^{13}C NMR spectra (and relative molecular weights) of both fractions. The spectrum of the soluble fraction has intense peaks of 1-pentene, indicating high comonomer concentration. Additional signals could be due to clustering (consecutive insertion of 1-pentene units

in the chain) and end-groups. The latter is significant, since the molecular weight is low. On the other hand, the crystallizable fraction is characterized by high molecular weight and low comonomer content. Thus the contribution of the comonomer to the melting and crystallization behaviour of the high molecular weight material is minimal. However small, it is nonetheless sufficient to cause changes in thermal properties, as shown earlier by DSC and CRYSTAF data.

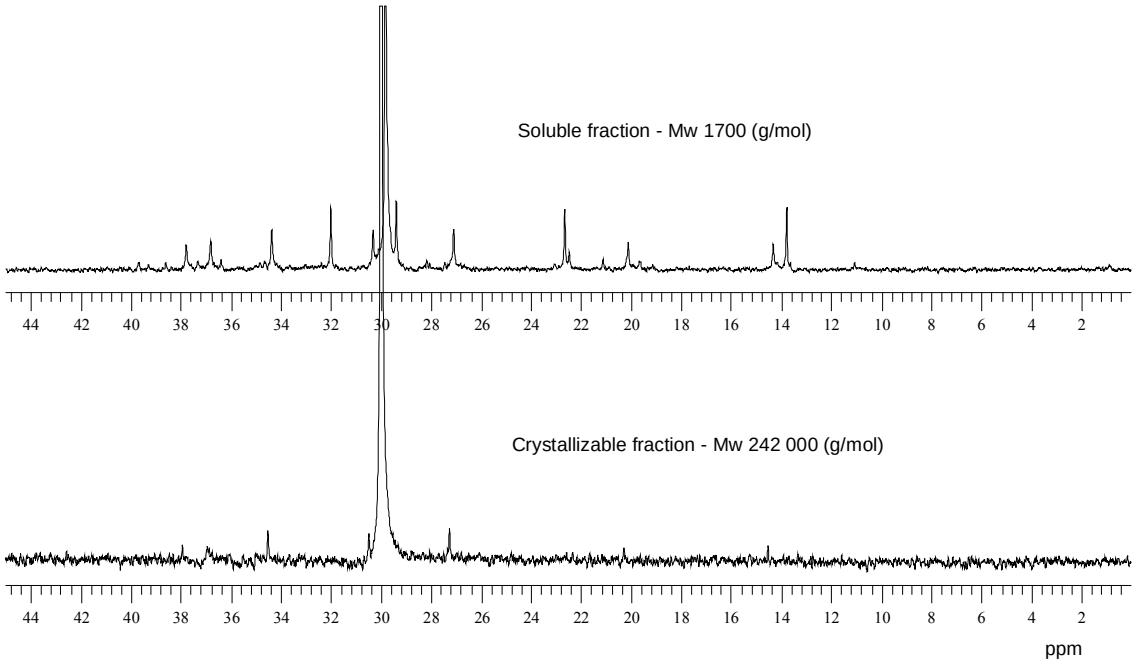

Figure 4.17: The ^{13}C NMR spectra for soluble and crystallizable fractions

From the spectra shown in Figure 4.17 the comonomer content of the soluble fraction can be calculated as about 16%, while the extracted polymer (crystallizable fraction) has a comonomer content of only 0.9%. It is clear that the higher than expected crystallization and melting temperatures shown in Figure 6 for the sample W6 are due

to the fact that a significant amount of the comonomer is located in the non-crystallizable (soluble) fraction of the copolymer. One would expect much lower melting and crystallization temperatures if the comonomer content of 6.9% mole was evenly distributed among all polymer chains. This is analogous to commercial LLDPE materials made by heterogeneous transition metal catalysts. The fractionation experiments (SEC-FTIR and Soxhlet extraction) paint a clearer picture of different thermal behaviour of the copolymers produced by the **4.1**, **4.2** and **4.3**/MAO catalyst systems as observed in DSC results. The experiment shows that it is not only the comonomer incorporation which affects the thermal properties, but also its distribution. Therefore, it is of note that the crystallization and melting temperatures and comonomer content vs. melting and crystallization temperature plots (Figures 4.6 and 4.7) have to be interpreted with the above in mind. The detailed results of further preparative TREF experiments of selected samples are discussed in the next chapter.

4.3.2 Copolymers synthesized using Cp*-containing catalyst systems

4.3.2.1 Molecular weight and molecular weight distribution

The copolymers, prepared using $Cp^*_2ZrCl_2$ (**4.4**) and $[(CO)_5W{=}C(Me)OZr(Cp^*)_2Cl]$ (**4.5**)/MAO, were synthesized under similar conditions as those used with Cp-containing analogues. Refer to Section 4.2.3 for exact details on the experimental

conditions (see also Scheme 4.4). The catalytic and molecular characterization data pertaining to the polymerizations are summarized in Table 4.2. The activities of these two catalyst systems (**4.4** and **4.5**/MAO) are generally lower than the activities of the unsubstituted cyclopentadinyl compounds (**4.1**, **4.2** and **4.3**/MAO). The catalyst **4.5**/MAO exhibits the lowest polymerization activities of all the catalyst systems. Reasons for poor activities are not clear.

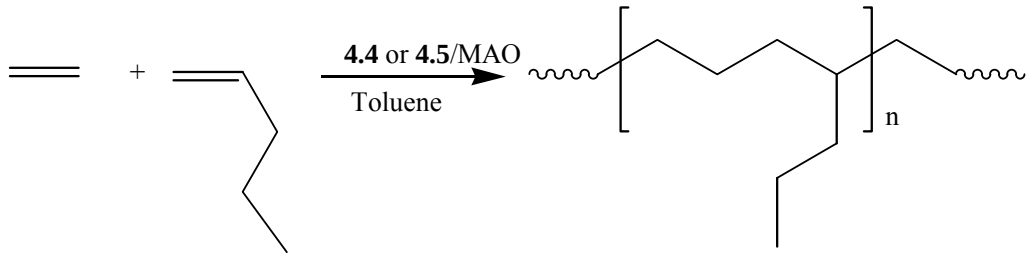

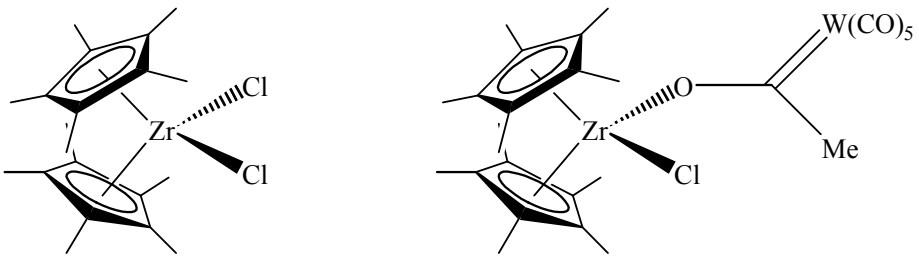

4.4 **4.5**

Scheme 4.4: Polymerization reaction scheme for ethylene/1-pentene copolymers

The molecular weights of **4.4**/MAO - catalyzed copolymers are higher – well above 100 000 g/mol - than those of copolymers synthesized with **4.1**/MAO. As explained previously, this was expected since the active zirconium center in **4.4**/MAO is more sterically hindered than in **4.1**/MAO. As a result **4.4**/MAO is expected to have fewer

chain transfer reactions than **4.1**/MAO. Molecular weights of copolymers produced with **4.5**/MAO are in the same range as samples obtained using **4.2** and **4.3**/MAO. The common factor to all four complexes (**4.2** – **4.5**) is once again the presence (in whatever form) of bulky ligands. The molecular weight distribution of the polymers obtained with **4.4**/MAO remained relatively narrow which is indicative of metallocene behaviour. Surprisingly, PDI's of ethylene/1-pentene copolymers produced with **4.5**/MAO are relatively narrow compared to copolymers synthesized with it's Cp analogue, **4.2**/MAO. Previously, (in Section 4.3.1 and Table 4.1), PDI's as high as 50 were observed for copolymers produced with **4.2**/MAO. The low PDI's of copolymers catalyzed by **4.5**/MAO catalyzed copolymers indicate that in order to achieve a greater control over molecular weight properties of copolymers produced with metalloxycarbenes, one needs to increase, to some extend, steric factors around the active center. However, high steric factors around the active center may also lead to a decrease in comonomer incorporation as was found with **4.4** and **4.5**/MAO. In fact, copolymers produced with the **4.5**/MAO – the catalyst system with the most sterically hindered active center - exhibits virtually no comonomer incorporation. Even with the amount of 1-pentene increased to more than 30 mol% in the feed, the melting temperature of the resulting copolymer remains high suggesting low comonomer concentration in the copolymer.

Table 4.3: Characterization results for ethylene/1-pentene copolymers synthesized with Cp* -containing catalyst systems

Sample Code	Catalyst No	1-pentene in feed [mol-%]	1-pentene in the copolymer [mol-%]	$T_{c\ DSC}$[a] (^oC)	$T_{m\ DSC}$[b] (^oC)	M_n[c] (g/mol)	M_w[c] (g/mol)	PDI[c]	Activity (Kg/(mol.h)
ZRS1	4.4	17.0	3.05	113.5	124.8	39 300	86 400	2.2	139.4
ZRS2	4.4	29.1	2.97	112.2	124.3	44 300	133 000	3.0	109.1
ZRS3	4.4	31.6	nd[d]	113.1	128.3	181 000	48 5000	2.7	187.9
ZRS4	4.4	33.9	1.16	113.3	127.3	52 500	141 700	2.7	236.4
ZRS5	4.4	38.1	1.68	114.0	128.3	64 400	181 200	2.8	251.5
WCPS1	4.5	13.3	0.72	112.4	130.7	12 800	97 500	7.6	52.7
WCPS2	4.5	17.0	1.64	114.7	126.6	18 700	106 000	5.6	106.7
WCPS3	4.5	20.4	nd	114.8	126.0	12 000	166 800	13.7	84.8
WCPS4	4.5	23.5	nd	114.9	128.2	38 200	230 000	6.0	78.8
WCPS5	4.5	23.0	nd	113.6	137.5	133 400	601 100	4.5	13.3
WCPS6	4.5	29.1	nd	111.2	124.2	38 400	164 000	4.3	63.6
WCPS7	4.5	33.9	nd	112.7	126.4	30 500	233 600	6.7	134.5

(a): crystallization temperature determined using DSC; (b): melting temperature determined using DSC ; (c): molecular weight property determined using SEC; (d): not detemined

4.4 CONCLUSIONS

Copolymers produced with the catalyst systems [$(CO)_5W$=C(Me)OZr$(Cp)_2Cl$] (**4.2**) and [$(CO)_5Cr$=C(Me)OZr$(Cp)_2Cl$] (**4.3**)/MAO show remarkable differences compared to materials synthesized with Cp_2ZrCl_2 (**4.1**)/MAO. These differences become obvious, when fractionation techniques such as CRYSTAF and SEC-FTIR are used. Emphasizing the role played by the anionic carbene complex ligand, copolymers produced with metalloxycarbenes display highly heterogeneous 1-pentene incorporation and higher molecular weight than those synthesized with the metallocenes Cp_2ZrCl_2 (**4.1**)/MAO. The SCBD's of the copolymers obtained using metalloxycarbenes clearly indicate that **4.2** and **4.3** behave more like a Ziegler-Natta than single site catalyst systems.

4.5 REFERENCES

1. Kaminsky, W.; Miri, M. *J. Polym. Sci., Part A: Polym. Che.m* **1985**, 23, 2151.

2. Heiland, K.; Kaminsky, W. *Makromol. Chem.* **1992**, 193, 601.

3. Quijada, R.; Dupont, J.; Silveira, D. C.; Miranda, M. S. L.; Scipioni, B. *Macromol. Rapid. Comm.* **1995**, 16, 357.

4. Kim, I.; Kim, S. Y.; Lee, M. H.; Do, Y.; Won, M. *J. Polym. Sci., Part A: Polym. Chem.* **1999**, 37, 2763.

5. Ewen, J. A. In *Catalytic polymerizations of olefins*; Keii, T.; Soga, K.; Eds.; Kodansha: Tokyo, **1986** p. 271.

6. Pietikäinen, P; Seppälä, J. V. *Macromolecules* **1994**, 27, 1325.

7. Fink, G.; Herfert, N.; Montag, P. In *Ziegler Catalysts*, Fink, G; Mulhaupt, R.; Brintzinger, H. H.; Eds; Springer: Berlin, **1995**, p. 159.

8. Escher, F. F. N.; Galland, B. B.; Ferreira, M. *J. Polym. Sci., Part A: Polym. Chem.* **2003**, 41, 2531.

9. Kissin, Y. V.; Mirabella, F. M.; Meverden, C. C. *J. Polym. Sci., Part A: Polym. Chem.* **2005**, 43, 4351.

10. Tang, L.; Hu, T.; Pan, L.; Sheng, Y. *J. Polym. Sci., Part A: Polym. Chem.* **2005**, 43, 6323.

11. Kaminsky, W. *J. Polym. Sci. Part A: Polym. Chem.* **2004**, 42, 3911.

12. Brüll, R.; Kgosane, D.; Neveling, A.; Pasch, H.; Raubenheimer, H. G.; Sanderson, R. D.; Wahner, U. M. *Macromol. Symp.* **2001**, 165, 11.

13. Sacchi, M. C.; Forlini, F.; Losio, S.; Tritto, I.; Wahner, U. M.; Tincul, I.; Joubert, D. J.; Sadiku, E. R. *Macromol. Chem. Phys* **2003**, 204,1643.

14. Wahner, U. M.; Tincul, I.; Joubert, D. J.; Sadiku, E. R.; Forlini, F.; Losio, S.; Tritto, I.; Sacchi, M. C. *Macromol. Chem. Phys.* **2003**, 204, 1738.

15. Costa, G.; Stagnaro, P.; Trefiletti, V.; Sacchi, M. C.; Forlini, F.; Alfonso, G. C.; Tincul, I.; Wahner, U. M. *Macromol. Chem. Phys.* **2004**, 205, 383.

16. Sacchi, M. C.; Forlini, F.; Losio, S.; Tritto, I.; Costa, G.; Stagnaro, P.; Tincul, I.; Wahner, U. M. *Macromol. Chem. Phys.* **2004**, 213, 57.

17. Graef, S. M.; Wahner, U. M.; van Reenen, A.J.; Brüll, R.; Sanderson, R. D.; Pasch, H. *J. Polym. Sci. Part A: Polym Chem.* **2002**, 40, 128.

18. Brüll, R.; Pasch, H.; Raubenheimer, H. G.; Sanderson, R. D.; van Reenen, A.J.; Wahner, U. M. *Macromol. Chem. Phys.* **2001**, 202, 1281.

19. van Reenen, A.J.; Brüll, R.; Wahner, U. M.; Raubenheimer, H. G.; Sanderson, R. D.; Pasch, H. *J. Polym. Sci., Part A: Polym. Chem.* **2000**, 38, 4110.

20. Brüll, R.; Luruli, N.; Pasch, H.; Raubenheimer, H. G.; Sadiku, E.R.; Sanderson, R. D.; van Reenen, A.J.; Wahner, U. M. *e-Polymer* **2003**, 061.

21. Mülhaupt, R. *Macromol. Chem. Phys*. **2003**, 204, 289.

22. Alt, H. G.; Koppl, A. *Chem. Rev*. **2000,** 100, 1205.

23. Coates, G. W. *Chem. Rev*. **2000,** 100, 1223.

24. Mitani, M.; Nakano, T.; Fujita, T. *Chem. Eur. J*. **2003**, 9, 2396.

25. Luruli, N.; Grumel, V.; Brüll, R.; Du Toit, A.; Pasch, H.; van Reenen, A. J; Raubenheimer, H. G.; *J Polym Sci Part A: Polym. Chem.* **2004**, 42, 5121.

26. Neveling A. *MSc Thesis*, University of Stellenbosch, Stellenbosch, South Africa. **1999**.

27. Nel J. *MSc Thesis*, University of Stellenbosch, Stellenbosch, South Africa. **2002**.

28. Ko, Y. S.; Woo, S. I.; *J. Polym. Sci. Part A: Polym Chem.* **2003**, 41, 2171.

29. Czaja, K.; Białek, M.; Utrata, A. *Polym. Sci. Part A: Polym. Chem.* **2004**, 42, 2512.

30. Naga, N.; Imanishi, Y.; *J. Polym. Sci. Part A: Polym. Chem.* **2003**, 41, 441.

31. Randall, J. C. *Polym. Charact. ESR NMR Symp.* **1980**, 6, 93.

32. Heiland, K.; Kaminsky, W. *Makromol. Chem. Phys.* **1992**, *193*, 601.

33. Naga, N.; Imanishi, Y.; *Macromol. Chem. Phys.* **2002**, 203, 771.

34. Schneider, M. J.; Suhm, J.; Mulhaupt, R.; Prosenc, M. H.;Brintzinger, H. H. *Macromolecules* **1997**, *30*, 3164.

35. Quijada, R.; Galland, G. B.; Mauler, R. S. *Macromol. Chem. Phys.* **1996**, *197*, 3091.

36. Byun, D. J.; Shin, D. K.; Kim, S. Y. *Polym. Bull.* **1999, 42**, 301.

37. Camurati, I.; Cavicchi, B.; Dall'Occo, T.; Piemontesi, F. *Macromol. Chem. Phys.* **2001**, 202, 701.

38. Lehmas, P.; Härkki, O.; Leino, R.; Luttikhedde, H. J. G.; Näsman, J. H.; Seppälä, J. V. *Macromol. Chem. Phys.* **1998**, 199, 1965.

39. Czaja, K.; Białek, M. *Polymer* **2001**, 42, 2289.

40. Starck, P.; Lehmus, P.; Seppälä, J. V.; *Polym. Eng. Sci*. **1999**, 39, 1444.

41. Alt, H. G.; Köppl, A.; *Chem. Rev.* **2000**, 100, 1205.

42. Resconi, L.; Cavallo, L.; Fait, A.; Piemontesi, F. *Chem. Rev.* **2000**, 100, 1253.

43. Xu, X.; Xu, J.; Feng, L.; Chen, W.; *J. Appl. Polym. Sci.* **2000**, 77, 1709.

44. Quijada, R.; Galland, G. B.; Freitas, L. L.; da Jornada, J. A. H.; Mauler, R. S.; Miranda, M. S. L. *Polym. Bull.* **1995**, 35, 299.

45. Mirabella, F. M.; Bafna, A.; *J. Polym. Sci. Part B: Polym. Phys.* **2002**, 40, 1637.

46. Soares, J.B.P.; Anantawaraskul, S. *J. Polym. Sci. Part B: Polym. Phys*. **2005**, 43, 1557.

47. Monrabal, B.; Blanco, J.; Nieto, J.; Soares, J.B.P. *J. Polym. Sci. Part A: Polym. Chem.* **1999**, 37, 89.

48. Monrabal, B. *Temperature rising elution fractionation and crystallization analysis fractionation*. In *Encyclopedia of Analytical Chemistry*, Ed, Mayers, R.A. **2000**, 14, page 1-20

49. Sarzotti, D. M.; Soares, J. B. P., Penlidis A. *J. Polym. Sci, B: Polym. Phys.* **2002**, 40, 2595.

50. Sarzotti, D. M.; Soares, J. B. P.; Simon, L. C.; Britto, L. J. D. *Polymer*, **2004**, 4787.

51. McRae, M.A.; Maddams, W. F. *Makromol. Chem*. 1976, 449.

52. Neves, C. J.; Monteiro, E.; Habert, A. C. *J. Appl. Polym. Sci.* **1993**, 50, 817.

53. Blitz, J. P.; McFaddin; D. C. *J. Appl. Polym. Sci.* **1994**, 51, 13.

54. Hongjun, C.; Xiaolie, L.; Dezhu, M.; Jianmin, W.; Hongsheng, T. *J. Appl. Polym. Sci.* **1999**, 71, 93.

55. Tackx, P.; Bremmers, S. *Polym. Matter. Sci. Eng.* **1998**, 78, 50.

56. Faldi, A.; Soares, J.B.P. *Polymer*, **2001**, 42, 3057.

57. Verdumen-Noël, L.; Baldo, L.; Bremmers, S. *Polymer*, **2001**, 42, 5523.

58. Kakugo, M.; Miyatake, T.; Mizunuma, K. *Macromolecules* **1991**, 24, 1469.

59. Graef, S. M.; Brüll, R.; Pasch, H.; Wahner, U. M. *e-Polymers* **2003**, 005.

5 Cross-fractionation of ethylene/1-pentene copolymers according to molecular weight using advanced fractionation techniques*

* Based on: **1**. Luruli, N.; Heinz, L.; Grumel, V.; Brüll, R.; Pasch, H.; Raubenheimer, H.G. *Polymer* **2006,** 47, 56. **2**. Luruli, N.; Pijpers, T.; Brüll, R.; Grumel, V.; Pasch, H.; Mathot, V. *J. Polym. Sci. Part B: Polym. Phys.* **2005**, in press. The SEC-FTIR fractionation was done at Deutsches Kunststoff-Institut (German Institute for Polymers) in Darmstadt, Germany under the supervision of Dr. R. Brüll and Prof. H. Pasch. The HPer DSC work was done at the Catholic University of Leuven, Belgium under the supervision of Thijs Pijpers and Prof. Vincent. Mathot.

ABSTRACT

The short chain branching distribution (SCBD) and thermal properties of selected ethylene/1-pentene copolymers were studied using Preparative Molecular Weight Fractionation (PMWF) and SEC-HPer DSC. These fractionation techniques allow a detailed study of SCBD and thermal properties to be conducted on a very narrow slice along the molecular weight axis. The PMWF showed that the molecular weight distribution profiles of the fractions of the copolymers produced with Cp_2ZrCl_2/MAO (**5.1**) have very narrow distribution characteristics. In contrast, the fractions of the copolymers obtained with metalloxycarbenes $[(CO)_5W=C(Me)OZr(Cp)_2Cl]$ (**5.1**) and $[(CO)_5Cr=C(Me)OZr(Cp)_2Cl]$ (**5.3**)/MAO had bimodal distributions across the entire molecular weight axis. Furthermore, the thermal properties of the deposits of these copolymers on a Germanium disc were studied using High Performance Differential Scanning Calorimetry (HPer DSC). Single SEC separations were used to accumulate fractions in the microgram range that were directly analyzed with regard to their thermal properties, thus allowing us to study SCBD and thermal behaviour simultaneously using very small amount of sample (less than 1 mg). HPer DSC showed a decrease in melting and crystallization temperatures towards the low molecular weight fractions of these copolymers.

5.1 INTRODUCTION

The knowledge of molecular weight distribution (MWD) and short chain branching distribution (SCBD) of polymers is important in understanding their properties during processing and application. This knowledge is also essential for tailoring or modifying catalyst structures or polymerization conditions during synthesis in order to influence the final properties of the polymers. Metallocene catalyst systems have long been claimed to produce polymers with narrow MWD or copolymers with uniform comonomer distribution[1,2]. While there is a lot of information on molecular weight properties of metallocene catalyzed copolymers, few detailed studies on SCBD are available. It is only until recently that details on SCBD of metallocene catalyzed polymers are beginning to emerge. SCBD has previously been studied using preparative TREF and CRYSTAF[3,4]. Preparative TREF involves fractionating the polymer according to crystallizability or solubility and then analyzing each fraction obtained after fractionation using NMR, DSC, SEC, FTIR or CRYSTAF. The disadvantage of TREF is that it is labor-intensive and takes long to analyze one sample. Although CRYSTAF is fast compared to TREF, the fractions cannot be analyzed separately. In addition, both TREF and CRYSTAF require high volumes of expensive and toxic solvents. Another way to study SCBD is by using SEC-FTIR. SEC-FTIR involves fractionating the polymer according to molecular weight by size exclusion chromatography (SEC) and subsequently profiling the SCBD using Fourier transform infrared (FTIR) spectroscopy off-line thus studying SCBD along the molecular weight axis. Typically, an eluent from SEC is deposited (usually less than

1 mg) on a Germanium disc via LC-Transform. Thereafter, FTIR scans are taken around the disc in order to profile the average comonomer distribution along the molecular weight as was shown in Chapter 4. Details about this procedure are readily available[5-10].

It has been shown that it is possible to combine SEC fractionation with conventional differential scanning calorimetry (DSC) in the case of HDPE's[11]. The recent progress in DSC technology has made it possible to combine SEC and high speed or high performance DSC (HPer DSC)* in a more quantitative way[11,12]. This allows one to not only study SCBD along the molecular weight axis but also the thermal properties (melting and crystallization temperature distributions) in much more detail.

HPer DSC has the ability to measure very small sample masses while scanning at high rates, up to 500 ^{o}C/min. Fast scanning rates also help to separate or reduce re-organizational thermal behaviour such as re-crystallization, melting and decomposition which may occur during heating. For example, during heating, polymer crystals can melt, re-crystallize, re-melt and finally decompose thus displaying multiple peaks. In order to assign peaks to a specific behaviour, the capability of variation of scanning at low to high rates turn out to be very helpful. Another advantage of HPer DSC is the ability to detect weak transitions. For this reason HPer DSC has been used in pharmaceutical analysis especially in analysis of the amorphous content of sugars[13,14]

*HPer DSC is now marketed by Perkin Elmer under the trade name Hyper DSC

In this chapter we report on a study of both SCBD and thermal properties of ethylene/1-pentene copolymers along with the molecular weight distribution. This is carried out using advanced fractionation techniques such as automated preparative molecular weight fractionation (PMWF) and the combination of SEC-FTIR and SEC-HPer DSC. As will be shown, single SEC separations or depositions are suitable to accumulate sufficient material for subsequent analysis of the thermal properties of the fractions by HPer DSC.

5.2 EXPERIMENTAL

5.2.1 Materials and equipments

The preparative molecular weight fractionation experiments were carried out using PREP mc2® equipment at the Deutsches Kunststoff-Institut (German Institute for Polymers, DKI), Germany. The solvents and filter papers used were purchased from Sigma Aldrich. The SEC fractionations for HPer DSC measurements were also conducted at DKI using a Waters 150 SEC. LC-Transform interface and Germanium discs were all purchased from LabConnections, Germany. The HPer DSC measurements were performed using a Perkin Elmer Diamond DSC at the Catholic University of Leuven, Belgium. The copolymers were synthesized as explained in Chapter 4.

5.2.2 Synthesis of ethylene/1-pentene copolymers

All reactions were carried out using standard Schlenk techniques. Polymerization reactions were performed under an inert gas atmosphere in a 350 ml stainless steel batch reactor (Parr) fitted with a glass liner, an inlet valve and pressure gauge. The samples chosen for fractionation in this chapter were selected from those shown in Table 4.1 in the previous chapter. The exact experimental details have already been discussed in Chapter 4. As a result of low comonomer incorporation, none of the copolymers synthesized with Cp*-containing catalysts were considered for cross-fractionation. Only samples synthesized with Cp-containing catalysts i.e. Cp_2ZrCl_2 (**5.1**), $[(CO)_5W{=}C(Me)OZr(Cp)_2Cl]$ (**5.2**) and $[(CO)_5Cr{=}C(Me)OZr(Cp)_2Cl]$ (**5.3**)/MAO were considered for cross-fractionation using both techniques. The samples selected for PMWF are ZR8, W5 and CR6. These were synthesized with Cp_2ZrCl_2 (**5.1**), $[(CO)_5W{=}C(Me)OZr(Cp)_2Cl]$ (**5.2**) and $[(CO)_5Cr{=}C(Me)OZr(Cp)_2Cl]$ (**5.3**)/MAO, respectively. For the fractionation using SEC-HPer-DSC two samples from each of two catalyst systems **5.1**/MAO and **5.3**/MAO respectively, were selected. The chosen samples were ZR2, ZR8, CR1 and CR15. The specific details of experimental procedures employed in PMWF and SEC-HPer-DSC measurements are discussed in the respective sections.

5.2.3 Analysis of the bulk properties of the samples

The characterization data for the bulk properties are shown in Table 5.1. Molecular weights of the polymers were determined using a PL 220 chromatograph from Polymer Laboratories packed with five Waters Styragel columns (HT 2 – 6) at a flow rate of 1 ml/min in 1,2,4-trichlorobenzene (140 ºC) relative to narrowly distributed polystyrene standards. The eluent was stabilized with BHT to prevent degradation.

The slow scanning (standard) DSC measurements of the bulk samples were performed using a Mettler Toledo DSC 822 under inert atmosphere. Two heating cycles and one cooling cycle were taken at heating and cooling rates of 10 °C/min, using about 6 mg of a sample per run.

Table 5.1: Summary of bulk properties for all the selected samples for cross-fractionation

Sample Code	Catalyst No.	1-pentene in the copolymer [mol-%]	$T_{c\ CRYSTAF}$ (^oC)	$T_{c\ DSC}$ (^oC)	$T_{m\ DSC}$ (^oC)	M_n (g/mol)	M_w (g/mol)	PDI
Zr2	1	9.0	78.7	106.2	114.7	7 000	26 000	3.8
Zr8	1	7.0	78.3	108.6	118.1	13 000	46 500	3.6
W5	2	3.9	82.3	111.0	124.6	18 300	218 400	11.9
CR1	3	9.1	79.2	107.2	115.9	7 600	35 000	4.7
CR15	3	8.3	80.4	104.8	109.8	15 200	43 100	2.8

5.3 PREPARATIVE MOLECULAR WEIGHT FRACTIONATION (PMWF)

PMWF involves fractionating polymers or copolymers using a combination of solvent /non-solvent. Preparative fractionation techniques, in general, are extremely useful in studying the microstructure of polyolefin copolymers in detail. Although the SCBD can easily be studied using SEC-FTIR, as already shown in the previous chapter, it is a challenge to study other parameters such as thermal properties of individual fractions due to very small mass associated with this technique. The advantage of using preparative methods is that the fractions can be studied in depth using other techniques like NMR and FTIR. Traditionally, the preparative fractionation involves dissolving the sample at high temperature using high boiling solvents (e.g TCB, xylene, etc) followed by fractionating the sample into individual fractions. The polymer is then separated according to crystallizability (CCD) or solubility. The fractions are collected at each temperature interval and analyzed off-line using other analytical techniques such as SEC, DSC, FTIR, and NMR. Preparative fractionation of semicrystalline polymers according to molecular weight is an old technique developed in the 1970's[15]. However, automated preparative molecular weight fractionation (PMWF) was introduced only recently by Monrabal[4].

5.3.1 PMWF experimental procedure

The preparative molecular weight fractionations (PMWF) were carried out with fully automated preparative TREF equipment (PREP mc2®)* using solvent/non-solvent gradient elution. The PREP mc2 is a fractionation instrument equipped with two reactors with an auto sampler as shown in Figures 5.1 and 5.2.

Figure 5.1: The PREP mc2 instrument fitted with autosampler

*PREP mc2® is commercial preparative TREF instrument manufactured by PolymerChar, Valancia, Spain.

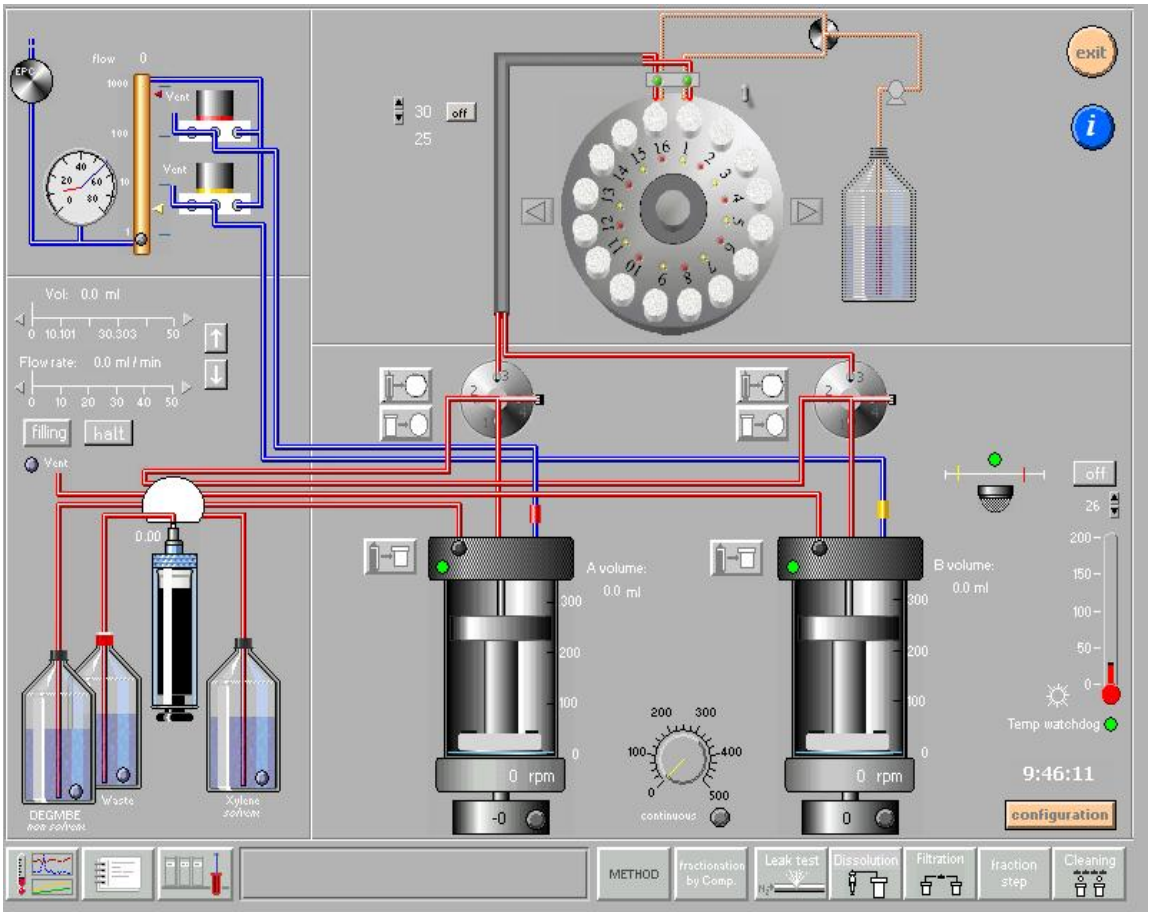

Figure 5.2: The PREP mc2 instrument fitted with autosampler and two reactors

The copolymer (500 mg) was dissolved in a combination of xylene (solvent) and diethyleneglycolmonobutylether (non-solvent) at 130 ^{o}C using a temperature program (Schemes 5.1 to 5.3). The temperature was then lowered to 110 ^{o}C at 30 ^{o}C/min. Finally, for elution, the temperature was raised to 120 ^{o}C at a rate of 20 ^{o}C/min. This cycle was repeated for each fraction and is the same for each temperature program shown in Schemes 5.1 to 5.3. However, the solvent/non-solvent compositions were varied as shown in Schemes 5.1 to 5.3. The efficiency of the fractionation programs was determined through trial and error using commercial LLDPE samples from

BASELL. Firstly, the conditions for fractionation were optimized using different solvent/non-solvent composition programs shown in Schemes 5.1 – 5.3. Scheme 5.1 shows a constant decrease of 10% in non-solvent while the composition was lowered irregularly in Scheme 5.1. When the copolymers were fractionated using solvent/non-solvent composition programs shown in Schemes 5.1 and 5.2, poor separation was achieved, i.e. separations resulted in few fractions with poor weight distribution. However, fractionating the copolymers using the composition program displayed in Scheme 5.3 resulted in better separation.

According to the program shown in Scheme 5.3, the fractions were collected at 6% intervals of solvent/non-solvent composition gradient starting from 75% of non-solvent. The fractionated polymers were precipitated in 100 ml of acetone while stirring and thoroughly washed with methanol. Finally, the polymer was dried overnight in an oven at 50 ^{o}C. The fractions were subsequently analyzed using SEC, DSC, FTIR, CRYSTAF and NMR. Fractions containing residual diethyleneglycolmonobutylether (DEGMBE) were crystallized from xylene and dried before performing further analysis.

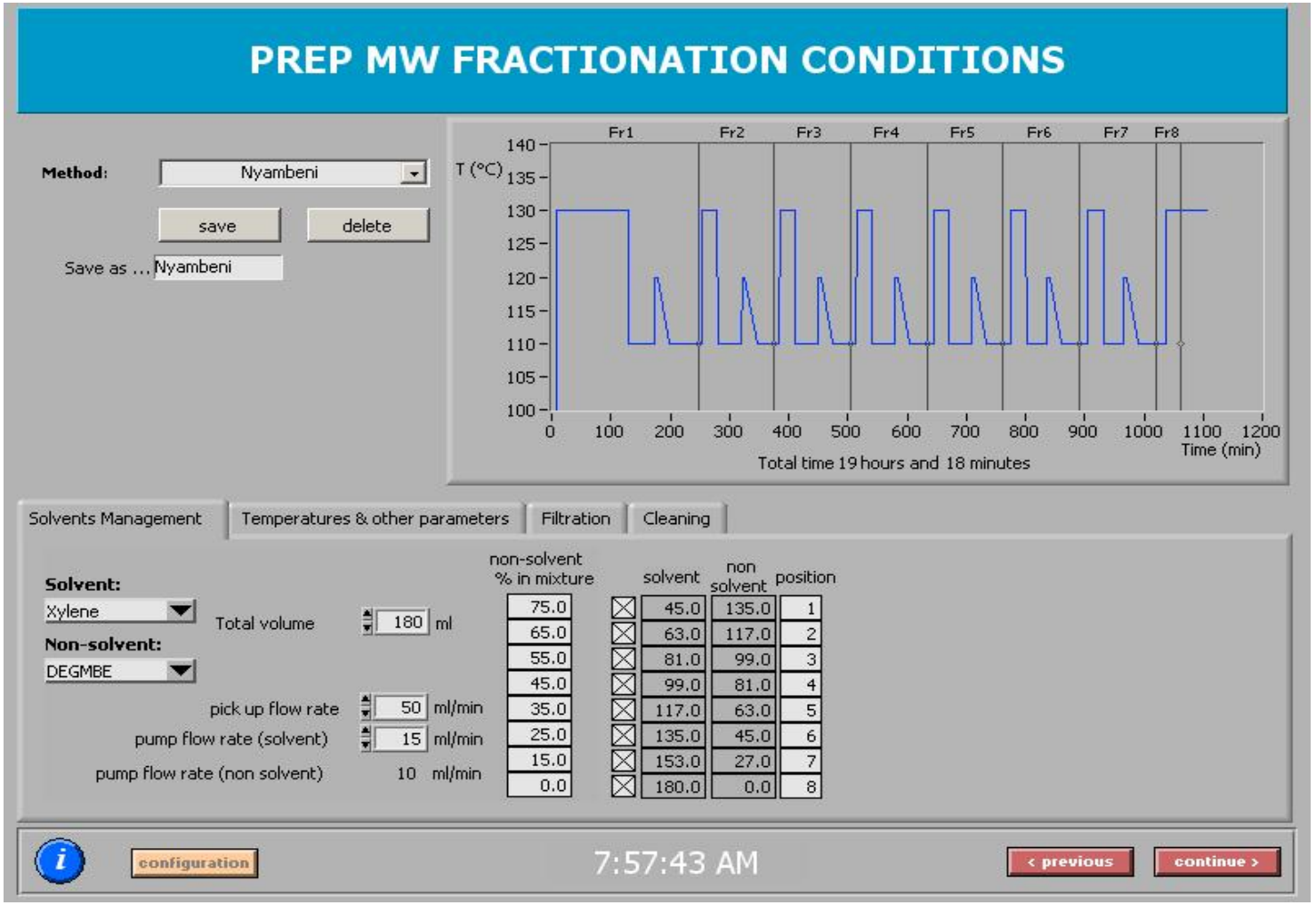

Scheme 5.1: Temperature program for preparative molecular weight fractionation (PMWF)

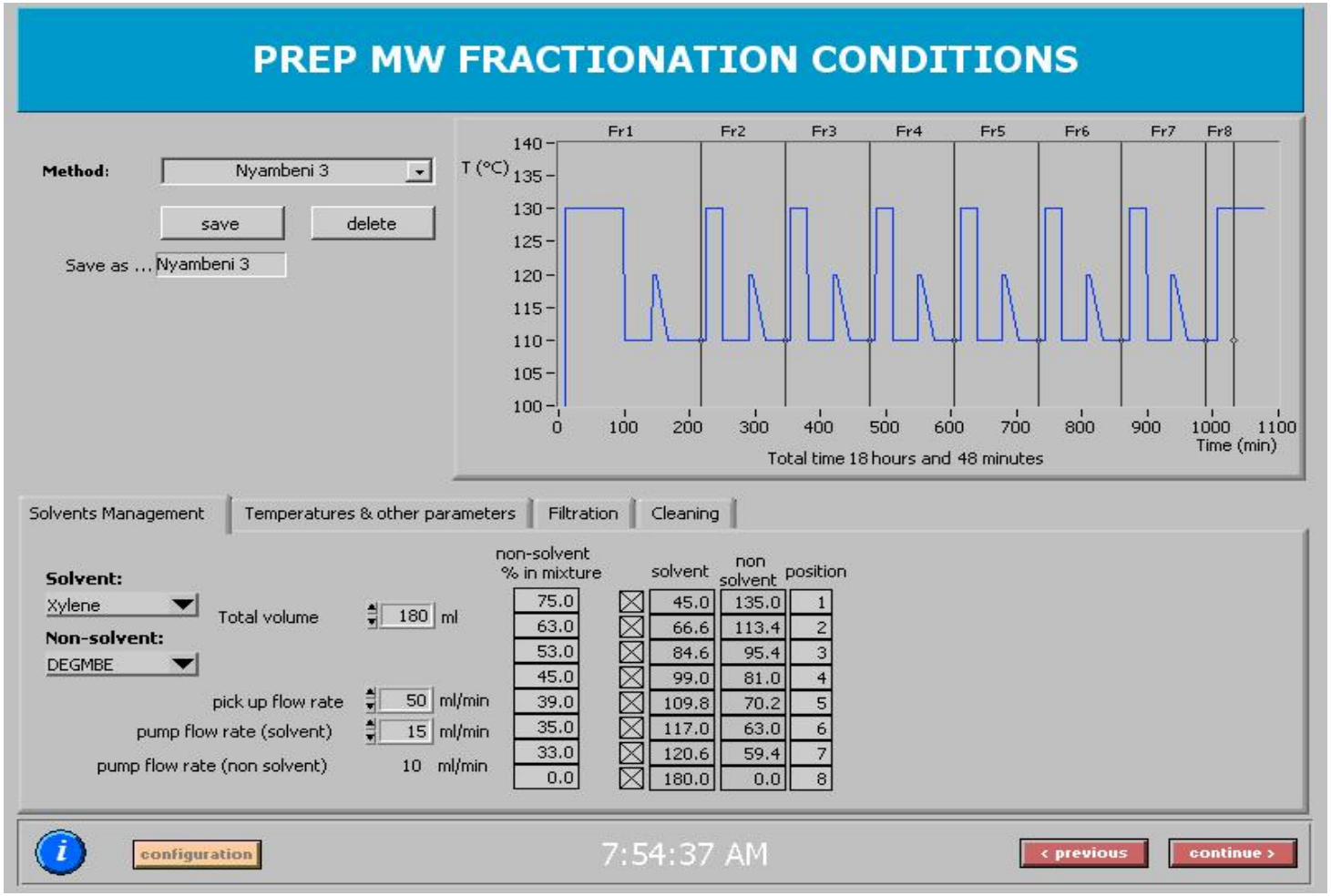

Scheme 5.2: Temperature program for preparative molecular weight fractionation (PMWF)

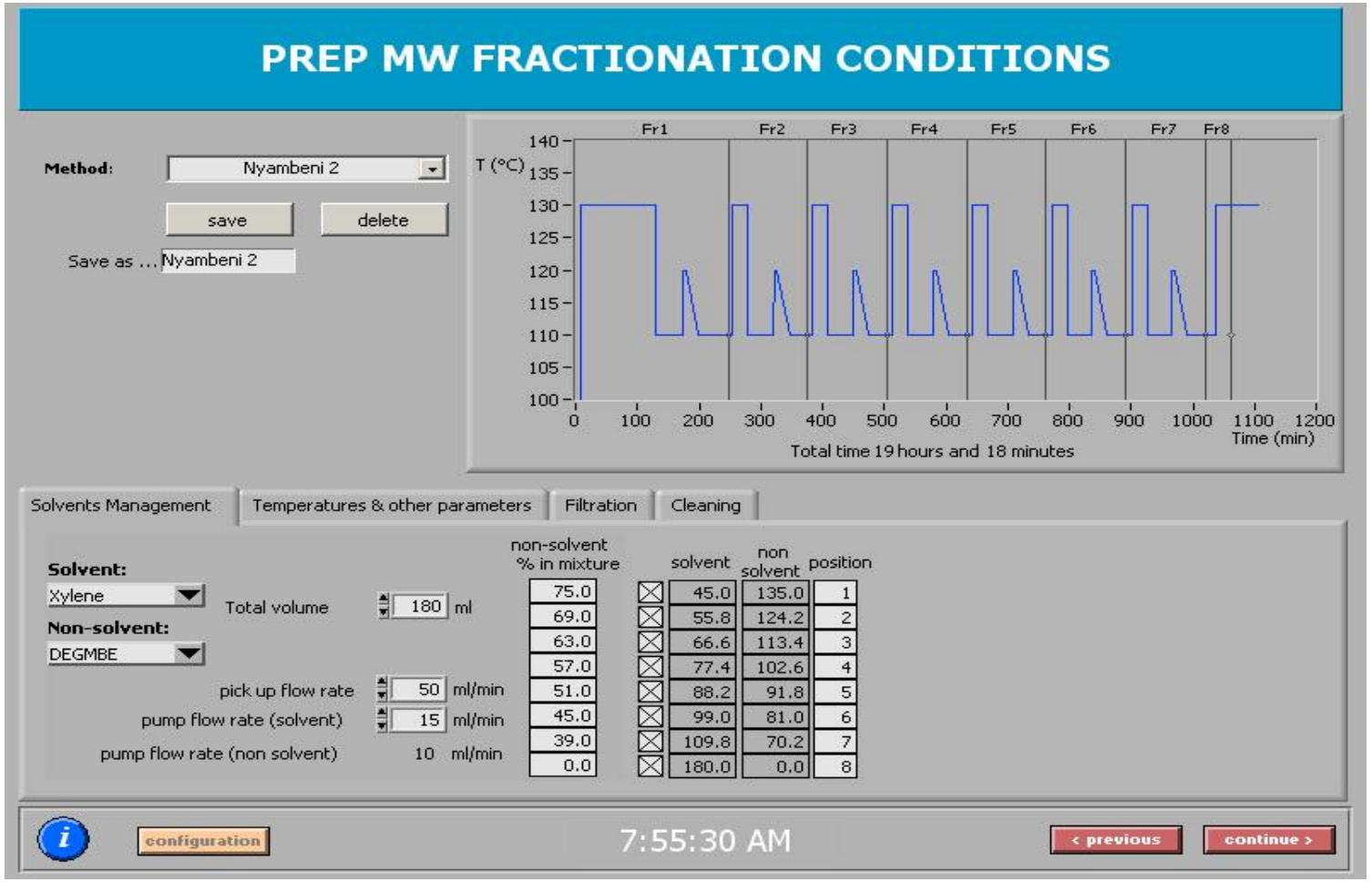

Scheme 5.3: Temperature program for preparative molecular weight fractionation (PMWF)

As mentioned previously, it is difficult to study some of the microstructural features, for example endgroups, using the SEC-FTIR technique. Profiling the unsaturated endgroups along the molecular weight axis using infrared absorption frequencies at 887, 908 and 966 cm^{-1} remained unsuccessful, as the thickness of the deposit on the Germanium disc was not sufficient. Fractionating the copolymers using preparative molecular weight fractionation techniques helps to overcome this problem since the fractions can be studied separately using either FTIR or ^{1}H-NMR. In addition to unsaturation, each fraction was also analyzed by DSC and with regard to thermal properties as well as molecular weight distribution. The characterization results from SEC and DSC are summarized in Tables 5.2 to 5.4.

Table 5.2: The summary of the preparative molecular weight fractionation data of sample ZR8

Frac No.	$T_{c\ DSC}$ (°C)	$T_{m\ DSC}$ (°C)	M_n (g/mol)	M_w (g/mol)	PDI	Yield (mg)	Weight % Yield
1	107.8	116.0	8 500	18 300	2.2	118.3	23.7
2	109.5	117.2	13 300	23 400	1.8	60.1	12.0
3	110.0	118.2	19 500	32 700	1.7	50.0	10.0
4	110.3	119.0	26 100	45 000	1.8	45.2	9.0
5	110.5	120.5	50 200	77 000	1.5	38.9	7.8
6	109.7	120.3	50 900	118 000	2.3	40.7	8.1
7	108.7	119.7	80 600	240 000	3.0	70.3	14.1

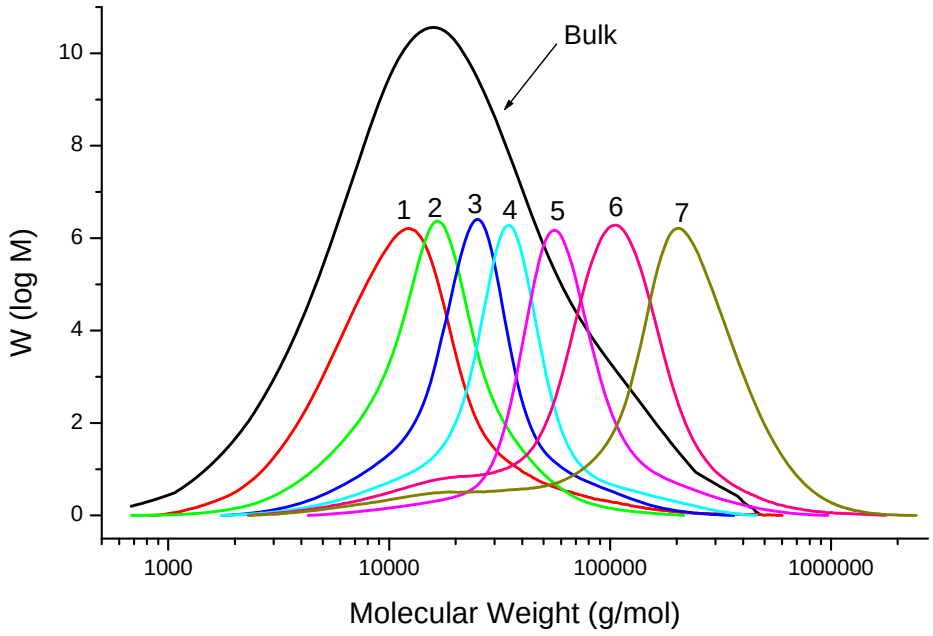

Figure 5.3: Molecular weight distribution of the bulk sample and PMWF fractions of sample ZR8 synthesized with **5.1**/MAO

Table 5.3: The summary of the preparative molecular weight fractionation data of sample W5

Frac No.	$T_{c\ DSC}$ (°C)	$T_{m\ DSC}$ (°C)	M_n (g/mol)	M_w (g/mol)	PDI	Yield (mg)	Weight % Yield
1	113.0	122.2	10 400	74 200	7.1	128.8	30.9
2	113.1	123.3	35 600	135 000	3.8	55.8	13.4
3	113.7	123.8	50 500	135 000	2.7	42.0	10.1
4	113.3	123.5	68 600	139 000	2.0	41.9	10.1
5	111.2	124.8	102 000	230 000	2.2	34.6	8.3
6	111.7	124.7	120 000	213 000	1.8	45.2	10.8
7	109.5	124.8	242 000	383 000	1.6	69.2	16.6

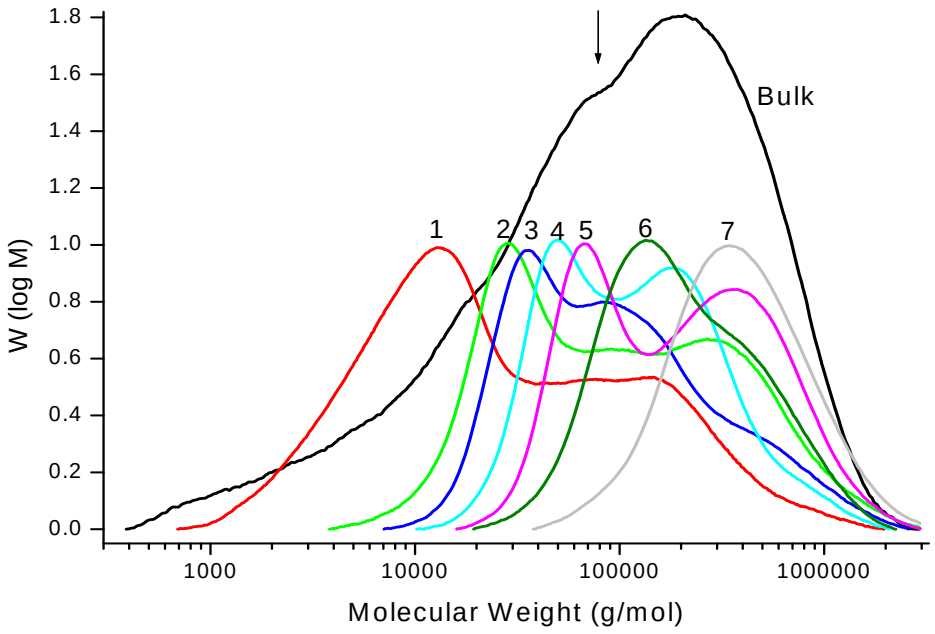

Figure 5.4: Molecular weight distribution of the bulk samples and PMWF fractions of sample W5 synthesized with **5.2**/MAO

Table 5.4: The summary of the preparative molecular weight fractionation data of sample CR6

Frac No.	$T_{c\ DSC}$ (^oC)	$T_{m\ DSC}$ (^oC)	M_n (g/mol)	M_w (g/mol)	PDI	Yield (mg)	Weight % Yield
1	105.7	114.0	9 000	16 200	1.8	112.6	22.9
2	106.7	115.5	33 300	64 500	1.9	61.3	12.4
3	107.3	116.7	39 800	77 700	2.0	48.7	9.9
4	107.3	116.8	52 600	81 200	1.4	40.8	8.3
5	106.3	116.7	66 300	84 700	1.3	42.1	8.5
6	104.7	116.3	9 700	117 900	1.2	70.3	14.3
7	102.8	118.3	191300	246 500	1.3	78.3	15.9
8	104.0	120.8	398 000	552 990	1.4	38.3	7.8

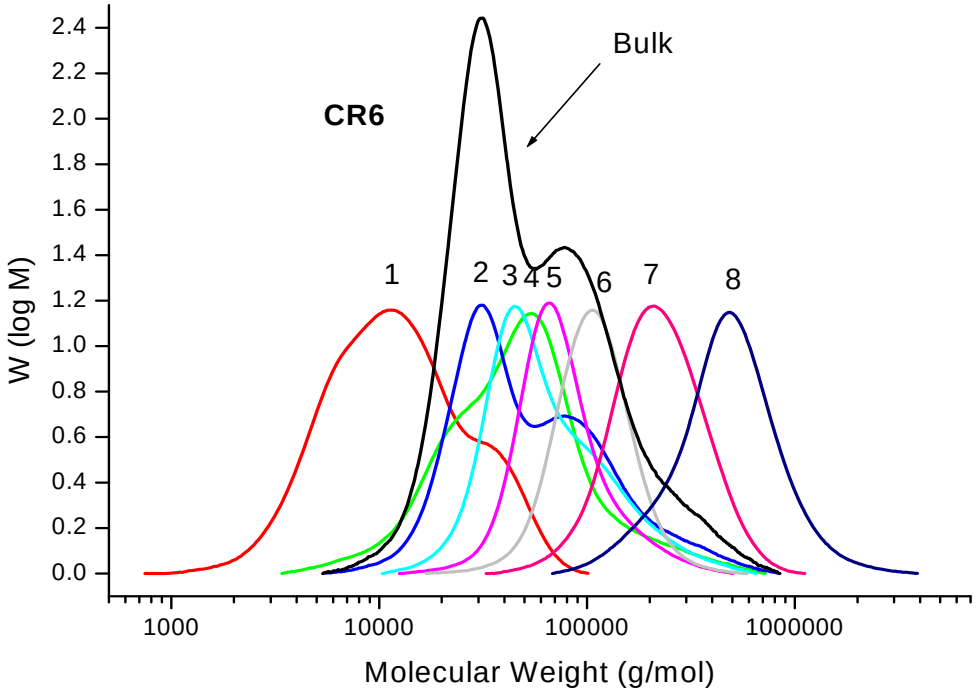

Figure 5.5: Molecular weight distribution of the bulk samples and PMWF fractions of sample CR6 synthesized with **5.3**/MAO

In general, as shown in Tables 5.2 – 5.4, total masses of the bulk samples are evenly distributed among the fractions. In all cases, the first fractions contain between 20 and 30% of the total materials while the rest of the fractions had around 10%. Very little sample mass was lost since the technique generates virtually no waste. Only a small amount of sample mass is lost during filtering or drying. The overlay of the molecular weight distribution curves for the fractions and the bulk of samples ZR8, W5 and CR6 shown in Figures 5.3, 5.4 and 5.5 respectively, clearly indicate that the separation takes place mainly according to molecular weight. However, it must be noted that it is impossible to separate exclusively according to molecular weight without the influence of chemical composition or *vice versa*[16].

It is clear that the fractions of sample ZR8 (Figure 5.3) show narrow polydispersities over a broad range of molecular weight while those synthesized with metalloxycarbenes (W5 and CR6) have broad and bimodal molecular weight distributions (Figures 5.4 and 5.5). Narrow molecular weight distribution of ZR8 fractions was expected since metallocenes are synonymous with this behaviour. Although the fractions of CR6 produced with $[(CO)_5Cr=C(Me)OZr(Cp)_2Cl]$ (**5.3**)/MAO have bimodal distributions, there are more fractions that are narrowly distributed compared to those of W6 synthesized with $[(CO)_5W=C(Me)OZr(Cp)_2Cl]$ (**5.2**)/MAO. Again, we observe here an intermediate behaviour with regard to molecular weight properties of the fractions of the copolymers produced with $[(CO)_5Cr=C(Me)OZr(Cp)_2Cl]$ (**5.3**)/MAO compared to those made with Cp_2ZrCl_2 (**5.1**) and $[(CO)_5W=C(Me)OZr(Cp)_2Cl]$ (**5.2**)/MAO.

It is interesting to note that the bimodality of W5 and CR6, fractions (Figures. 5.4 and 5.5) occur around the same molecular weight range where the bimodal distribution of the bulk sample is found.

As expected from the results of the SEC-FTIR analysis, first few fractions (with low average molecular weight) for all the samples (ZR8, W5 and CR6) have low melting and crystallization temperatures as measured by DSC (see Figures 5.6, 5.7 and 5.8 and also compare with Tables 5.2, 5.3 and 5.4). This corresponds well with the SEC-FTIR results, explained in Chapter 4, that show the 1-pentene concentration to be high in the low molecular weight fractions. The melting curves of ZR8 and CR6 broadened towards the low molecular weight fractions and finally develop multiple curves. Almost all the melting peaks of CR6 display multiple transitions while those of ZR8 only occurred towards the low molecular weight fractions. On the other hand, the melting curves of W6 remain constant with a slight decrease in the melting temperatures towards the low molecular weight fractions. Multiple DSC transition behaviour, as mentioned in Chapter 4, has previously been associated with broader CCD of the copolymers[17]. It is interesting to note that the low molecular weight fractions of ZR8 have multiple melting peaks indicating that broadening of the CCD occurs towards low molecular weight region.

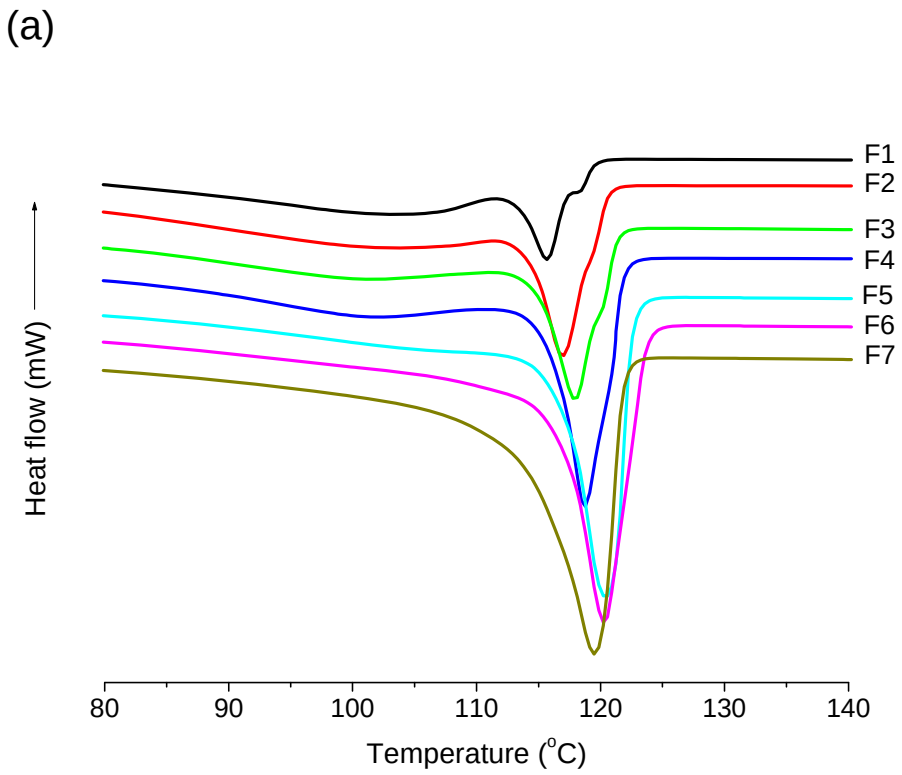

Figure 5.6: DSC curves (melting region) of ZR8 molecular weight fractions of copolymers synthesized with **5.1**/MAO

(b)

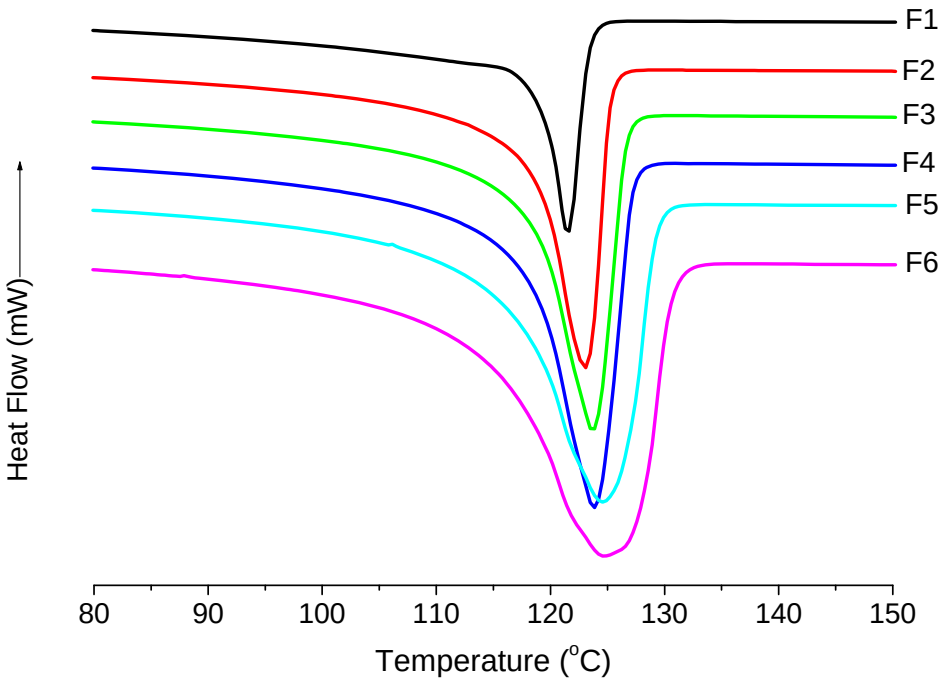

Figure 5.7: DSC curves (melting region) of W5 molecular weight fractions of copolymers synthesized with **5.2**/MAO

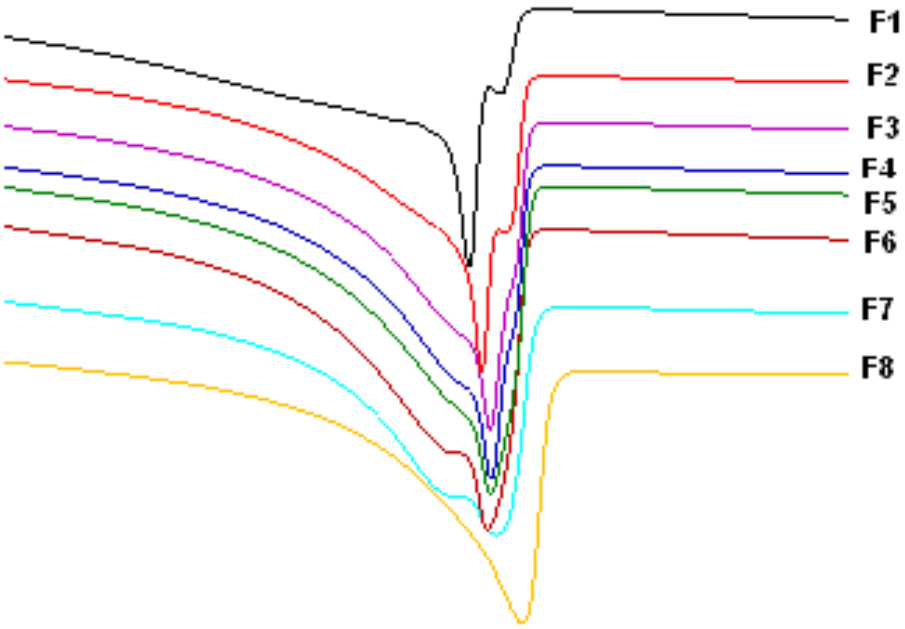

Figure 5.8: DSC curves (melting region) of CR6 molecular weight fractions of copolymers synthesized with **5.3**/MAO

The relative concentrations of vinyl and trans-vinylene endgroups were analyzed by IR spectroscopy. As seen in Figures. 5.9, 5.10 and 5.11 the concentration of the endgroups from copolymers made by all three catalyst systems is higher in the low molecular weight fractions. Since the vibration of the vinylidene groups overlaps with the CH_3-rocking vibration of the comonomer, the relative concentration of the vinylidene endgroups was determined from the ^{1}H-NMR spectra using the resonances between 4.6 – 4.8 ppm. It is difficult to identify the endgroups of high molecular

weight fractions in the ^{1}H-NMR spectrum. To avoid the molecular weight effect, we only analyzed the vinylidene content of the first three fractions of each sample i.e. with relatively low molecular weight. Figure 5.12, which shows an overlay of ^{1}H-NMR spectra of the first three fractions of W5, clearly indicates that vinylidene concentration is high in the first fraction while the other two contain virtually no trace thereof. The vinylidene concentration investigated using ^{1}H-NMR for fractions of the other two samples (ZR8 and CR6) displayed similar behaviour as observed for W5

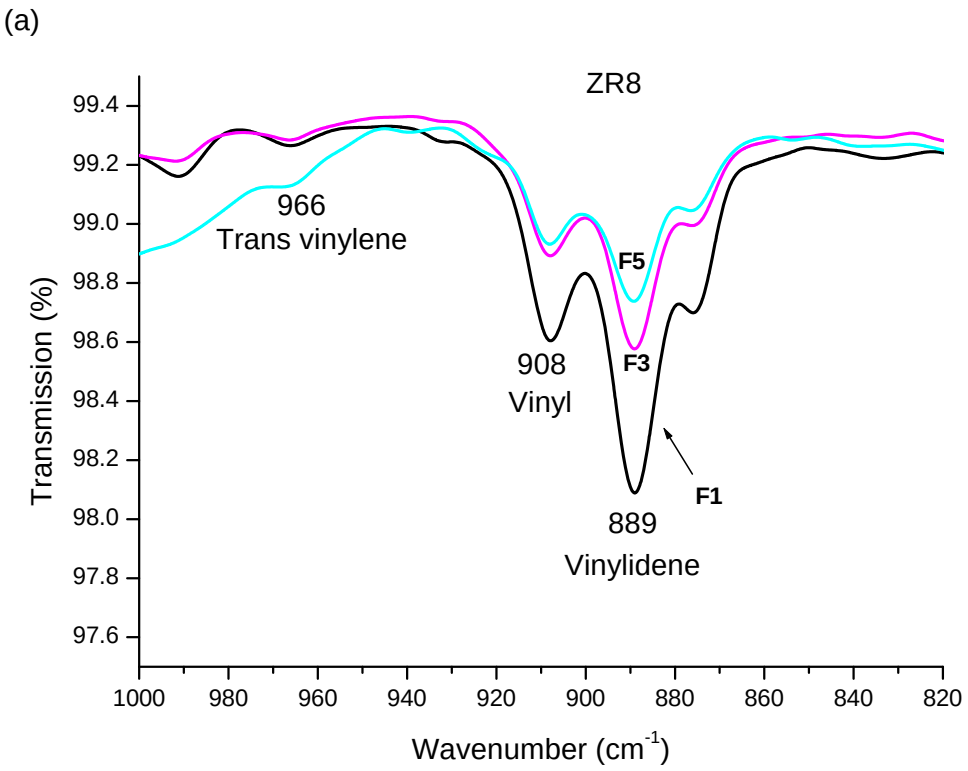

Figure 5.9: Enlargement of the unsaturated endgroup region in the FTIR spectra of ZR8 fractions

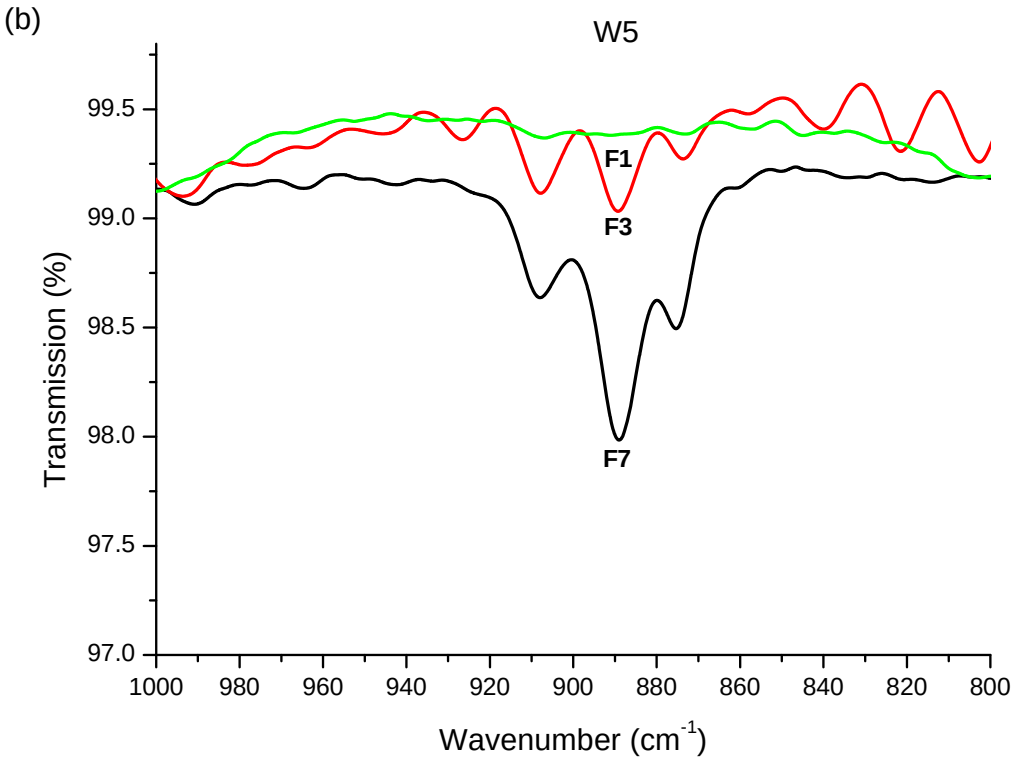

Figure 5.10: Enlargement of the unsaturated endgroup region in the FTIR spectra of W5 fractions.

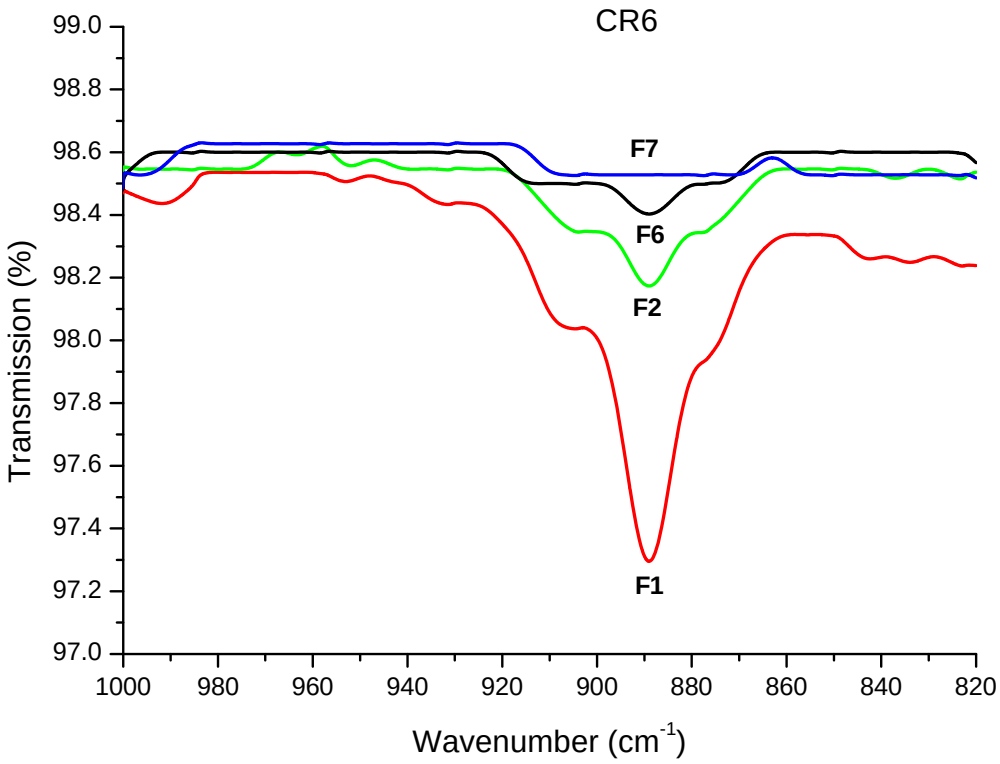

Figure 5.11: Enlargement of the unsaturated endgroup region in the FTIR spectra of CR6 fractions**.**

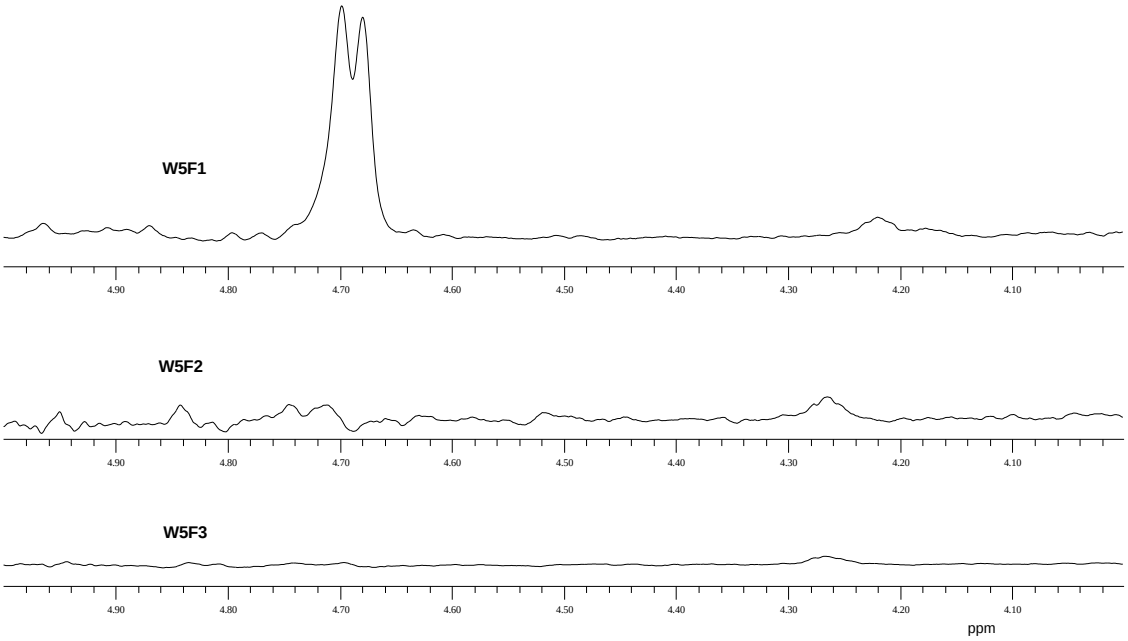

Figure 5.12: ^{1}H-NMR spectra in the vinylidene endgroup region of W5 fractions.

5.4 CROSS-FRACTIONATION USING SEC-FTIR AND SEC-DSC

An LC-Transform Model 300 from LabConnections, coupled to a Waters 150C chromatograph (columns HT 2 – 6) was used for the SEC-FTIR analyses. The stage temperature was 160 °C, the temperature of the nozzle 125 °C and the transfer line was operated at 150 °C.

Infrared spectra were acquired using a Nicolet Nexus spectrometer in transflection mode and Omnic 5.2 software for interpretation. Typically 60 scans at a resolution of 2 cm^{-1} were accumulated for each sample.

Four samples were selected for the fractionation using SEC-HPer DSC. These are ZR2 and ZR8 made using Cp_2ZrCl_2 (**5.1**)/MAO. The other two are CR1 and CR15 synthesized using $[(CO)_5Cr=C(Me)OZr(Cp)_2Cl]$ (**5.3**)/MAO. The fractions were deposited on a Germanium disc via the LC-Tansform using higher angle speed (20 ^oC/min) starting from 0 to 360 degrees. Thereafter, the FTIR scans were taken around the Germanium disc. The details about fractionating ethylene/1-pentene copolymers using the LC-Transform approach have already been explained in detail in Chapter 4.

For cross-fractionation, the Germanium disc was immersed in dichloromethane for separating the film. With the use of a degree arc placed above the disc and a fine knife, the desired angle size is scraped. The polymer collected is then placed on a pre-weighed aluminium foil. To avoid contamination, latex gloves were used throughout. Aluminium foil with the same mass as the foil containing the sample is used as a reference. Measurements of subsequent fractions were carried out in aluminium foil of always the same mass.

All measurements at high scanning rates were carried out in a Perkin Elmer Diamond DSC purged with helium/neon gas (25 ml/min). The samples were held for 5 minutes at 150 ºC and then cooled down to -100 ºC at 50 ºC/min (entirely linear). After stabilizing at -100 ºC for 5 minutes, the sample was heated up to 150 ºC at 150

ºC/min and kept there for 2 minutes. Finally the sample was cooled down to room temperature at 200 ºC/min. The samples were not heated higher than 150 ºC in order to avoid degradation since they were not stabilized.

5.4.1 The DSC analysis of the bulk properties of the selected samples

The samples have a comonomer content of between 7 and 9 mol% (Table 5.1). The weight average molecular weights vary between 25 and 50 000 g/mol and polydispersities between 3 and 5. Since there was no significant difference between first and second heating DSC curves, only the second heating curve was recorded. Figure 5.13 shows the second heating curves of all four samples measured using a standard method, i.e. heating at 10 ^{o}C/min from 0 to 160 ^{o}C. As displayed in Figure 5.13, samples have broad (ZR8 and CR15) and multiple melting peaks (ZR2 and CR1). Although multiple peak curves need further investigation using high scanning rates, broad melting peaks observed during slow heating, give an early indication that the two samples may have broad distributions of the thermal properties. The SEC-FTIR analysis of these samples in Chapter 4 showed a heterogeneous distribution of 1-pentene throughout the molecular weight distribution.

Applying high scanning rates on ZR2, as described in the experimental section, using HPer DSC, eliminates the third peak which was observed during heating at 10 ^{o}C/min. This peak can be attributed to the re-crystallization of crystals occurring as a result of slow heating since polymer chains have enough time to melt, re-crystallize

and re-melt. However, two distinct melting peaks at 115.2 and 101.0 ^{o}C and a broad crystallization peak are still present (see Figure 5.14) even after applying a fast heating rate which may be an indication that ZR2 has a broad SCBD. Sample CR1 also behaved in the same way as ZR2 under high scanning rates, i.e. the third peak disappeared while the other two remained (see Figure 5.14). The same apply to the other two samples (ZR8 and CR15) with broad melting curves. It is only at high scanning rates that re-crystallization during melting can be eliminated and "real" melting observed.

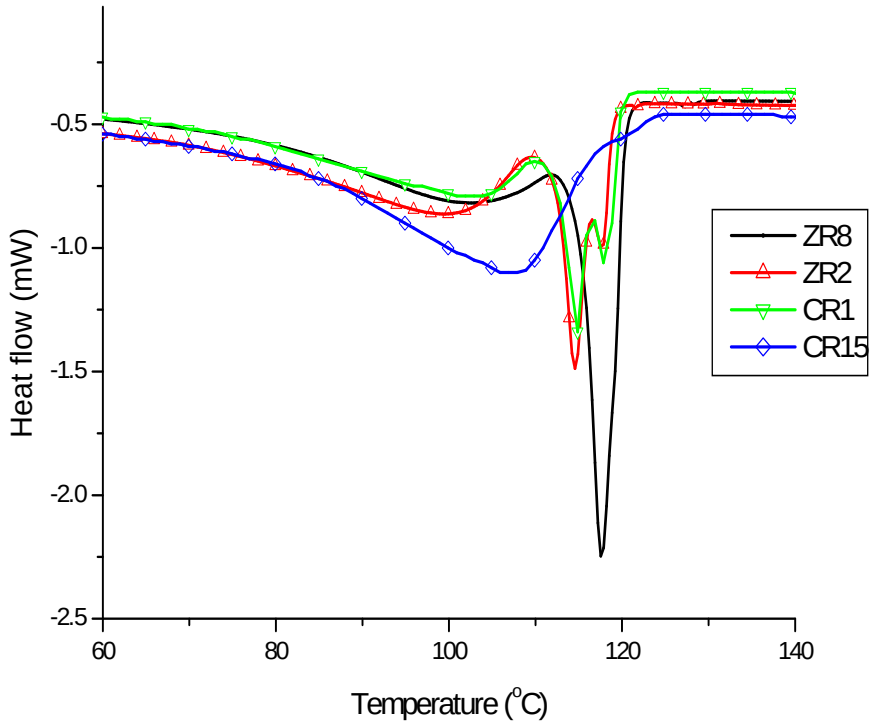

Figure 5.13: The second heating curves of the bulk samples from conventional DSC measured at 10 ^{o}C/min.

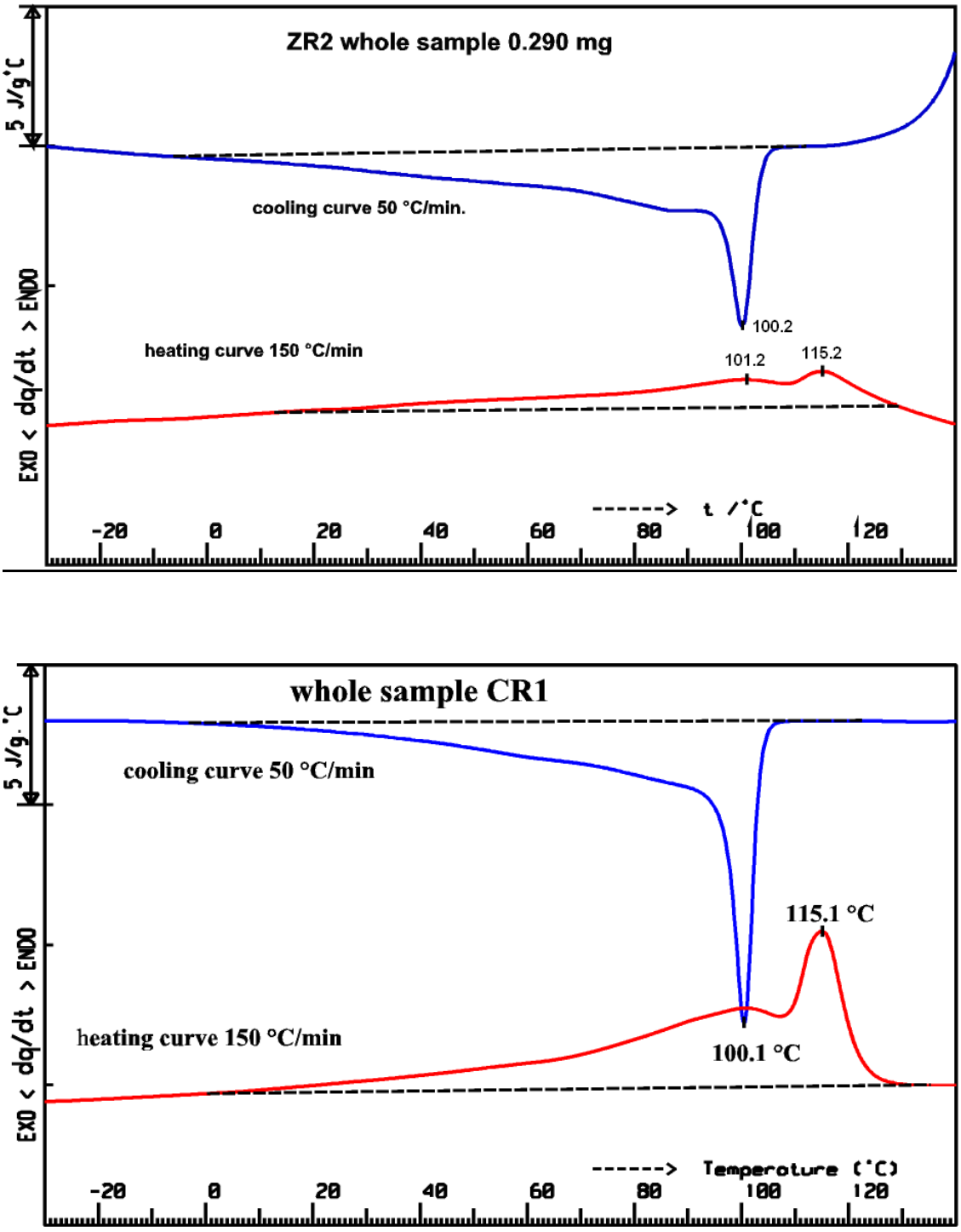

Figure 5.14: The cooling and heating curves of bulk samples ZR2 and CR1 measured using HPer DSC

The ability to scan (heat or cool) at various rates, including high rates, allows one to distinguish multiple thermal transitions such as cold crystallization, re-crystallization or decomposition after melting with high degree of certainty. HPer DSC proves to be a very valuable tool, in addition to standard DSC, due to the improved capability to interpret this multiple thermal behaviour

5.4.2 Cross-fractionation

In order to relate the thermal properties to the comonomer distribution of these copolymers along the molecular weight axis, we must first profile the distribution of 1-pentene using SEC-FTIR. The distribution of the average of CH_3 groups (caused by both 1-pentene and end groups) along the molecular weight axis is obtained by taking FTIR scans from SEC fractions using the LC Transform interface. The details of SEC-FTIR will not be repeated in this chapter as it has already been explained and discussed in Chapter 4. It was shown that the two catalyst system produce copolymers with heterogeneous comonomer distributions along the molecular weight axis. The results further indicated that average concentration of 1-pentene is higher towards the low molecular weight fractions for all these four samples (the concentration of 1-pentene is equivalent to the relative CH_3 concentration which correlates to the number of end groups).

A typical coordination polymerization mechanism associated with most metallocene catalyst systems for ethylene/α-olefin copolymerization would follow 1,2-insertion of

a comonomer after ethylene insertion and terminated via β-hydride elimination.[18-22] Busico et al. showed that Cp_2ZrCl_2/MAO at low polymerization temperatures follows 1,2-insertion and terminated via β-hydride elimination for propylene polymerization.[18] If we assume that this is the preferred polymerization mechanism, then for every chain we have a contribution of one CH_3-group from chain end and a significantly higher number of CH_3-goups from the comonomer (Figure 5.15). Taking this into account, we can therefore conclude that the CH_3 endgroup contribution from ethylene is negligible and no endgroup correction is necessary. This assumption can be validated by simply comparing the SEC-FTIR results with those obtained using other fractionation techniques (Soxhlet and PMWF) as shown in Chapter 4.

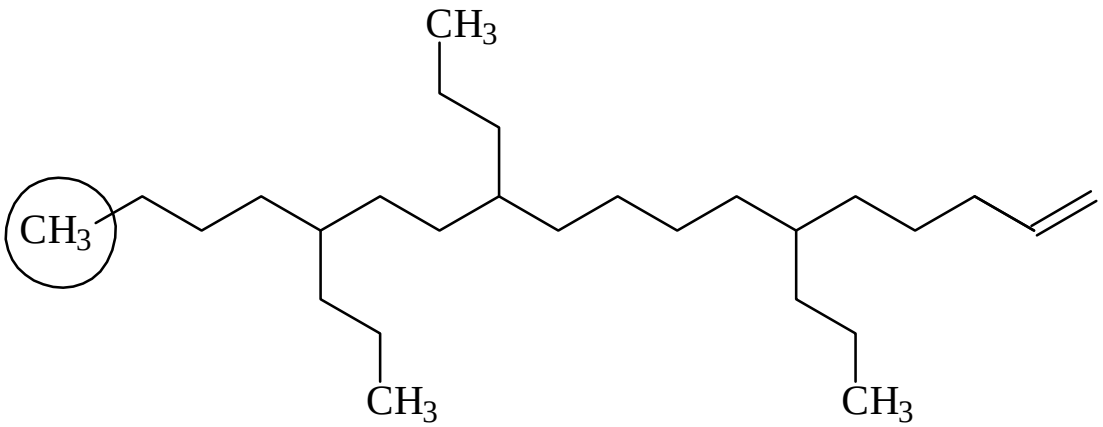

Figure 5.15: Typical structure of ethylene/α-olefin copolymer

For a better insight into the distribution of SCB, the thermal properties (melting and crystallization) of these samples along the molecular weight axis were studied using HPer DSC. This was done by isolating fractions around the Germanium disc and subsequently measuring melting and crystallization temperatures. It must be pointed

out that although calibration to determine the exact molecular weight of each fraction was not done, it is possible to relate the fractions to relative molecular weights. Since SEC uses hydrodynamic volume for separation, high molecular weight materials are eluted first, therefore the first fractions represent the high molecular weight material while the last corresponds to lower molecular weight materials.

As explained in the experimental section, dichloromethane is used as a liquid to facilitate the removal the film from the Germanium disc. It has been proven that dichloromethane does not dissolve the copolymer[11]. Subsequently, the film is split at different angles with the help of a degree arc. This is further explained in Scheme 5.4 which shows a film deposited on a Germanium disc and divided into fractions according to different angles.

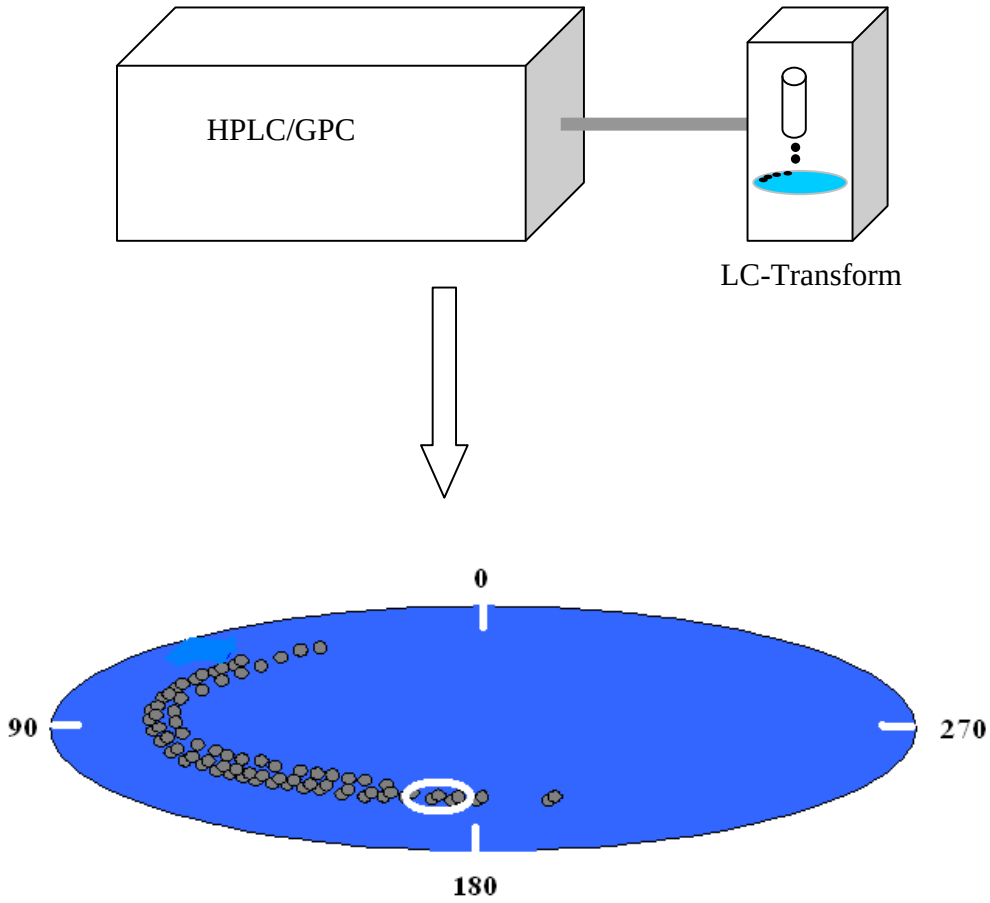

Scheme 5.4: Scheme showing polymer fractionation for HPer DSC measurements

5.4.2.1 The HPer DSC fractionation results of samples ZR2 and ZR8

The melting and crystallization temperatures together with the masses of the fractions of ZR2 and ZR8 are displayed in Tables 5.5 and 5.6, respectively. Generally the sample mass of each fraction was far below 1 mg as shown in Tables 5.5 and 5.6. For sample ZR2, the melting of the individual fractions takes place over a broad temperature range from 102 to 122 ^{o}C (20 degrees difference).

Table 5.5: Ethylene/1-pentene fractions of sample ZR2

Fraction	Mass (mg)	Angle (degree)	T_c (°C)	T_m (°C)
Bulk	0.290	-	100.2	115.2
1	0.018	90-120	102.1	122.6
2	0.018	120-150	100.4	117.9
3	0.096	150-180	99.9	118.2
4	0.148	180-210	102.6	118.1
5	0.072	210-240	104.2	117.8
6	0.052	240-270	102.2	116.0
7	0.080	270-300	98.9	111.1
8	0.030	300-330	95.4	118.2
9	0.072	330-350	92.5	102.0

Table 5.6: Ethylene/1-pentene fractions of sample ZR8

Fraction	Mass (mg)	Angle (degree)	T_c (°C)	T_m (°C)
Bulk	0.230	-	102.8	115.3
1	0.010	70-100	nd	nd
2	0.010	100-130	100.6	115.6
3	0.038	130-150	101.1	116.1
4	0.028	150-180	101.3	118.4
5	0.012	180-210	103.6	119.3
6	0.010	210-240	103.8	117.8
7	0.066	240-270	102.1	115.8
8	0.072	270-300	100.1	113.3
9	0.034	300-330	97.4	109.9

nd = not determined

Similarly, crystallization temperatures ranged from 92 to 104 ^{o}C (about 10 degrees difference). Although the range of melting temperatures for the fractions of sample ZR8 (see Table 5.6) is slightly narrower compared to ZR2, the behaviour is similar. This finally gives a more detailed picture about the SCBD of the copolymers and also the polymerization behaviour of Cp_2ZrCl_2(**5.1**)/MAO under the chosen conditions. From the SEC-FTIR and SEC-HPer DSC results one can conclude that **5.1** and **5.2**/MAO produces copolymers with broad or non-uniform SCBD. The

heterogeneous comonomer distribution on copolymers obtained by both catalyst systems can be expected since they do not have a bridging ligand which could restrict the rotation or movements of the Cp-ligands during polymerization. It has previously been speculated that Cp_2ZrCl_2/MAO probably has more than one active catalytic species which behaves differently during polymerization hence the possibility to produce heterogeneous copolymers[23].

Examples of the melting and the corresponding crystallization curves are shown in Figures 5.16 (a and b) and 5.17 (a and b) for samples ZR2 and ZR8, respectively. It must be pointed out that even though the sample mass is very low (due to the fact that the sample mass was obtained after single deposition), well pronounced thermal transitions can be obtained as a result of the high sensitivity of HPer DSC. Furthermore, multiple film deposition can lead to improved DSC curves. Figure 5.16 shows cooling and broad melting curves for ZR2 fractions. This can be attributed to the fact that ZR8 has a lower total comonomer content (Table 5.1), therefore leading to a higher crystallinity. Nevertheless, meaningful information could still be extracted from these curves as already demonstrated. The highest melting and crystallization peak temperatures of the fractions were plotted against fraction numbers (Figures 5.18 and 19). Neglecting the fact that all fractions have broad thermal transitions, the plots reflect heterogeneity with respect to SCB and decrease in both melting and crystallization peak temperatures towards the low M_w fractions.

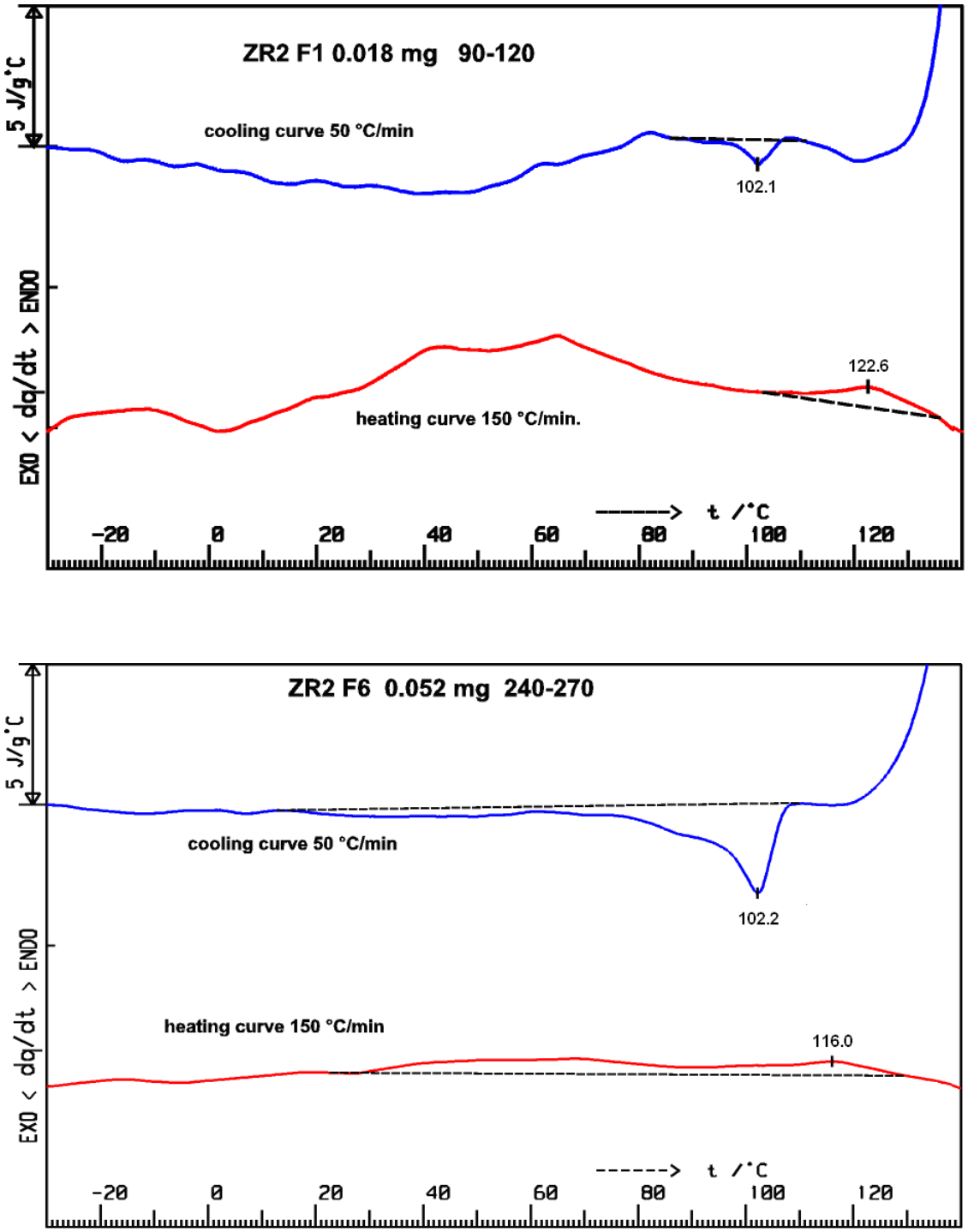

Figure 5.16 (a): Cooling and heating curves of ZR2 fractions F1 and F6 measured using HPer DSC

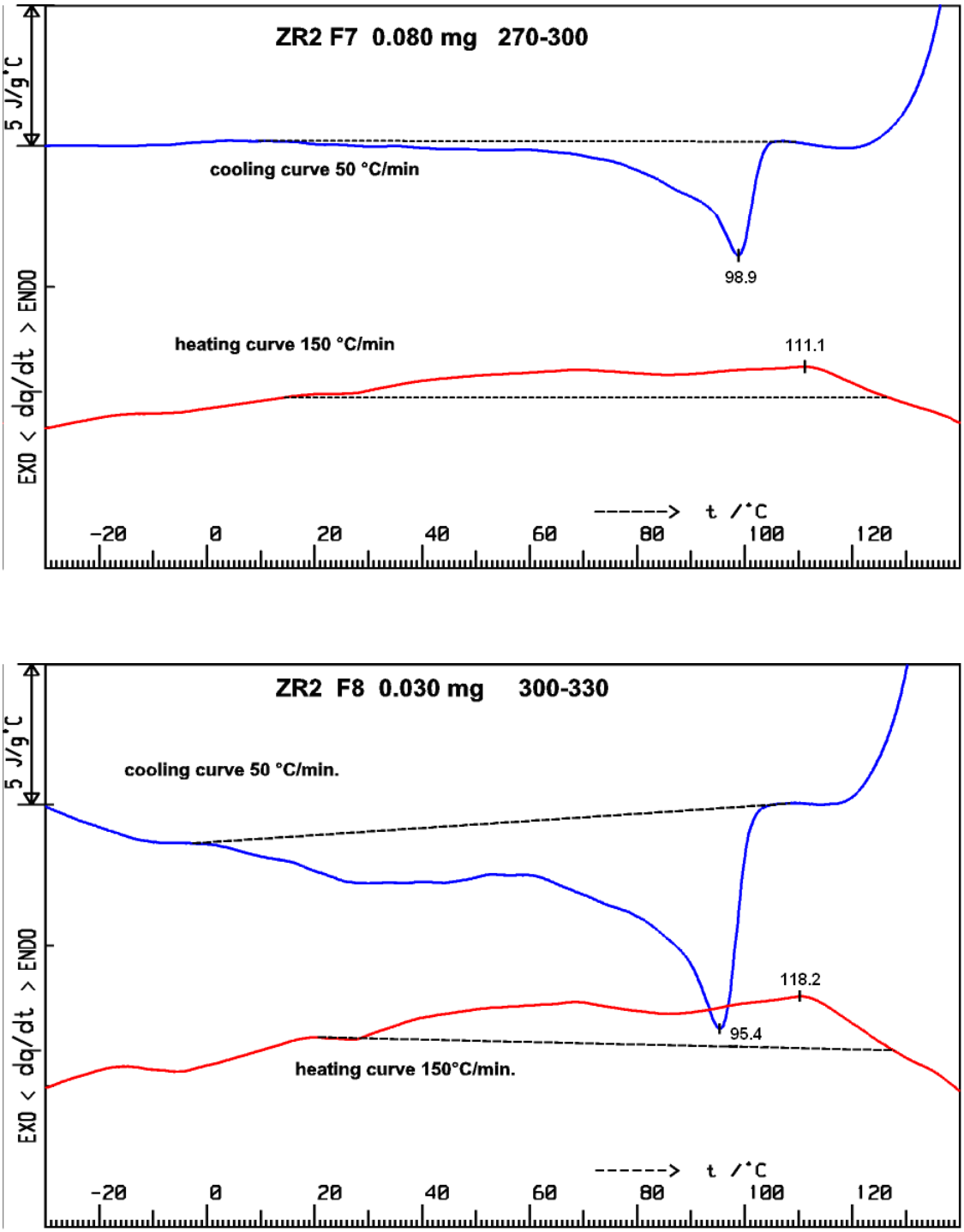

Figure 5.16 (b): Cooling and heating curves of ZR2 fractions F1 and F6 measured using HPer DSC

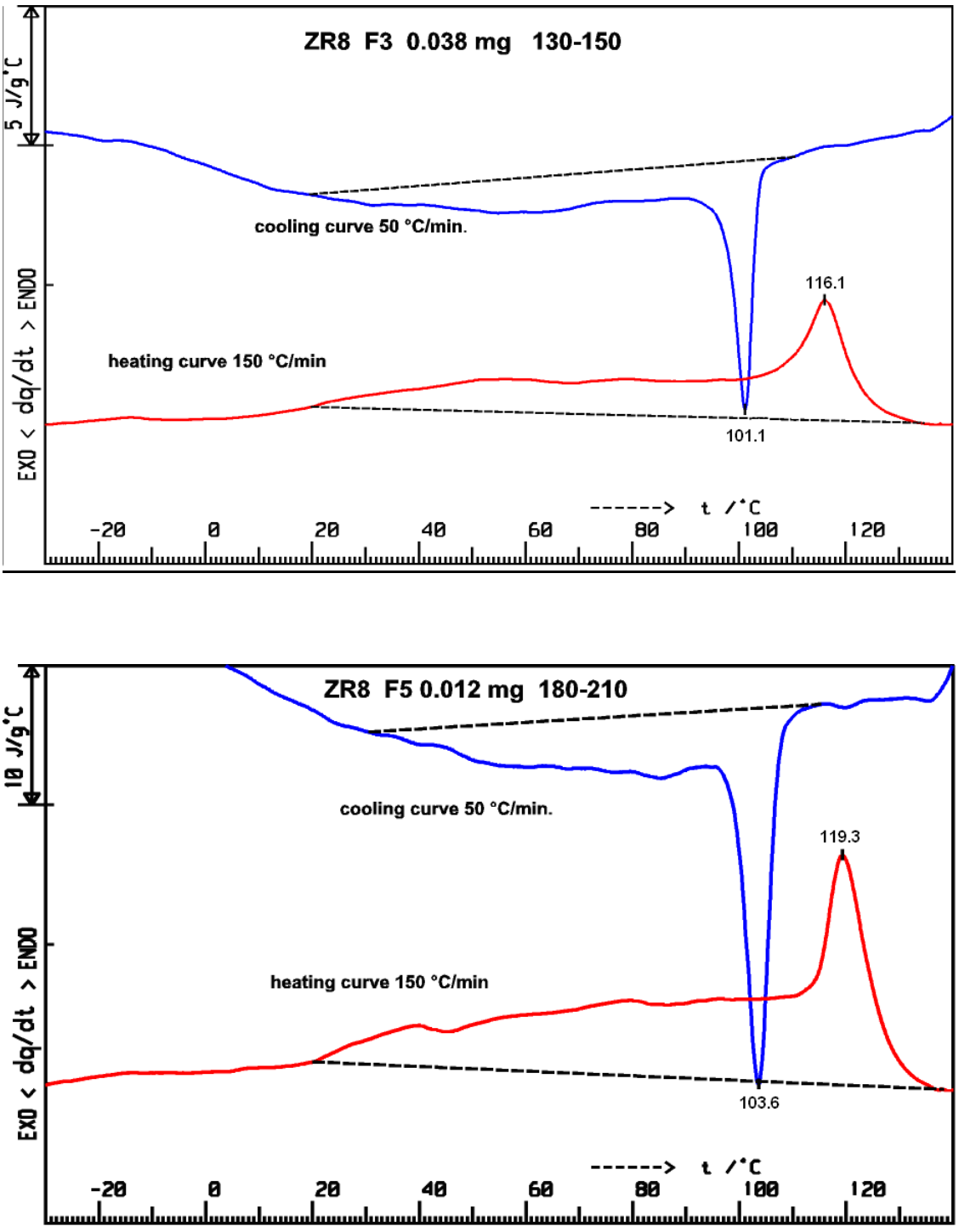

Figure 5.17 (a): Cooling and heating curves of ZR8 fractions measured using HPer DSC

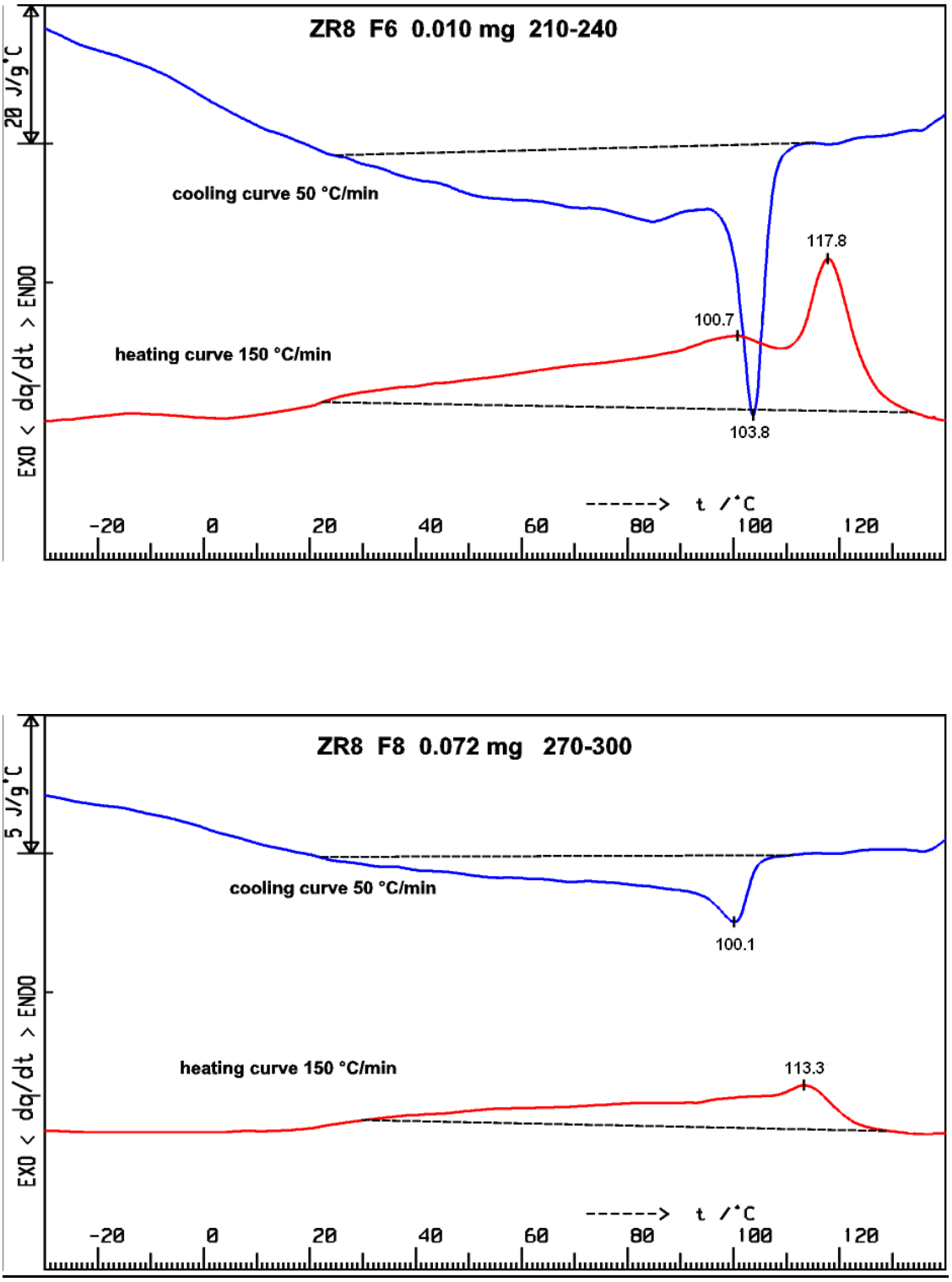

Figure 5.17 (b): Cooling and heating curves of ZR8 fractions measured using HPer DSC

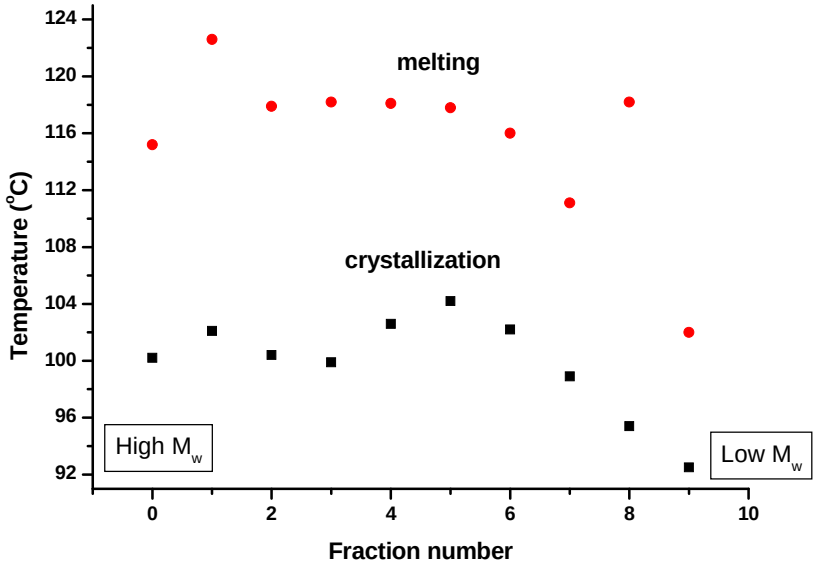

Figure 5.18: Melting temperatures of ZR2 fractions vs. fraction numbers

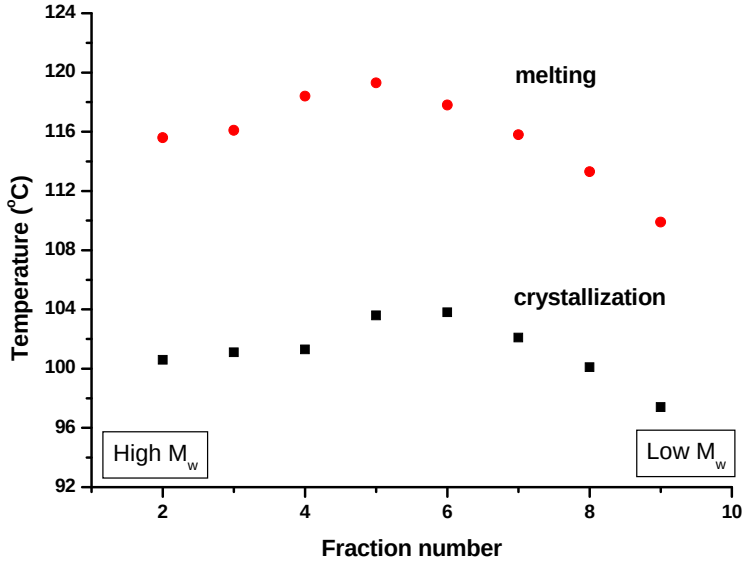

Figure 5.19: Melting temperatures of ZR8 fractions vs. fraction numbers

*5.4.2.2 The HPer DSC fractionation results of samples CR1and CR15 obtained using [(CO)$_5$Cr=C(Me)OZr(Cp)$_2$Cl](**5.3**)/MAO*

The fractionation results of CR1 are displayed in Table 5.7 while those of CR15 are Table A5.1 in Appendix A. The melting and crystallization curves of the selected fractions of both samples are shown in Figures 5.20 and 5.21. As observed previously with ZR2 and ZR8 analysis, the masses of the fractions are in the microgram range (far below 1mg). Once again, the melting and crystallization curves for both CR1 (Figure 5.20) and CR15 (Figure 5.21) do not show any loss of critical information. Melting and crystallization temperatures can clearly be extracted from these curves thus again substantiating the high level of sensitivity of HPer DSC already seen for ZR2 and ZR8.

Figure 5.20 and 5.21 indicate that the melting and crystallization generally take place over a broad temperature range. The plots of the melting and crystallization temperatures vs. fraction numbers (Figure 5.22 and 5.23) follow behaviour similar to that observed for ZR2 and ZR8 i.e a decrease of melting and crystallization temperatures towards high fractions (low molecular weight).

Table 5.7: Ethylene/1-pentene fractions of sample CR1

Fraction	Mass (mg)	Angle (degree)	T_c (°C)	T_m (°C)
Bulk	0.540	-	100.1	115.1
1	0.030	90-120	104.1	118.7
2	0.022	120-140	103.4	117.7
3	0.016	140-160	102.1	118.6
4	0.014	160-180	100.9	115.7
5	0.008	180-190	101.6	116
6	0.016	190-200	102.3	116.2
7	0.010	200-210	102.9	116.2
8	0.033	210-220	102.8	116.5
9	0.042	220-260	101.6	116.5
10	0.136	260-300	97.4	110.9
11	0.056	300-340	90.6	105.1

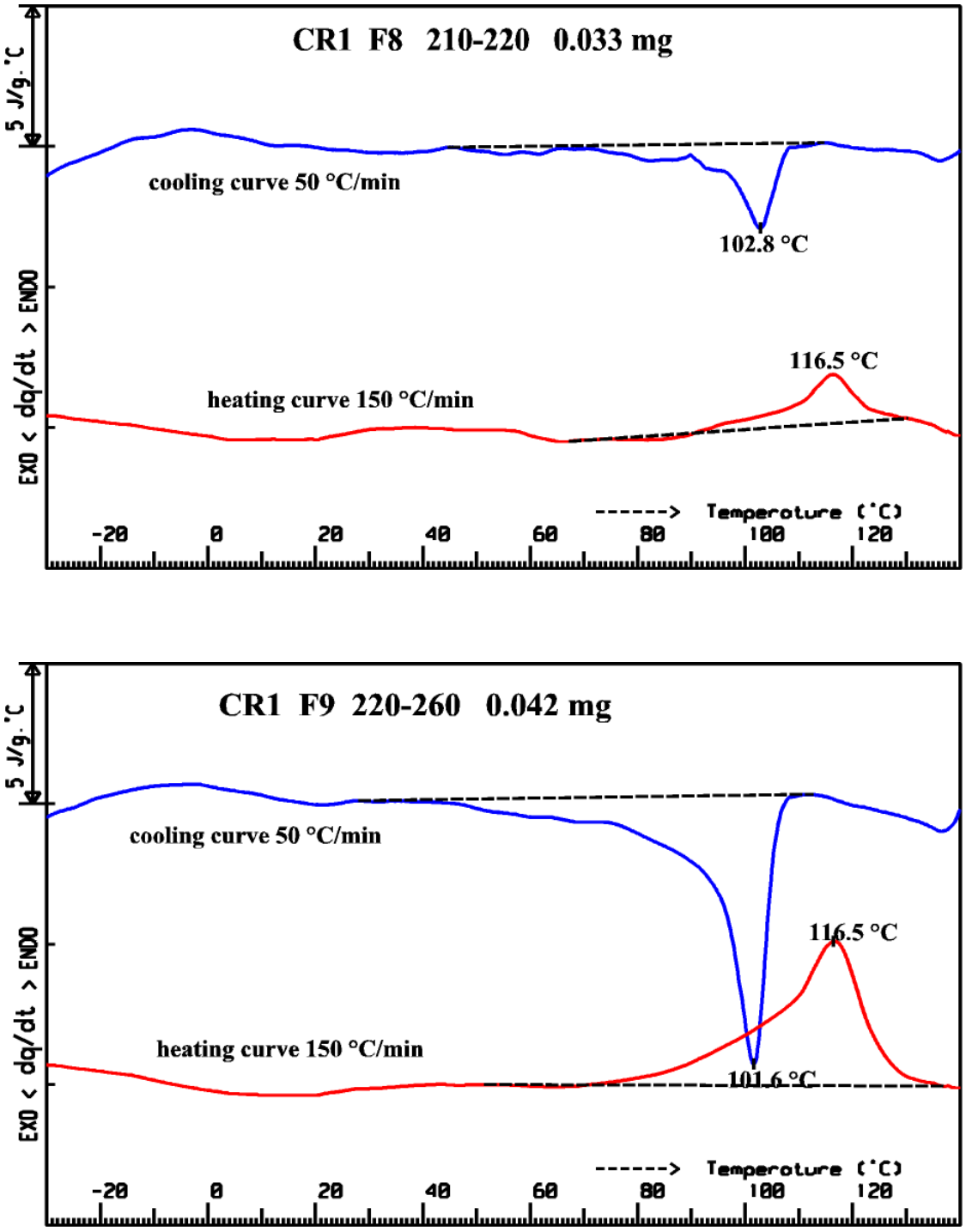

Figure 5.20: Cooling and heating curves of CR1 fractions (F8 and 9) measured using HPer DSC

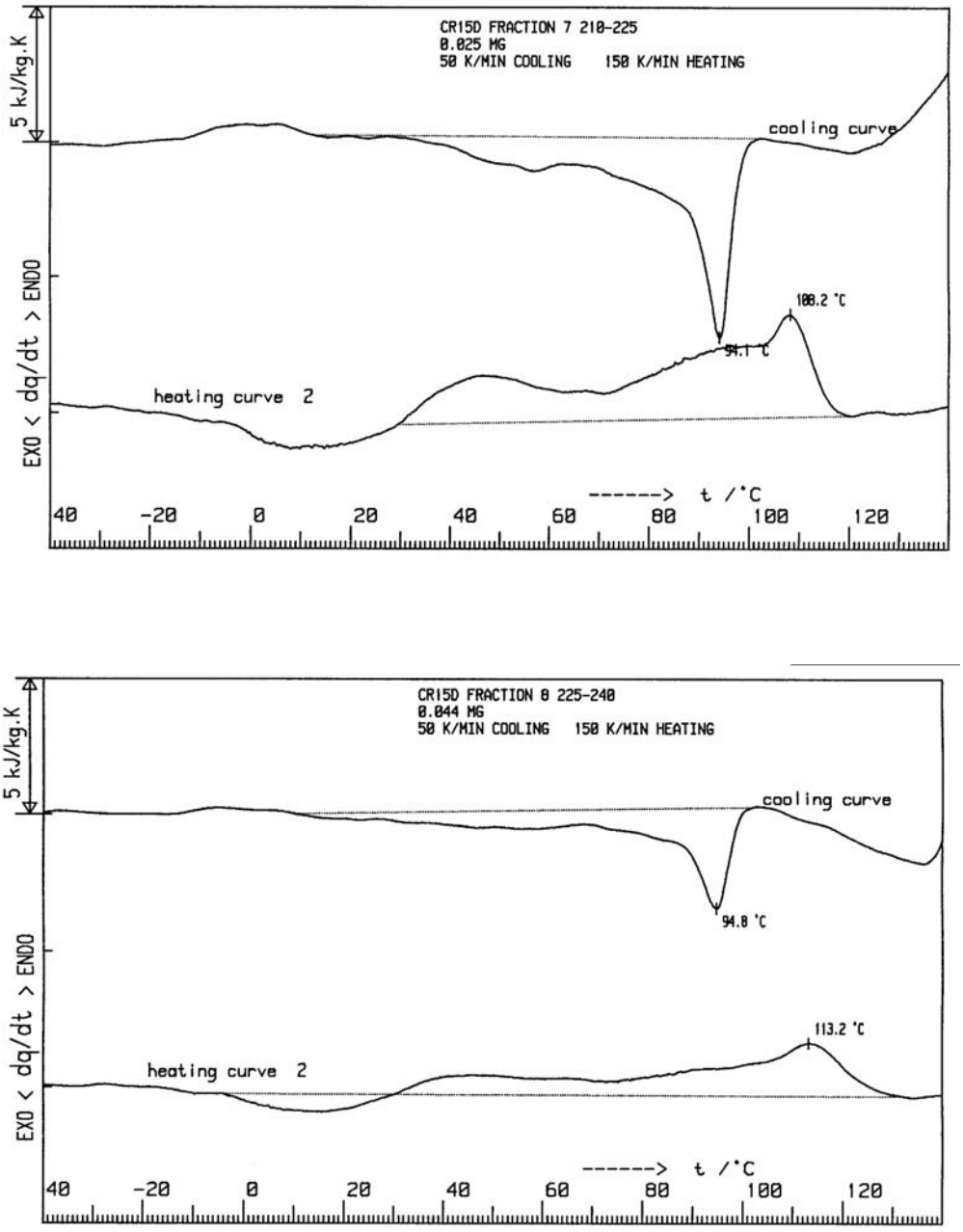

Figure 5.21: Cooling and heating curves of CR15 fractions measured using HPer DSC

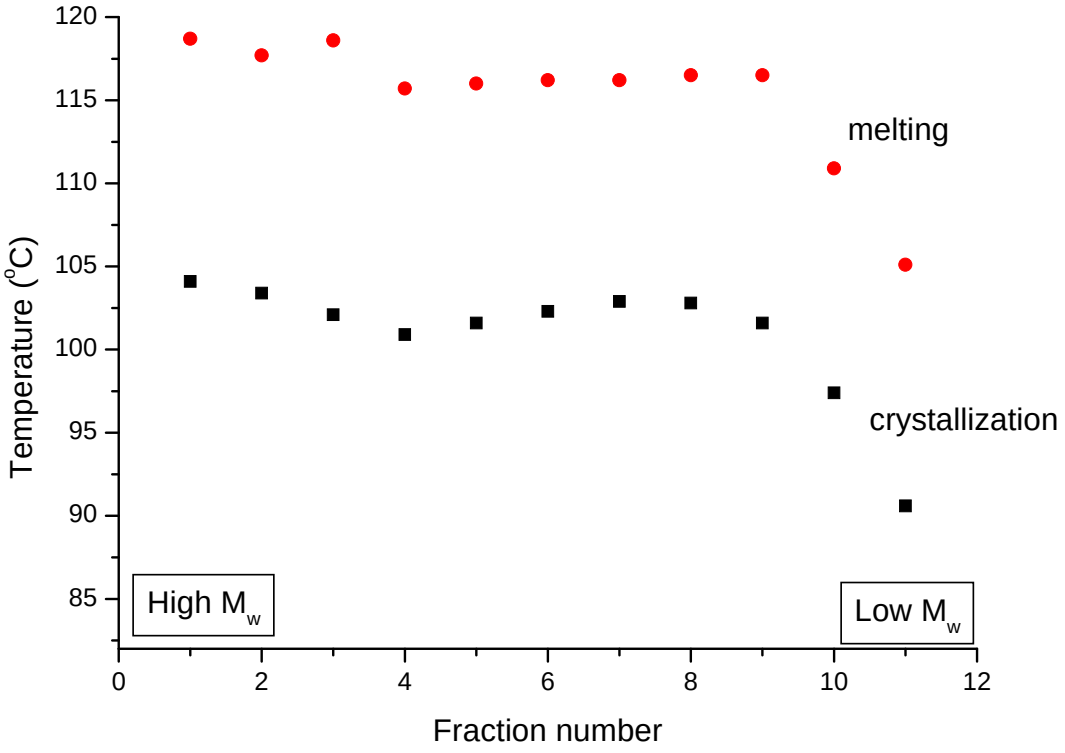

Figure 5.22: Melting and crystallization temperatures of CR1 fractions vs. fraction numbers

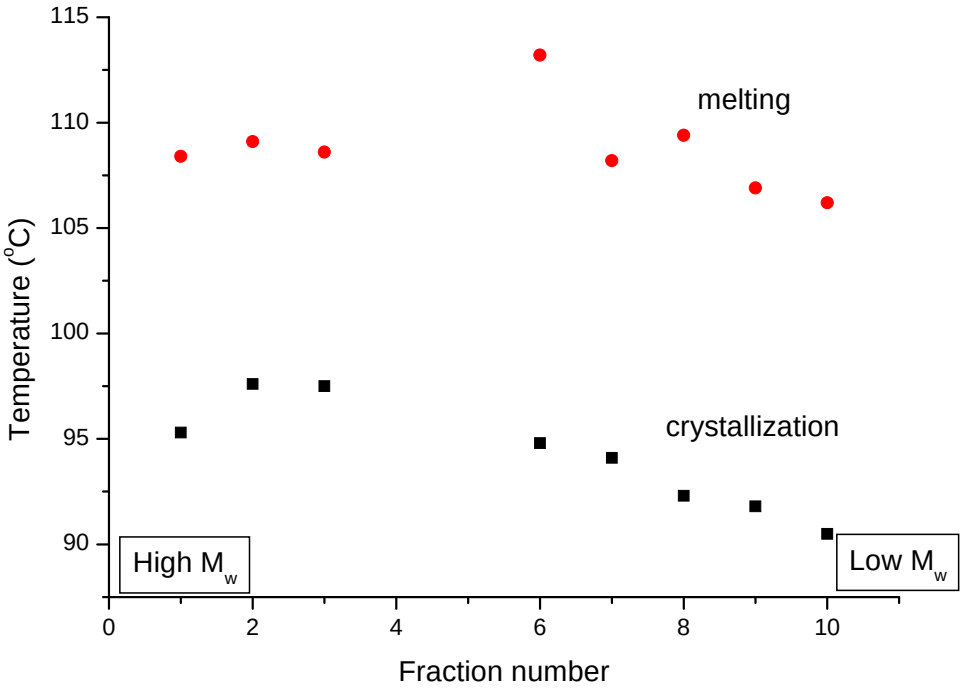

Figure 5.23: Melting temperatures of CR15 fractions vs. fraction numbers

For all four samples obtained with Cp_2ZrCl_2(**5.1**) and $[(CO)_5Cr{=}C(Me)OZr(Cp)_2Cl]$(**5.3**)/MAO catalysts, it is evident that the low molecular weight fractions have the lowest melting and crystallization temperatures as expected. For the high molecular weight fractions one would expect T_c and T_m to decrease with constant SCB and increasing molecular weight (decreasing fraction number), because analogous measurements on LDPE fractions - though performed at 5 k/min - already show such a decrease having a *constant* SCB [24,25]. The fact that T_c and T_m in this report show approx. *constant* values points to a *decrease* of SCB with molecular weight, confirming the FTIR results. However, using the LDPE results as reference data is not optimal because the type of SCB is rather undefined, and we

await better data from homogeneous copolymers having a constant comonomer (SCB) as function of molecular weight.

The decrease of T_c (see Figure 5.24) and T_m values (HPer DSC) with increasing SCB, is in good agreement with the SEC-FTIR plots, which indicate high comonomer concentration in the low molecular weight region and standard DSC measurements which indicated that the bulk samples have a broad SCBD.

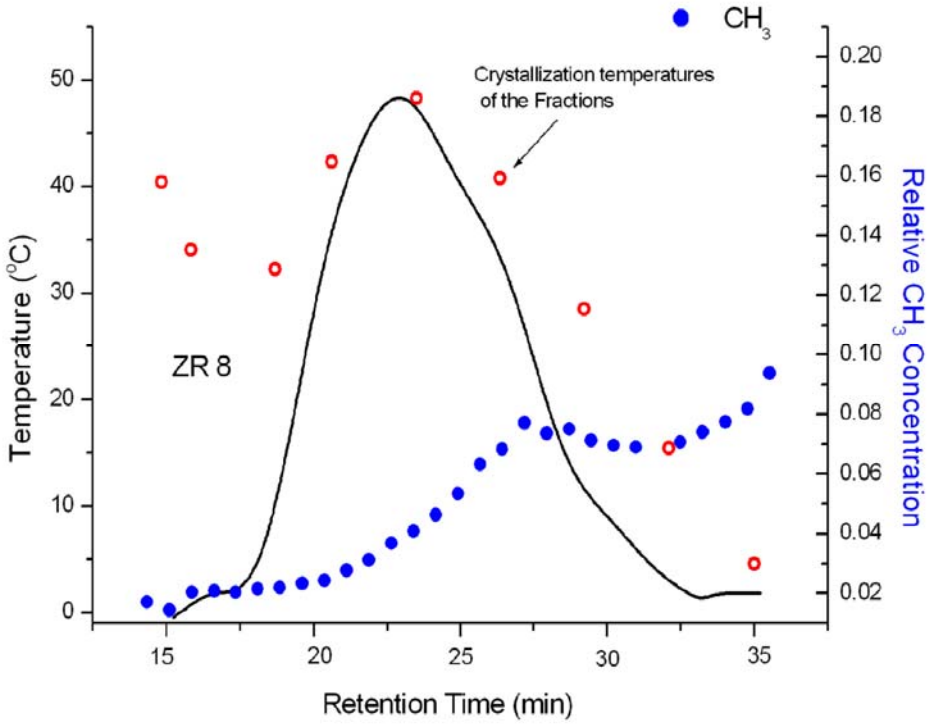

Figure 5.24: An overlay of crystallization temperatures of ZR8 fractions from HPer DSC and molecular weight distribution

HPer DSC technique adds a new dimension to the SEC-FTIR fractionation. The ability to measure very small amounts of sample and the ability to detect weak signals makes it possible to study thermal properties along the molecular weight axis. In

addition, the use of HPer DSC as a complementary method to SEC-FTIR, allows the study of SCBD and thermal properties in a very short period compared to TREF or CRYSTAF. Scheme 5.5, illustrates the culmination of the two methods.

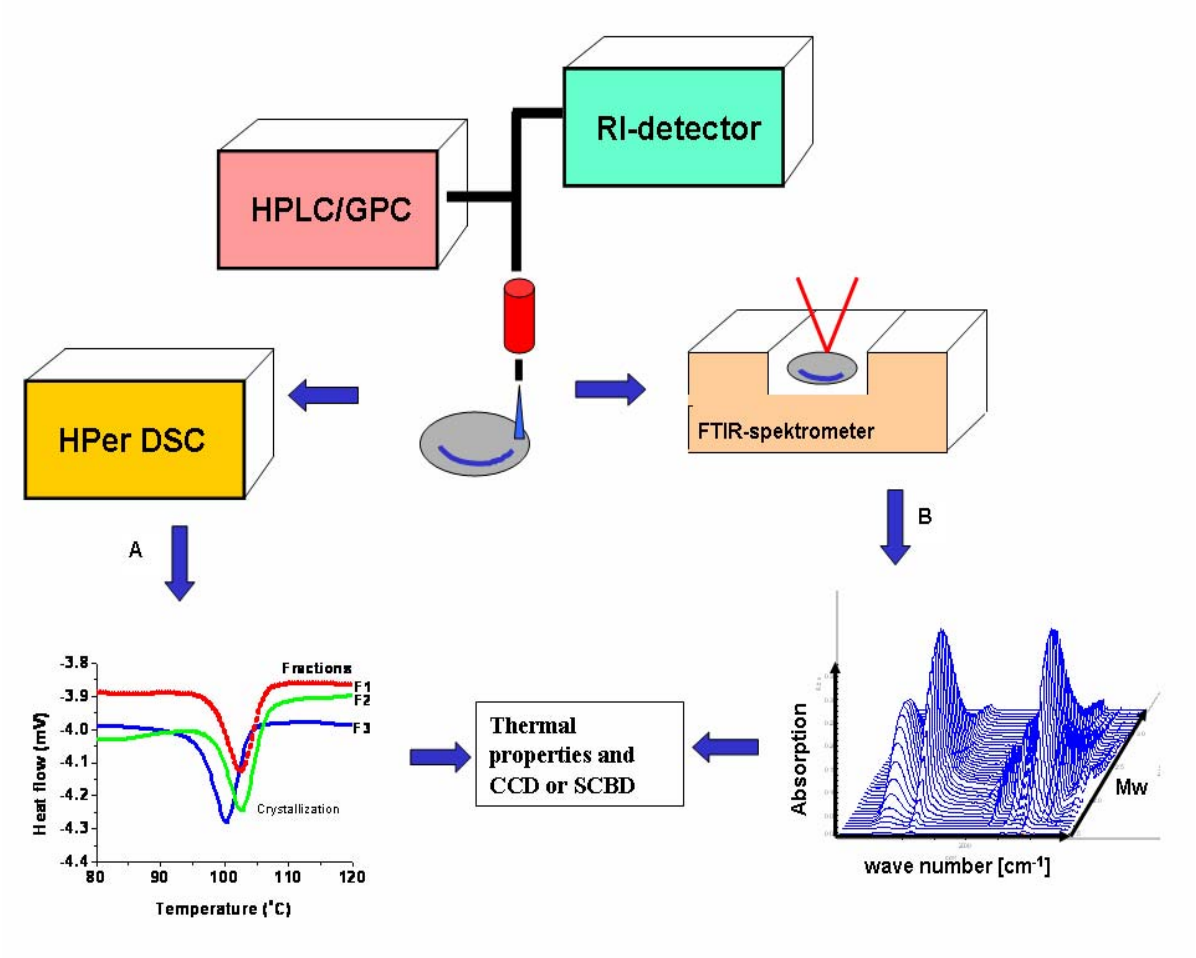

Scheme 5.5: Scheme showing polymer cross-fractionation techniques HPer DSC (A) SEC-FTIR (B)

The chemical composition distribution of the copolymers produced by the metallocene Cp_2ZrCl_2 and the metalloxycarbene ([$(CO)_5W$=C(Me)OZr$(Cp)_2$Cl] and [$(CO)_5$Cr=C(Me)OZr$(Cp)_2$Cl]) catalyst systems along the molecular weight axis is summarized by a schematic representation shown in Figure. 5.25. The heterogeneous comonomer distribution occurs in both cases with high comonomer concentration towards low molecular weight. However, metalloxycarbene-catalyzed copolymers show a sharper increase of the comonomer content at copolymers chains with low molecular weight.

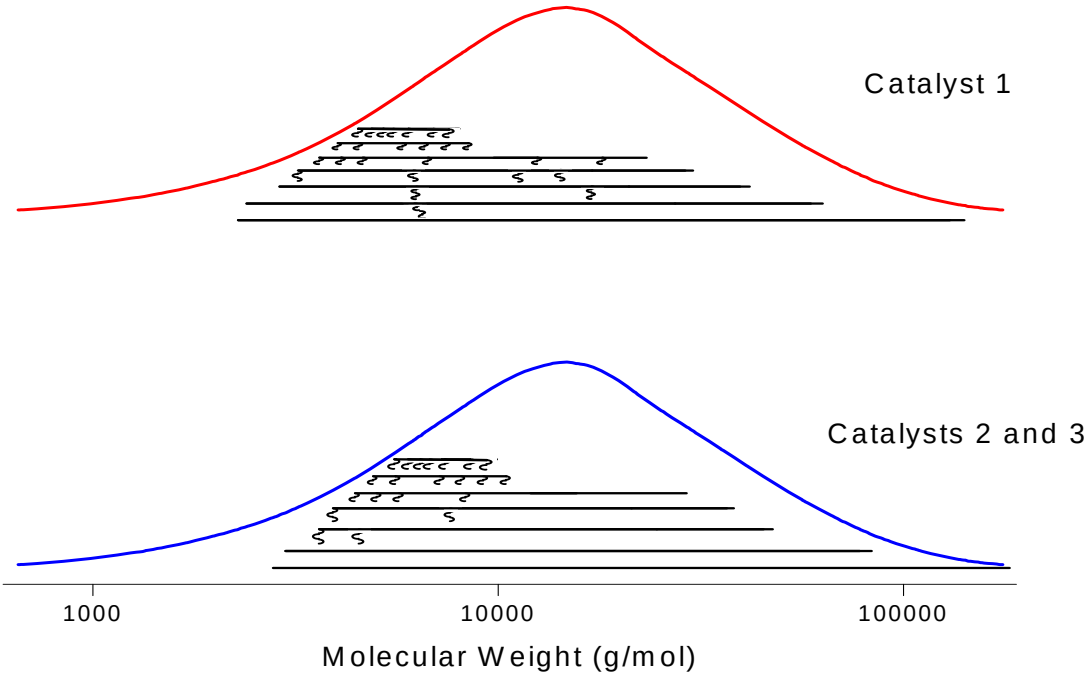

Figure 5.25: Schematic representation of comonomer distribution along the molecular weight axis

5.5 CONCLUSIONS

Ethylene/1-pentene copolymers synthesized with Cp_2ZrCl_2(**5.1**), $[(CO)_5W{=}C(Me)OZr(Cp)_2Cl]$(**5.2**) and $[(CO)_5Cr{=}C(Me)OZr(Cp)_2Cl]$(**5.3**)/MAO show a broad short chain branching distribution as analyzed using PMWF and SEC-DSC. The heterogeneous copolymers produced by all three catalysts may indicate that each of the catalyst systems may have more than one active site behaving differently during polymerization. Taking full advantage of HPer DSC's ability to scan at high rates, re-crystallization peaks, occurring during heating, can be separated from "real" melting. Using PMWF and by combining SEC-FTIR and HPer DSC techniques we were able to show that it is possible to:

1. study SCBD, and consequently thermal properties, along the molecular weight axis using SEC-FTIR and HPer DSC, respectively;

2. use HPer DSC to complement SEC-FTIR and thus provide valuable information about polymer properties on narrow sub-classes of molecular weight distribution in a reasonably short analysis time.

3. we can conclude that $[(CO)_5W{=}C(Me)OZr(Cp)_2Cl]$(**5.2**) and $[(CO)_5Cr{=}C(Me)OZr(Cp)_2Cl]$(**5.3**)/MAO produce copolymers that are more heterogeneous with regard to SCBD than those synthesized with Cp_2ZrCl_2(**5.1**).

5.6 REFERENCES

1. Kaminsky, W. *J. Polym. Sci. Part A: Polym. Chem.* **2004**, 42, 3911.

2. Kaminsky, W. *Macromol. Symp.* **2002**, 177, 61.

3. Soares, J.B.P.; Anantawaraskul, S. *J. Polym. Sci. Part B: Polym. Phys.* **2005**, 43, 1557.

4. Monrabal, B. *Temperature rising elution fractionation and crystallization analysis fractionation*. In Encyclopedia of Analytical Chemistry, Ed, Mayers, R.A. **2000**, 14, page 1-20.

5. DesLauriers, P. J.; Rohlfing, D. C.; Hsieh, E. T. *Polymer* **2002**, 43, 159.

6. Willis, J. N.; Wheeler. L. *Adv. Chem. Ser.* **1995**, 247, 253.

7. Tackx, P.; Bremmers, S. *Polym. Mater. Sci. Eng.* **1998**, 78, 50.

8. Luruli, N.; Grumel, V.; Brüll, R.; Du Toit, A.; Pasch, H.; van Reenen, A.J.; Raubenheimer, H.G. *J. Polym. Sci. Part A: Polym. Chem.* **2004,** 42, 5121.

9. de Goede, S.; Brüll, R.; Pasch, H.; Marshall, N. *Macromol. Symp.* **2003,** 193, 35.

10. Graef, S. M.; Brüll, R.; Pasch, H.; Wahner, U. M. *e-Polymers* **2003**, 005.

11. Mathot, V. B. F. *J. Therm. Anal. Cal*. **2001**, 64, 15.

12. Pijpers, M.F.J.; Mathot, V.B.F.; Goderis, B.; Scherrenberg, R.; van der Vegte, E. *Macromolecules* **2002**; 35, 3601.

13. McGregor, C.; Saunders, H.M.; Buckton, G.; Saklatvala, R.D. *Thermochim. Acta* **2004**, 417, 231.

14. Abdulkarim, S.M, Long, K.; Lai, O.M.; Muhammad, S.K.S.; Ghazali, H.M. *Food Chemistry* **2005**, 93, 253.

15. Bergström, C.; Avela, E. *J. Appl. Polym. Sci.* **1979**, 23,163.

16. Francuskiewicz, F. *Polymer Fractionation*, Springer-Verlab, Berlin, **1994**. Chapter 12, p177.

17. Xu, X.; Xu, T.; Feng, L.; Chen, W. *J. Appl. Polym. Sci.* **2000**, 77, 1709.

18. Busico, V.; Cipullo, R. *Prog. Polym. Sci.* **2001**, 26, 443.

19. Resconi, L.; Piemontesi, F.; Franciscono, G.; Abis, L.; Fiorani, T. *J. Am. Chem. Soc.* **1992**, 114, 1025.

20. Ewen, J. *J. Am. Chem. Soc*. **1984**, 106, 6355.

21. Zambelli, A.; Ammendola, P.; Grassi, A.; Longo, P.; Proto, A. *Macromolecules* **1986**, 19, 2703.

22. Cheng, H.; Ewen, J. *Makromol. Chem*. **1989**, 190, 1931.

23. Heiland, K; Kaminsky, W; *Makromol. Chem. Phys.* **1992**, 193, 601.

24. Mathot, V.B.F.; Pijpers, M.F.J. *Polym. Bull.* **1984**, 11, 297.

25. Mathot, V.B.F. *The Crystallization and Melting Region*. In *Calorimetry and Thermal Analysis of Polymers*, Ed,. Mathot ,V.B.F. Hanser Publishers, Munich Vienna New York **1994**, Ch. 9, 231-299.

6 General conclusion and recommendations

6.1 General conclusions

Reaction between anionic Fischer-type carbene complex salts and various metallocenes furnished metalloxycarbene complexes. Most of these complexes when activated with MAO, are active for oligomerizing, polymerizing and copolymerizing α-olefins. Certain metalloxycarbenes/MAO are more active catalyst systems than Cp_2ZrCl_2/MAO and produce polymers with high molecular weight and, broad and bimodal molecular weight distribution. In particular, ethylene/1-pentene copolymers obtained using metalloxycarbenes/MAO are highly heterogeneous in terms of comonomer distribution compared to those produced with metallocenes. The high molecular weight of polymers or copolymers obtained with metalloxycarbenes/MAO catalysts, in general, compared to those obtained with Cp_2ZrCl_2/MAO, indicate that the anionic Fischer carbene ligand probably influences the polymerization processes sterilally. In addition, broad and bimodal molecular weight distribution as well as heterogeneous comonomer distribution point to the fact that metalloxycarbene/MAO catalysts behave vastly different. These results have led to speculative proposal that these novel catalyst systems could be multi-

sited. An in-depth study of the polymer properties has been made possible by the availability of advanced and recently developed fractionation analytical techniques such Preparative molecular weight fractionation (PMWF) and a combination of SEC and high performance DSC (SEC-HPer DSC).

6.2 Recommendations

The following further investigations should be considered:

- A more detailed investigation into the role that the second metal plays in influencing the catalytic activity and stability of metalloxycarbenes should be carried out.

- Molecular weight calibration of the SEC instrument for SEC-FTIR measurements would make the short chain branching distribution plots more accurate and also give a clearer picture as to what extent the molecular weight influences the melting and crystallization temperatures in HPer DSC fractionation.
- The polymer fractions obtained during preparative molecular weight fractionation, if not dried properly, normally contain residuals of non-solvent (diethyleneglycolmonobutylether, DGMBE). The residuals of DGMBE can significantly affect DSC results and therefore, other solvents should be investigated for drying preparative molecular weight fractions in order to overcome this problem.

- Whether chemical composition play any role at all during preparative molecular weight fractionation.

- The extent to which dichloromethane, diluent used during HPer DSC fractionation, influences the results, needs further investigation.

Appendix A

Chapter 4

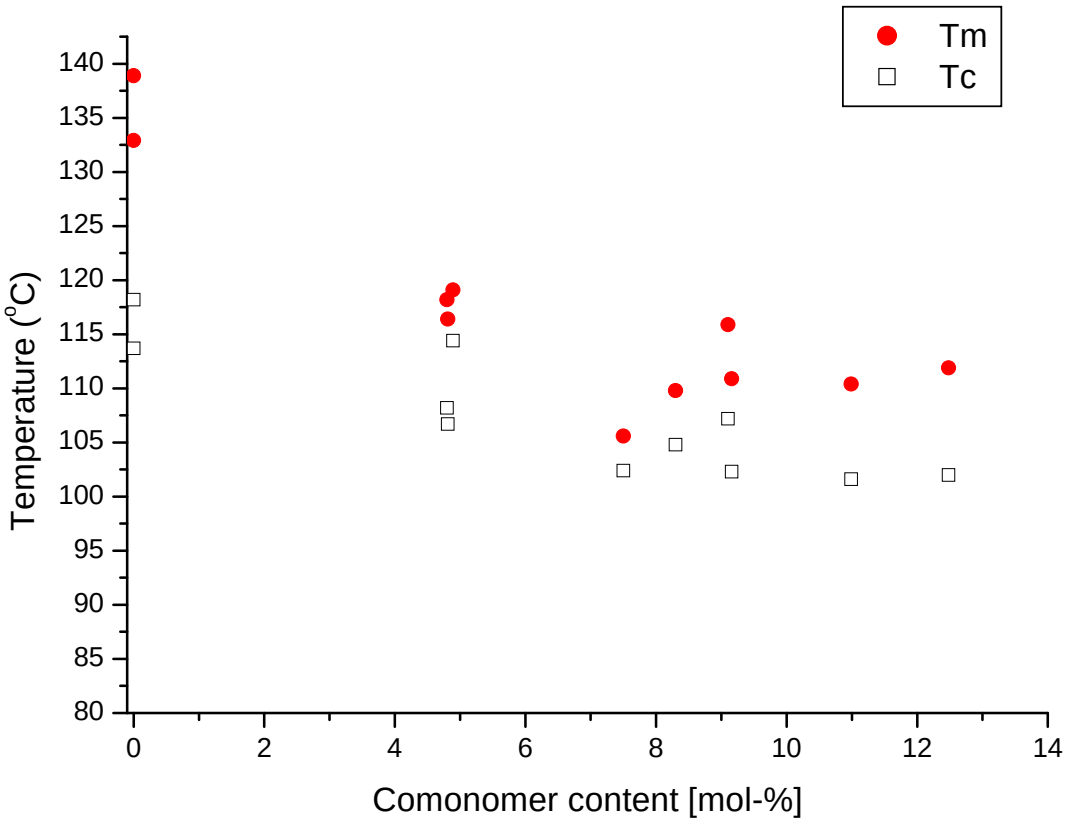

Figure A4.1: Melting and crystallization temperatures vs comonomer content for copolymers produced with $[(CO)_5Cr=C(Me)OZr(Cp)_2Cl]$ (4.3)/M**AO**

Chapter 5

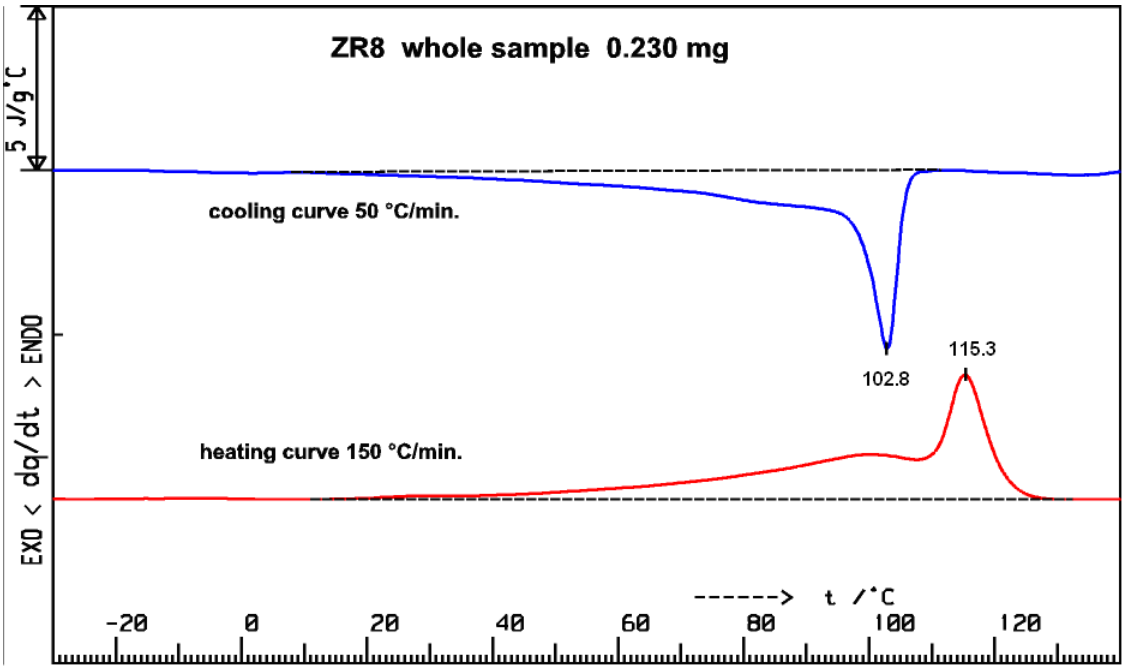

Figure A5.1: The cooling and heating curves of bulk sample ZR8 measured using HPer DSC.

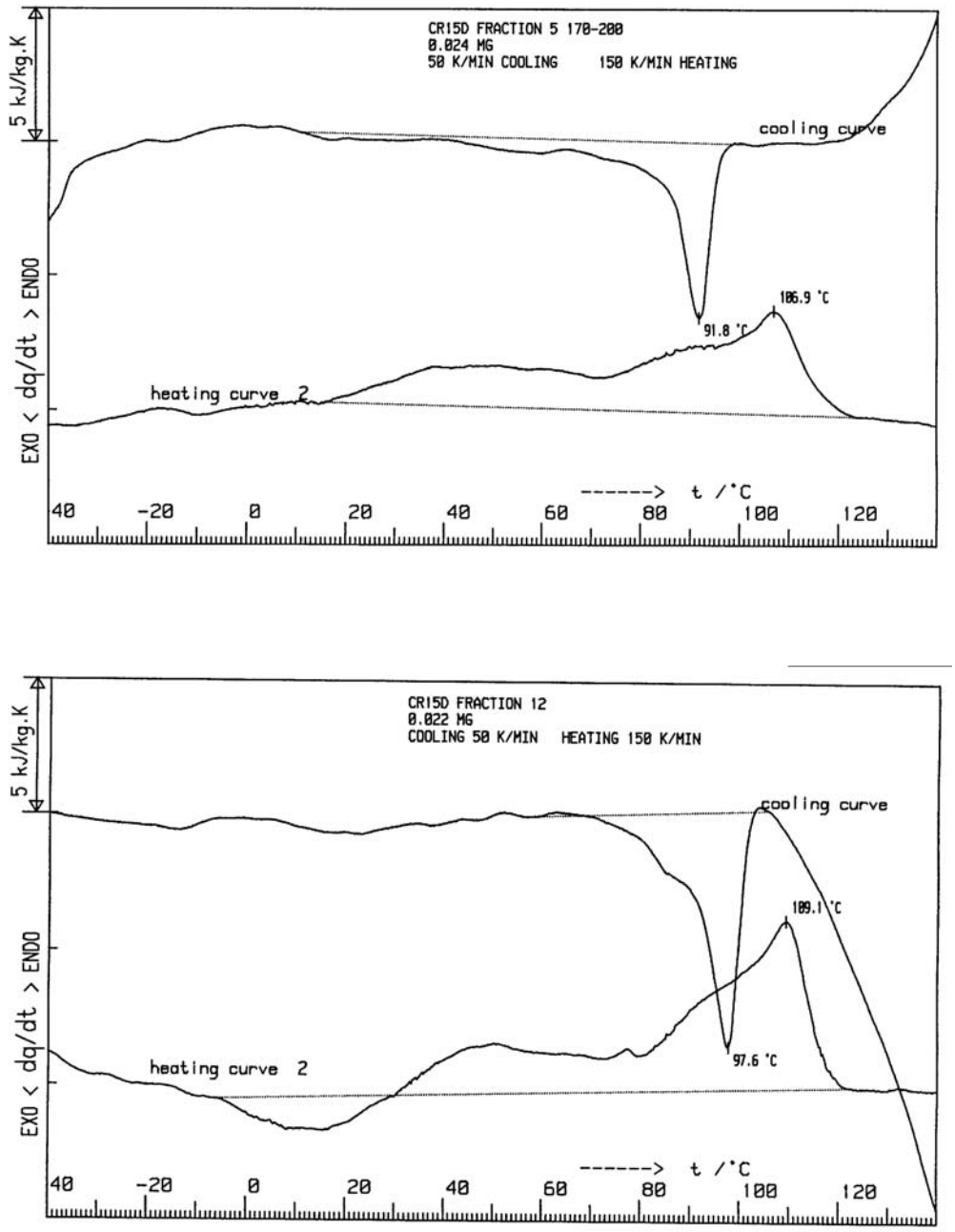

Figure A5.1: Selected cooling and heating curves of CR15 fractions measured using HPer DSC

Table A5.1: Ethylene/1-pentene fractions of sample CR15

Fraction	Angle (^{o})	Weight (mg)	Tc (^{o}C)	Tm (^{o}C)
1	nd	nd	nd	nd
2	nd	nd	nd	nd
3	nd	nd	nd	nd
4	140-170	0.06	90.5	106.2
5	170-200	0.024	91.8	106.9
6	200-210	0.016	92.3	109.4
7	210-225	0.025	94.1	108.2
8	225-240	0.044	94.8	113.2
11	270-290	0.022	97.5	108.6
12	290-320	0.022	97.6	109.1
13	320-350	0.01	95.3	108.4

nd = not determined